JC03 Rec'd PCT/PTO 31 JAN 2001

FORM PTO-1390 (Modified) (REV 10-95) U.S. DEPARTMENT OF COMMERCE PATENT AND TRADEMARK OFFICE		
TRANSMITTAL LETTER TO THE UNITED STATES DESIGNATED/ELECTED OFFICE (DO/EO/US) CONCERNING A FILING UNDER 35 U.S.C. 371		ATTORNEY'S DOCKET NUMBER: 56326-032 (IOPL-007) U.S. APPLICATION NO. (IF KNOWN, SEE 37 CFR): 60/094,602 09/762077
INTERNATIONAL APPLICATION NO.: PCT/US99/17338	INTERNATIONAL FILING DATE: July 30, 1999	PRIORITY DATE CLAIMED: July 30, 1998

TITLE OF INVENTION
INFRARED RADIATION SOURCES, SENSORS AND SOURCE COMBINATIONS AND METHODS OF MANUFACTURE

APPLICANT(S) FOR DO/EO/US
Edward A. Johnson

Applicant herewith submits to the United States Designated/Elected Office (DO/EO/US) the following items and other information:

1. ☒ This is a **FIRST** submission of items concerning a filing under 35 U.S.C. 371.
2. ☐ This is a **SECOND** or **SUBSEQUENT** submission of items concerning a filing under 35 U.S.C. 371.
3. ☐ This is an express request to begin national examination procedures (35 U.S.C. 371(f)) at any time rather than delay examination until the expiration of the applicable time limit set in 35 U.S.C. 371(b) and PCT Articles 22 and 39(1).
4. ☒ A proper Demand for International Preliminary Examination was made by the 19th month from the earliest claimed priority date.
5. ☐ A copy of the International Application as filed (35 U.S.C. 371 (c) (2))
   a. ☐ is transmitted herewith (required only if not transmitted by the International Bureau).
   b. ☐ has been transmitted by the International Bureau.
   c. ☒ is not required, as the application was filed in the United States Receiving Office (RO/US).
6. ☐ A translation of the International Application into English (35 U.S.C. 371(c)(2)).
7. ☒ A copy of the International Search Report (PCT/ISA/210).
8. ☐ Amendments to the claims of the International Application under PCT Article 19 (35 U.S.C. 371 (c)(3))
   a. ☐ are transmitted herewith (required only if not transmitted by the International Bureau).
   b. ☐ have been transmitted by the International Bureau.
   c. ☐ have not been made; however, the time limit for making such amendments has NOT expired.
   d. ☐ have not been made and will not be made.
9. ☐ A translation of the amendments to the claims under PCT Article 19 (35 U.S.C. 371(c)(3)).
10. ☐ An oath or declaration of the inventor(s) (35 U.S.C. 371 (c)(4)).
11. ☒ A copy of the International Preliminary Examination Report (PCT/IPEA/409).
12. ☐ A translation of the annexes to the International Preliminary Examination Report under PCT Article 36 (35 U.S.C. 371 (c)(5)).

Items 13 to 18 below concern document(s) or information included:

13. ☐ An Information Disclosure Statement under 37 CFR 1.97 and 1.98.
14. ☐ An assignment document for recording. A separate cover sheet in compliance with 37 CFR 3.28 and 3.31 is included.
15. ☐ A **FIRST** preliminary amendment.
    A **SECOND** or **SUBSEQUENT** preliminary amendment.
16. ☐ A substitute specification.
17. ☐ A change of power of attorney and/or address letter.
18. ☒ Certificate of Mailing by Express Mail
19. ☐ Other items or information:

U.S. APPLICATION NO. (IF KNOWN, SEE 37 CFR 09/762,077)	INTERNATIONAL APPLICATION NO. PCT/US99/17338	ATTORNEY'S DOCKET NUMBER 56326-032 (IOPL-007)

20. The following fees are submitted:.		CALCULATIONS PTO USE ONLY	
BASIC NATIONAL FEE (37 CFR 1.492 (a) (1) - (5)) :			
☐ Search Report has been prepared by the EPO or JPO	**$840.00**		
☐ International preliminary examination fee paid to USPTO (37 CFR 1.482)	**$670.00**		
☐ No international preliminary examination fee paid to USPTO (37 CFR 1.482) but international search fee paid to USPTO (37 CFR 1.445(a)(2))	**$760.00**		
☐ Neither international preliminary examination fee (37 CFR 1.482) nor international search fee (37 CFR 1.445(a)(2) paid to USPTO	**$970.00**		
☒ International preliminary examination fee paid to USPTO (37 CFR 1.482) and all claims satisfied provisions of PCT Article 33(2)-(4)	**$96.00**		
ENTER APPROPRIATE BASIC FEE AMOUNT =		**$96.00**	
Surcharge of **$130.00** for furnishing the oath or declaration later than ☐ 20 ☒ 30 months from the earliest claimed priority date (37 CFR 1.492 (e)).		**$130.00**	

CLAIMS	NUMBER FILED	NUMBER EXTRA	RATE		
Total claims	29 - 20 =	9	x $18.00	**$162.00**	
Independent claims	4 - 3 =	1	x $78.00	**$78.00**	
Multiple Dependent Claims **(check if applicable).**			☐	**$0.00**	
TOTAL OF ABOVE CALCULATIONS =				**$466.00**	
Reduction of 1/2 for filing by small entity, if applicable. Verified Small Entity Statement must also be filed (Note 37 CFR 1.9, 1.27, 1.28) **(check if applicable).**			☒	**$233.00**	
SUBTOTAL =				**$233.00**	
Processing fee of **$130.00** for furnishing the English translation later than ☐ 20 ☐ 30 months from the earliest claimed priority date (37 CFR 1.492 (f)).			+	**$0.00**	
TOTAL NATIONAL FEE =				**$233.00**	
Fee for recording the enclosed assignment (37 CFR 1.21(h)). The assignment must be accompanied by an appropriate cover sheet (37 CFR 3.28, 3.31) **(check if applicable).**			☐	**$0.00**	
TOTAL FEES ENCLOSED =				**$233.00**	
				Amount to be: refunded	$
				charged	$

☒ A check in the amount of **$233.00** to cover the above fees is enclosed.

☐ Please charge my Deposit Account No. in the amount of to cover the above fees.
A duplicate copy of this sheet is enclosed.

☒ The Commissioner is hereby authorized to charge any fees which may be required, or credit any overpayment to Deposit Account No. **50-1133** A duplicate copy of this sheet is enclosed.

NOTE: Where an appropriate time limit under 37 CFR 1.494 or 1.495 has not been met, a petition to revive (37 CFR 1.137(a) or (b)) must be filed and granted to restore the application to pending status.

SEND ALL CORRESPONDENCE TO:

Mark G. Lappin, P.C.
McDermott Will & Emery
28 State Street
Boston, MA 02109-1775
Tel: 617/535-4043
Fax: 617/535-3800

SIGNATURE

Mark G. Lappin, P.C.
NAME

26,618
REGISTRATION NUMBER

January 30, 2001
DATE

INFRARED RADIATION SOURCES, SENSORS AND SOURCE COMBINATIONS, AND METHODS OF MANUFACTURE

RELATED APPLICATIONS

This application is a continuation-in-part of commonly owned and copending U.S. Patent Application Serial No. 08/905,599, filed on August 4, 1997, now U.S. Patent No. 5,838,016, granted November 17, 1998, and U.S. Provisional Patent Application Serial No. 60/094,602, filed on July 30, 1998, and PCT Application No. PCT/US98/25771, filed December 4, 1998, International Publication No. WO99/28729, which are all hereby expressly incorporated by reference. Related PCT Application No. US99/07781, filed April 9, 1999, is an appendix to this application.

FIELD OF THE INVENTION

This invention relates to optical radiation sources and relates in particular to blackbody radiation sources whose wavelength-dependent surface emissivity is modified in order to radiate with higher power efficiency and/or to radiate within a desired wavelength controlled spectral band. The invention also relates to sensors incorporating sources and to systems and methods embodying same.

BACKGROUND OF THE INVENTION

Non-dispersive Infrared (NDIR) techniques utilizing the characteristic absorption bands of gases in the infrared have long been considered as one of the best methods for gas measurement. These techniques take advantage of the fact that various gases exhibit substantial absorption at specific wavelengths in the infrared radiation spectrum. The term "non-dispersive" refers to the type of apparatus incorporating the NDIR technique, typically including a narrow band pass interference filter (as opposed to a "dispersive" element such as a prism or a diffraction grating to isolate and pass radiation in a particular wavelength band from a spectrally broad band infrared source. The gas concentration is discerned from the detected intensity modulation of source radiation emanating from the source and passed by the filter coincident in wavelength with a strong absorption band of the gas to be measured.

A prior art NDIR gas analyzer typically includes an infrared source with a motor-driven mechanical chopper to modulate the source so that synchronous detection is used to discriminate spurious infrared radiation from surroundings; a pump to push gas through a sample chamber; a narrow band-pass interference filter; a sensitive infrared detector, inexpensive infrared optics and windows to focus the infrared energy from the source onto the detector. Despite the fact that the NDIR gas measurement technique is one of the best methodologies that had ever been devised, it has not enjoyed wide application because of its complexity and high cost of implementation.

Several components play essential roles in making the NDIR technique work for gas measurement. The radiation source is one such component; and in order for NDIR methodology to work efficaciously, this source must provide broad spectral output and give high power in the band of interest. A blackbody radiation source is generally used for this component because it can be heated to a temperature that provides high intensity radiation within any wavelength region. Because the blackbody output spectral distribution and intensity are uniquely determined by the temperature of the source, the spectral peak intensity can be adjusted by varying the temperature of the blackbody source. By the well-known Wien's Displacement Law the peak intensity of a blackbody radiation source of temperature T is at a wavelength λ_{max} equivalent to $2.898 \times 10^{-3}/T$ where T is measured in degrees Kelvin (1°K) and λ_{max} is measured in meters. By the process of T and the size of the blackbody radiator, a desired intensity of blackbody radiation selected wavelength λ can be attained.

The so-called "Nernst Glower," consisting of a heating element of a tungsten filament) embedded in a ceramic slab, has long been used for the blackbody source of most prior art NDIR gas detection systems. Despite the fact that the Nernst Glower gives off an amount of infrared energy with an emissivity close to unity, its power efficiency (i.e., efficiency from electrical to useable optical energy) is notoriously low. The large amount of unwanted heat is also a major drawback in the use of the Nernst Glower in any NDIR gas measurement systems. Furthermore, the large heat capacity of the Nernst Glower makes it a necessarily slow device in terms of intensity modulation. In many cases, it can only be used as a steady state or DC radiation source; and thus a mechanical

chopper is needed to generate synchronous modulated signals, further adding to the complexity of NDIR gas measurement systems.

The prior art has attempted to replace the blackbody radiator with hot filament as an approximation to a blackbody. However, such a filament does not have high emission over all wavelengths because there is spatial temperature variation within the filament; it is not an ideal blackbody source. Optical radiation sources, such as a hot filament lamp, are thus often referred to as "quasi-blackbody" sources. In addition, hot filament radiators typically are used by a quartz bulb which is substantially opaque for wavelengths, longer than about 4.5μm reducing its applicability to gas detection through longer wavelength absorption lines. Prior art hot filaments are thus not particularly good infrared radiation sources for use with NDIR gas sensors.

The prior art has attempted to improve NDIR sensors. In U.S. Patent No. 4,876,413 (the '414 patent), published in April of 1975, Bridgham describes an infrared radiation source that includes a thin film resistor heater with highly emissive material Cr_3Si on a substrate. The thin film heater is positioned between a pair of thin metal elements serving as sensing electrodes on a very thin (<0.005" typical) insulating substrate. The entire thin film heater is packaged in a standard TO-5 heater equipped with a focusing reflector and pins supporting the heater structure.

While the source of the '413 patent advances infrared radiator sources in terms of higher emissivity and wider spectral emissions, it does not offer size or speed advance over the classic tungsten lamp. Furthermore, its construction is rather fragile and the heater cannot withstand temperatures above ~700°C, severely limiting the maximum allowable output. Finally, its overall power efficiency is rather poor and the low cost and useable life of this radiator has not been satisfactorily proven. Consequently, the source of the '413 patent has not found wide application in NDIR gas measurement systems.

In U.S. Patent No. 4,644,141 published in February of 1987, Hager et al. advances a heater structure first proposed in the '413 patent, except that a combination of silicon, silicon oxides and a platinum metal pattern are used as the heating element to optimize the performance of the overall heater structure. Nevertheless, other than a slight improvement in power efficiency over the device of '413 patent, there is no fundamental advancement over the prior art.

Over the past several years, significant technical progress has been made in the area of optical sources as set forth in the inventor's own prior application of U.S. Serial No. 08/511,070, filed on August 3, 1995. Such optical sources have greatly increased the reliability and cost-effectiveness of NDIR gas sensors.

The present invention has several objects in providing further improvements and advantages in source and sensor embodiments as compared to the prior art. One object of the invention is to provide sources which function as tuned waveband emitters that preferentially emit radiation into a wavelength band of interest as compared to blackbody or gray-body radiators. Another object of the invention provides in integrated circuit sensor include selectively tuned radiation source. Still another object of the invention provides methods and devices for sensing gas constituents without certain of the difficulties and problems of prior art NDIR devices.

These and other objects will become apparent in the description which follows.

SUMMARY OF THE INVENTION

As used herein, "on chip" refers to integrated circuits and the like which are processed through microelectronic fabrication techniques to provide circuitry and/or processes (including A/D processing) on a semiconductor element or chip.

As used herein, "SOURCE" generally means tuned waveband emitters constructed according to the invention that preferentially emit radiation into a wavelength band of interest. Certain SOURCES, for example, include those tuned radiation sources described in the commonly assigned and copending U.S.S.N. 08/905,599, filed on August 4, 1997, now U.S. Patent No. 5,838,016, granted November 17, 1998, and U.S.S.N. 08/511,070, filed on August 3, 1995, now abandoned (the latter also being incorporated herein by reference). Still other SOURCES including tuned cavity emitters, chemical and microelectronic/semiconductor emitters, and other etched electro-mechanical, chemically-treated, ion-bombarded and lithographically created surfaces which permit spectral control and which provide narrow band incoherent emissions tailored to specific end-user needs and requirements.

The invention has many objectives in providing improved sources and sensors. It also utilizes and is complimentary to certain art encompassing other areas including

NDIR gas measurement technology, silicon micro-machined thermopile, optical beam configurations and fabrication techniques. As such, the following patents and publications providing information and background to the specification and are herein incorporated by reference. U.S. Patent No. 4,620,104; U.S. Patent no. 4,644,141; U.S. Patent No. 4,859,858; U.S. Patent No. 4,926,992; U.S. Patent No. 5,060,508; U.S. Patent No. 5,074,490; U.S. Patent No. 5,128,514; U.S. Patent No. 5,152,870; U.S. patent No. 5,220,173; U.S. Patent no. 5,324,951; U.S. Patent No. 5,444,249,249; Hutley et al., The Total Absorption Of Light By A Diffractive Grating, Optics Communications, 19(3), pp. 431-436 (1976); Loewen et al., Dielectric Coated Gratings: A Curious Property, Applied Optics, Vol. 16(11), pp. 3009-3011 (1977); Rajic et al., Design, Fabrication, And Testing Of Micro-Optical Sensors Containing Multiple Aspheres, SPIE, Vol. 2356, pp. 452-462 (1995); Gupta et al., Infrared Filters Using Metallica Photonic Band Gap Structures On Flexible Substrates, Appl Phys. Lett., 71(17), pp. 2412-2444 (1997); and Rehse et al., Nanolithography With Metastable Iron Atoms: Enhanced Rate Of Contamination Resist Formation For Nanostructure Fabrication, Appl. Phys. Lett., 71(10), pp. 1427-1429 (1997).

In one aspect, the invention provides an integrated circuit sensor (ICS). The ICS has a tuned narrow band emitter (e.g., a SOURCE of the invention) and a tuned narrow band detector fabricated on a single silicon die, Optics (e.g., reflective optics or a silicon slab waveguide) capture source emissions and refocus the captured energy onto the detector. Control electronics are preferably included and are preferably incorporated "on chip" to facilitate packaging issues. A solar cell can also be integrated with the sensor to provide power. The sensor can further be integrated with other features described herein or contained in related applications.

In another aspect, the invention provides a Hybrid Infrared Gas and Thermal Sensor Head ("HIRGS"). A SOURCE is integrated with an uncooled detector (e.g., a microbolometer detector), and a reflector (e.g., a parabolic reflector) into a package such as a single transistor can. Source drive electronics and detector readout electronics and preferably included with the HIRGS and can also be provided "on chip". The detector is also preferably "tuned" to the waveband emissions of the SOURCE.

In still another aspect, the invention provides an Integrated Gas Sensor ("IGS"). A SOURCE is coupled to illumination optics which pass a beam (of tuned magnetic radiation) into a gas sample or stream. A detector (preferably with receiving optics) is arranged to capture the beam and convert the beam into electrical signals. An electronics system is used to diagnose the beam intensity and spectral characteristics to analyze the gas, e.g., to determine the % concentration of a particular gas.

In another aspect, an alternative IGS includes a SOURCE which incorporates a gas cell sample (or gas flow cell). Wavelength compatible optics preferably collect SOURCE emissions to efficiently illuminate the cell. A mirror (e.g., a flat mirror) positioned on the opposite side of the cell reflects the SOURCE emissions back through the cell and to a detector (also preferably with optics to improve collection efficiency). The detector is positioned to collect the reflected beam adjacent to the SOURCE. An electronics subsystem is used to diagnose the beam intensity and spectral intensities to determine characteristics of the gas, e.g., concentration of a particular gas.

In one aspect, methodology is provided for manufacturing a microbolometer-based SOURCE and integrated sensor. The sensor includes one microbolometer arranged to emit tuned radiation, optics to collect and transmit the radiation to a sample under study for a specific purpose (e.g., to illuminate a gas cell or a solid surface), and another microbolometer arranged to collect at least part of the post sample (i.e., transmitted through the gas or scattered from the surface) radiation. As known in the art, microbolometers function by efficiently collecting infrared radiation within an absorbing microbridge cavity; and the absorbed energy changes the resistance of the bridge electronics, indicating an amount of radiation. The efficient thermal mass of the bridge permits very fast dissipation of radiant energy so that multiple microbolometer can efficiently take high speed IR picture frames (i.e, each microbolometer operating as a pixel in a picture in accord with the invention, the source microbolometer operates in reverse: electric energy drives the microbolometer to radiate heat and to emit radiation in the band of the cavity. The sister microbolometer detector is tuned to the same band and the two microbolometer effectively emit and recover tuned electromagnetic radiation.

In another aspect, a tuned cavity band emitter SOURCE is provided. The SOURCE of this aspect has an emissivity curve which differs - selectively and

beneficially-from a standard blackbody curve. It thus functions as a selective incoherent band emitting infrared source. This SOURCE can thus include a metal foil filament such as provided in U.S. Patent Application Serial No. 08/905,599; and can further include a metal transistor can be coupled to the SOURCE. The SOURCE of this aspect can also be constructed with spectral control, including supporting electronics, to function as an incoherent narrow band emitter. Preferably, the surface of the emitting SOURCE of this aspect is dark. It also includes a sharp spectral transition between a high absorbing band and a highly reflecting out of band, thereby functioning as a "band emitter".

By way of background, prior art incoherent sources radiate in a manner representative of a blackbody curve. However, most applications and products utilize only a small band within the spectrum relative to that blackbody curve (by way of example, most devices are used to generate energy within a defined band; and other radiation can result in noise). These prior art sources thus inefficiently emit energy into the band. Accordingly, when the prior art source is brought to temperature, the blackbody emissions at the center of the measurement band represent only a tiny fraction of the total radiant output falls within the desired measurement band. The invention solves this dilemma.

In accord with the invention, the SOURCE emitter surface of one aspect is modified to become an effective band emitter. By suppressing out-of-band emission sensors and systems utilizing the SOURCE trade out-of-band photons (noise) for in-band photon (signal). In essence, the SOURCE becomes a near-perfect reflecting surface for out-of-band radiation and a highly efficient absorber for in-band radiation corresponding to an array of absorbers. The size, shape, and spacing of these cavities are designed to absorb at a pre-selected resonance wavelength. The size of these cavities should be about $\lambda/2\pi$ for the desired wavelength of medium and longwave infrared radiation (e.g., 3-5μm and/or 8-12μm), the cavity sizes are within the limits of state of the art microlithography and microfabrication techniques. Thus, this aspect of the invention includes a SOURCE with manually applied cavities disposed thereover with microlithography.

In another aspect, the invention provides mid-and long-wavelength infrared sensors for gas detector applications utilizing a non-blackbody, narrow-band radiator. The SOURCE of this aspect includes sub-micron scale surface structures which facilitate

control of the radiator emission spectrum. The source thus combines blackbody radiator functionality with a surface that selectively filters wavelength emissions.

In another aspect, an optical radiation SOURCE is provided which optimizes the following three parameters for improved waveband emissions: operating temperature T(°K), emitting area A, and surface emissivity ϵ (λ). The SOURCE utilizes structure which emphasizes the emitting surface characteristics (e.g., cavity structure) of the radiator and which optimizes its emitting area and its emissivity to maximize power output in the optimized waveband.

Another aspect of the invention provides an optical radiation SOURCE with an output that is "spectrally tailored" relative to the emission a perfect blackbody by modifying surface emissivity so as to maximize power output in a desired and controlled spectral wavelength.

In another aspect, the optical radiation SOURCE of the invention has a thin structure with a well-defined outwardly facing surface that emits optical radiation. The thin structure includes a resistive element in the form of a thin film or foil supported by a substrate and configured with surface structure as discussed above. The optical radiator SOURCE is powered by electrical current passed through its resistive element. The texture of the outwardly facing filament is methodically and controllably modified by well-known techniques - such as electrolytic plasma etching, ion-milling, and preferably in combination with photo-lithographic masking technology - such that the emissivity of the radiator SOURCE possesses an emissivity near to unity with well-defined and controllable spectral wavelength band.

The invention is next described further in connection with preferred embodiments, and it will become apparent that various additions, subtractions, and modifications may be made by those skilled in the art without departing from the scope of the invention.

BRIEF DESCRIPTION OF THE DRAWINGS

The foregoing and other objects of this invention, the various features thereof, as well as the invention itself, may be more fully understood from the following description, when read together with the accompanying drawings in which:

PAGE INTENTIONALLY LEFT BLANK

PAGE INTENTIONALLY LEFT BLANK

DESCRIPTION OF PREFERRED EMBODIMENTS:

I. Reflector Source with Reflector housing in front of planar emitter which is normal to the emission axis, in conjunction with textured source

One form of the invention is a relatively low power reflector infrared (IR) source with an improved texture, smaller (compared to the prior art) filament, and with an integral reflector.

A common design issue for IR sources is the requirement for significantly more useful signal, particularly in the LWIR, with significantly less required drive power. The present invention effects such changes by including reduced filament size, improved filament texture, and by incorporating a reflector into the source package. This allows, for example, for medical instruments (including anesthesia monitors or critical care systems), industrial safety instruments, and automotive emission monitoring.

FIG. 1A shows an IR source 10 of the invention having relatively high usable signal with relatively low drive power. A relatively small filament 110 is used with a molded reflector 12 to provide a "search light" type beam-former, illuminating a narrow forward cone (as shown in Fig. 1B) and eliminating the need for discrete optical (lens) elements. The smaller filament of the invention also uses less power compared to the prior art ("standard") as shown in FIG. 1C.

This source 10 reduces the required parts count and integration complexity for instrument environments, by integrating relatively high functionality into a single component by reducing or eliminating the need for separate optical elements and providing an output illumination cone which is compatible with standard thin film interference filters.

FIG. 1D shows an IR source 10' which is similar to source 10 but includes an "M"-shaped filament 11', and a formed-sheet reflector 12'.

This form of IR source does not require extensive tooling or automation. Preferably, the source utilizes a laser cut filament cut from thin self-supporting metal foils which are treated in large (e.g., 10 cm square) sheets. Again, preferably, the filament size is relatively small (for example, 250 parts per 10 cm square).

II. **Radiation Source with Parabolic or compound parabolic "Winston" collimator, in conjunction with textured source**

FIG. 2 shows another exemplary form of IR source of the invention, particularly including straight parabolic, or compound parabolic collimators configured in combination with a textured source. The embodiment of FIG. 2 shows a single loop, single bar filament with a "behind the source" concentrators. FIG. 3A shows a "two-sided" emitter with a "behind the source" concentrator. FIGS. 3B-3D show exemplary filament emitters.

FIG. 4 shows a "flat pack" construction source which allows a variety of reflector configurations. By utilizing double sided emission, the filament effectively doubles its active area and provides twice the usable in-band signal flux at a given temperature.

Other filament configurations provide additional "shine-through" illumination for rear-mounted reflectors, for example, as shown in FIGS. 5 and 6. In FIG. 6, the filament is "sideways", i.e., the reflector axis is in the plane of the filament.

III. Tuned band emitter sources

A. Tuned band emitter "photonic band gap" filament

The incorporated PCT Application No. PCT/US98/25771 discloses IR sources with metal foil filaments, and particularly shows an embodiment in a Tx metal transistor can. That form of source effects spectral control, and teaches use of spectral control to construct an incoherent narrow band emitter. In the prior art, the emitting surface has been modified to make it dark, but significant spectral control has not been accomplished. In accordance with the present invention, there are sharp spectral transitions between highly absorbing, in band, and highly reflecting, out of band, thereby effecting a band emitter. Traditional incoherent sources are constrained by the blackbody curve. The blackbody curve assures that, even if the source temperature is brought to peak with the blackbody distribution at the center of the measurement band, only a small fraction of the total radiant output falls within the desired measurement band.

In accordance with the present invention, the emitter surface (and the consequent surface spectrum) is shaped and textured so that the blackbody curve helps to define a band emitter. By suppressing out-of-band emission, this allows an instrument designer to

trade out-of-band photons (noise) for in-band photons (signal.) This is effected with a highly reflecting surface having an array of absorbing cavities thereon. The size, shape, and spacing of these cavities are established to absorb at a pre-selected resonance wavelength. As determined from incoherent scattering theory, the size of these cavities is preferably about l/2p for the desired wavelength. For wavelengths in the MWIR and/or LWIR gas bands, these sizes are well within the limits of current microlithography and microfabrication techniques.

The blackbody curve naturally rolls off more steeply on the short wavelength side, so it naturally defines the short wavelength band edge, even if the surface emissivity does not exhibit a sharp short wavelength cut-off.

Spectral control

The small surface texture features which make the infrared source of the invention work are preferably made by a random seed texturing process. These features make the surface a selective emitter with full blackbody-like emissivity at short wavelengths but little or no emissivity at longer wavelengths.

Spectral selection is determined using random textured infrared emitters for gas detector applications. A non-blackbody, narrow-band radiator replaces the function of a traditional interference filter and dramatically improves the efficiency of the surface as an in-band emitter. By building a surface which is dark (high emissivity) in-band, and shiny (low emissivity) outside that band, the ratio of usable bandpass flux-to-total flux maximized, and therefore maximizing instrument sensitivity. Sub-micron scale surface structures control the radiator emission spectrum. In effect, the function of the blackbody radiator surface is combined with the function of the bolometer element, and together with some of the function of a thin film interference filter into a single component.

To achieve device miniaturization, it is important to achieve tight spectral control of the infrared emission. This enables maximum infrared absorption signal with minimum parasitic heating of the neighboring detector element.

The infrared emitters for gas detection are preferably made using random seed texturing of the radiator surfaces. FIG. 7 shows spectral irradiance (relative units) as a function of wavelength for a textured metal foil filament of the invention, as compared with a conventional 575CBB filament. The exemplary metal foil radiator displays

spectral narrowing dl/l ~ 0.5 (FWHM), by random texture. A mixture of small and large surface feature sizes accounts for the spectral width. Lithographic techniques are used to produce well controlled surface features for narrow emission waveband

For an ideal blackbody under these conditions, only a few percent of the total flux is in-band. But the textured metal radiator surfaces suppress long wavelength radiation and therefore improves this ratio. The conversion efficiency of a radiator surface (where neither the surface preparation or the operating temperature were optimized for this purpose) is around 4%. Further improvements can be effected by tuning the spectral emission band specifically for this purpose and carefully maintaining the appropriate operating temperature during the measurement. Preferably, a tuned cavity band emitter with spectral resolution (dl/l) around 0.1, is achieved which is comparable to that achieved with micromesh reflective filters. This level of surface topology (and therefore spectral) control, is achieved using lithographic surface modification techniques.

An exemplary emission device is based on the mask pattern shown in FIGS. 7A(a) and 7A(b). The patterns in the center of the mask labeled 8,10 and 12B or N are crosses, either broad (B) or narrow (N) as shown in the detail. Numbering corresponds to the wavelength (i.e., 8, 10, or 12 microns) of the peak absorption. Other patterns can be annular rings and tripoles. The patterns are etched into polished silicon wafers, 1-3, μm deep. A thin layer of aluminum may be evaporated onto the surface of a wafer to change the background emissivity from that of silicon ($\epsilon \approx 0.7$) to that of aluminum ($\epsilon \approx 0.1$).

The reflection spectra from the exemplary patterned silicon wafer (without an aluminum coating) are shown in FIG. 8A(c). The absorption peaks are consistently shorter than the target wavelengths (by about 20%) and depend on the feature size as well as the unit cell size (feature spacing).

In FIG 7A(c) the spectra are shown as a ratio with the reflectance of an untreated silicon area on the same wafer. Two areas (12N and 12B, respectively) of the wafer show spectral absorption features related to the size and spacing of patterns on the wafer surface.

With controllable band emission devices of the invention, thermal emission from photonic bandgap surface structures show distinct peaks with a wavelength proportionally to the geometry of the structure. This permits sensor-on-a-chip configurations, for example,

where thermal radiation from a "designed" textured surface can be concentrated into a narrow band with low values of $\Delta\lambda/\lambda$. The sensitivity of the detector approaches theoretical limits.

FIG. 7B shows emission spectra from aluminized patterned silicon surface heated to 500°C showing distinct peaks with wavelength varying as geometrical scale factor. In that figure, all sites on the wafer were heated to the same temperature. The surface structure causes sharp emission peaks which appear over a spectral range of nearly an octave. The emission peaks on the aluminum coated wafer have shifted to shorter wavelengths. Various embodiments may use coated wafers, uncoated wafers, and wafers with different doping.

FIG. 7B shows a curve fit to the date from FIG 7B for a cross design as shown in FIG. 7B. The upper (black) curve illustrates the emission spectrum from an ideal blackbody at 773 K. The lower curve is the semi-empirical thermal model used for estimating instrument signal to noise. It consists of a graybody (with emissivity of 0.48) at a temperature of 773 K, plus excess emission at a peak wavelength of 6.89 microns and an emission width of $\Delta\lambda/\lambda \leq 0.16$. The upper curve in FIG. 7B shows a measured emission data, demonstrating a short wavelength cutoff. Random ion-beam produced texture provides devices with long wavelength cutoff.

In FIG. 7C, the background blackbody emission from the silicon wafer has a relatively high emissivity of at least 0.48 whereas the emissivity of a good aluminum film is below 0.1. Patterns with a larger fraction of open area (and hence cleaner coatings) show sharper emission peaks.

The reflectance and remittance peaks from FIGS. 7B and 7C exhibit a systematic short wavelength-side deviation from their target wavelengths, but demonstrate that PBG peak position and halfwidth are related to size and spacing of the periodic features. FIGS. 7D(a) and 7D(b) show emission wavelength versus etched cavity size (measured as width of cross' leg) and versus cavity-to-cavity spacing. For a 4.65 μm emitter, the cross' leg is about 1.45 μm wide with center-to-center spacing of about 4μm.

IC compatible fabrication

Substantially regular patterns on thin foils are formed by plating or depositing metal films. In one form, a silicon substrate is used as a mechanical support for the foil during subsequent processing.

Subtractive processes based on deliberate, lithographic seed island formation are used with ion beam surface texturing processes. Lithographic masking and exposure schemes are used to achieve the required patterning. Typical lead solder glass materials, used for fabrication of thick film circuits, have a low sputter removal rate, and they are screen printed and chemically removed after processing. Diamond-like carbon films, deposited by chemical vapor deposition, have extremely low removal rates but are not easily patterned. Typical layer thicknesses of the solder glass are a few thousandths of an inch (50-100 mm) and this is comparable to the resolution achievable with screen printing equipment. Conventional microlithography for electronics can produce lines and spaces at least an order of magnitude smaller (two orders of magnitude for state-of-the-art VLSI processes) although the ability to faithfully transfer a pattern to the metal foil is somewhat limited by the thickness of the mask layer. Since the typical size of the pillars which comprise the surface texture is around a micron, micron scale antenna replication is used.

The following method places a regular array of micron-scale structures of a refractory metal oxide on the surface of high TCR self-supporting metal foils. The resultant structure has a surface which is a selective infrared absorber in itself or alternatively, is an improved starting material for texturing using ion milling techniques. The steps listed are conventional photolithographic procedures.

Thin metal foils are deposited on silicon wafers for process compatibility and ease of downstream handling. Alternatively, self-supporting silicon microbridges are used as the individual emitter elements.

After appropriate cleaning of support disc and foil, the drilled/milled area of the disc is coated with a film of positive photoresist, for example, applied with a clean brush, and the foil is placed over the holes and pressed or rolled into good contact with the disc. Effectively, the holes in the disc are covered, the disc is then held down on a vacuum chuck for the next step.

Positive photoresist is next applied to the entire disc, using a conventional spinner followed by a conventional soft-bake step. The ramp rate up to baking temperature is maintained to be relatively low to allow solvent in the resist layer which bonds the foil to the disc to be released slowly and thus avoid lifting the foil from the disc. A resist formulation designed for use with reflective substrates is useful for this step.

Masking, exposure, and development of the top layer of photoresist is performed in a conventional manner. Clear areas in the mask are positive images of the features to appear on the foil. The hard-bake phase drives off solvents to make the resist film vacuum-worthy.

In cases where a plasma cleaning step is not possible in the equipment used for film deposition, the assembly is then given a short exposure to an oxygen plasma in apparatus for ashing photoresist. The objective is insuring adhesion of the deposited film. Deposition of a refractory oxide film is next done by laser deposition, which allows maintenance of low substrate temperatures. The refractory film covers the entire disc/foil assembly, contacting and, preferably adhering to the foil through the openings in the photoresist.

In the next step, the coated disc/foil assembly is soaked in acetone (or photoresist stripper), in some cases with gentle ultrasonic vibration, to complete the lift-off of photoresist and overlying refractory film and free the foil from the supporting disc. After separation from the support disc, the foil is then cleaned and used "as is", or mounted in an ion mill for texturing as a self-seeded material.

The most desirable packaging alternative is to leave the metal foil intact on the silicon wafer. However, in some forms of the invention, the radiator elements are heated electrically for ready measurement of input power and conversion efficiency. In order to achieve this, the radiator elements are thermally and electrically isolated from their surroundings. A "window-frame" pattern of cut-outs in the silicon substrate is used so that the actual radiator elements are suspended on the remaining silicon, as shown in FIGS. 8A and 8B(a)-8B(c).

FIGS. 8A (ten steps, 1-10) and 8B(a)-8B(c) show the basic window-frame construction technique for forming individual radiator elements on a silicon die. Elements are left on the silicon wafer as a support during microtexturing and then silicon via's are etched from underneath to produce suspended radiator elements.

Integrated source and drive/stabilization electronics

Wavelength selective bolometer surface

Computer modeling is used to determine the optimum surface shape for desired emission characteristics, based in part on transmission through conductive screen and

dielectric-mounted mask arrays. In such models, an incoming electromagnetic wave is considered to produce surface excitations (plasmons) in the metallic screen or grid, and this in turn produces the transmitted wave. The plasmons are considered to be excited directly in order to produce a wave emitted from a surface which has the desired frequency band filter behavior.

FIGS. 9A and 9B show the conversion efficiency gains using lithographic feature design and fabrication. Such IR sources illustrate a spectral narrowing of 0.5, which gives them almost a factor of four efficiency advantage over an ideal blackbody. By bringing emission width to 0.1 (FIG. 9A), the width achieved to date for filter transmission width, another factor of 4-5x in conversion efficiency is obtained (FIG. 9B).

The size and shape of the repetitive surface feature control the details of the emission spectrum: the peak frequency in the transmission band; the width of the transmission band; the location of the minima which define the band; the steepness of the intensity falloff.

A two-dimensional array with 90° rotation symmetry serves to minimize polarization dependence of the effect, and variation of the details of the repetitive feature (replace a square unit mask by a plus-sign shape, e.g.) enhances desired spectral characteristics. The resonant frequency of the transmitted wave scales linearly with the length of the unit cell in the grid, as expected by analogy with grating studies. Other details depend sensitively upon feature shape (as mentioned previously), the width of lines which create the feature, and feature-to-feature variations. Other features of a textured surface - height of surface features, wall profile shape have an effect, as well.

Existing theoretical studies on transmission properties use models and analogs for prediction. Scalar diffraction theory has been used, as well as a transmission line analog: both with reasonable success. The drawback of such models is that their applicability to a particular situation can only be certified by experimental tests. *A priori* determination of a region of applicability of particular models is not assured.

In accordance with the invention, transmission line analogs comprise the models for prediction of emission from grids and periodic masks. In these models, each element (unit cell) of the grid is modeled as a simple circuit consisting of a resistance, capacitance and inductance whose values are adjusted so that circuit current matches output field strength of the unit cell. A grid then consists of a large number of identical circuits coupled together

with capacitors (for capacitive grids, consisting of conducting elements out of contact with one another) or inductors (for inductive grids, consisting of continuous conductors as in a wire mesh.) The collection of connected circuits implies an output current which are solved by techniques common in transmission line analysis. Analyses such as these are used in calculating transmission properties of grids and masks.

A first principle approach, using Maxwell's equations, is used to establish the validity of this model, and to determine the appropriate R, C, and L values for a given unit element size and shape. The coupling values are similarly found. Once the model has been shown valid for the frequency range of interest, the model is used to simplify analysis of the complete grid. When variation in the unit cell parameters is to be investigated, the analysis becomes more complicated, and the results are cast into a matrix inversion problem where standard computer techniques are employed.

Maxwell's Equations are used as a basis to predict the surface emission, and polarization independence, and then to calculate the emission spectrum of the unit surface cell. Assuming 90 degree rotation symmetry and an infinite grid size, this result is expanded to represent emission from a large surface. Then, small square grids (10x10 features, for example) with random feature-to-feature variation are modeled to determine a representation of the effects of fabrication artifacts and variations.

Integrated circuit sensor

Pitch/catch source and detector on the same die

The invention further includes a turbulence-based infrared hydrocarbon leak detector which is radically simpler than conventional infrared absorption instruments. Two aspects make this possible. First, a simple structured IR instrument is configured by building a tuned infrared source and conventional infrared detector into a single package. Second, digital signal processing techniques are used to overcome the DC and low frequency drift which characterizes most nondispersive infrared measurements. The sensor does not provide an absolute concentration measurement for hydrocarbons but it is particularly sensitive to the high frequency "noise" caused by the turbulence accompanying changes in local gas concentration. This provides a robust leak detection capability for gases which are not normally present in the sampling environment. Combined with a simple reflector plate to

define the gas sampling region, this sensor provides a rugged, reliable, field- and flight-worthy hydrocarbon leak detection capability.

FIG. 10 shows a novel, low-cost infrared hydrocarbon leak sensor using an integrated source and detector in an open path atmospheric gas measurement. As a leak detector, the sensor discards low frequency "signal" in favor of the high frequency "noise" associated with changes in local gas concentration. In one form, the entire sensor engine mounts on a TO-8 transistor header.

Hot bolometer sensor (with and without separate filter)

An aspect of the invention can be used to form an infrared gas monitoring component to build an integrated on-board exhaust NOx meter. Silicon micromachining technology is used to build a sensor which is radically simpler than conventional infrared absorption instruments. Infrared absorption instruments traditionally contain a source of infrared radiation, a means of spectral selection for the gas under study, an absorption cell with associated gas sample handling and/or conditioning, any necessary optics, a sensitive infrared detector, and associated signal processing electronics. The invention simplifies and reduces the cost of an IR instrument by integrating the function of the infrared source and infrared detector into a single self-supporting thin-film bolometer element. This element is packaged with inexpensive molded plastic optics and a conventional spectral filter to make a transistor-size "sensor engine." Combined with a simple reflector plate to define the gas sampling region, this sensor engine provides a complete gas sensor instrument which is extremely inexpensive and which will approach the sensitivity of conventional infrared absorption instruments.

FIG. 11A shows a novel, low-cost infrared gas sensor engine 100 using a heated bolometer element as both source and detector in an open path atmospheric gas measurement. The bolometer element reaches radiative equilibrium with its surroundings at a slightly lower temperature if gas absorption frustrates light re-imaging on the element. The compound parabolic concentrator defines a relatively narrow illumination cone and the passive reflector is designed to provide a pupil-image of the spectral filter onto itself. The entire sensor engine can be mounted on a TO-8 transistor header. FIG. 11B shows a detailed view of the sensor engine 100.

Achieving tight spectral control of the infrared emission is important in making the heated bolometer element work well. The device is particularly effective if the amount of radiation absorbed by gas molecules under study is made measurably large in terms of the overall thermal budget of the bolometer surface. Preferably, a tuned cavity band emitter is constructed with spectral resolution (dl/l) around 0.1, roughly the performance achieved to date with micromesh reflective filters. This raises the conversion efficiency to nearly 15% for the NOx problem. This level of surface topology (and therefore spectral) control, is achieved through micro-electro-mechanical systems (MEMS) technologies

The embodiments of the sensor engine shown in FIGS. 11A and 11B include a single bolometer which both emits and detects radiation. Those configurations permit construction of devices, such as gas detectors, which are compact and employ a minimum number of component parts. In some instances, however, it is useful to construct such devices with separate radiations sources and sensors. Exemplary devices using separate radiation sources and detectors are shown in FIGS. 11C-11I.

In FIG. 11C, radiation source 102 and radiation detector 104 are mounted on a silicon die 106, facing a reflector 108 disposed across a test region 110. The reflector 108 is positioned to effect an optical path between the source 102 and detector 104. The test region 110 is constructed so that an applied test gas flow passes between the source 102/detector 104 pair and the reflector 108, intercepting the optical path. The silicon die 106 includes integrated processing circuitry 112 coupled between the detector 104 and a data output port 116. An electrical control 118 is coupled to source 102 for driving source 102 to emit radiation, preferably infrared radiation with a spectral range including an absorption line of the gas to be detected.

FIG. 11D shows a configuration similar to that in FIG. 11C, but where the source 102 and detector 104 are housed in a closed chamber C, and the reflector (mirror) 108 is external to the chamber C, with the optical path between the source 102/detector 104 and reflector 108 passing through an optically transmissive window W. With this configuration, the gas under test is isolated from the source and detector and any other instrumentation.

FIG. 11E shows an embodiments similar to that in FIG. 11C, but where the source 102 and detector 104 are mounted within an enclosure E disposed on a single can

120. The enclosure E establishes a test gas flow path therethrough, which intercepts the optical path between source 102/detector 104 and the reflector 108.

FIG. 11F shows an embodiment wherein a source 102 is disposed opposite to a detector 104, wherein a collimating lens 122 establishes a collimated radiation beam through a test gas flow to a lens 124. Lense 124 focuses the resultant beam onto a detector 104.

FIG. 11G shows a source 102 which is activated by an optical beam B directed from a high energy laser L (by way of lens 132, reflector 134 and lens 136). The source 102 is back-illuminated, so that emitted radiation propagates from an emission surface toward a reflector 108A, which in turn directs that radiation across a test gas flow to a reflector 108B. Reflector 108B focuses the radiation incident thereon to a detector 104 which is coupled to a data output port 116.

FIG. 11H shows source 102 and detector 104 on opposite sides of a support, each facing a respective one of reflectors 108A and 108B. Source 102 is electrically driven to emit radiation which propagates to reflector 108A. Reflector 108A directs the radiation incident thereon across the test gas flow to reflector 108B. Reflector 108B focuses the radiation incident thereon to the detector 104.

FIG. 11I shows source 102 and detector 104 mounted on the same substrate S, and opposite to a reflector 108. A lens 142 directs radiation from source 102 to reflector 108. Reflector 108 directs radiation incident thereon to a lens 144, which in turn focuses that radiation onto detector 104. An optically transmissive test gas cell 148 (containing a gas to be identified) is disposed between the lenses 142 and 144 and the reflector 108. Detector 104 provides via data out port 116, a signal to a reference data comparator 150, which compares a received signal (from detector 104) to reference information, for example to permit identification of one or more components in the gas in test gas cell 148.

Wheatstone bridge drive circuit

An individual emitter die is packaged, together with individual infrared detector pixel elements and thin film interference filter windows in TO-8 transistor cans using standard process equipment.

Drive and readout schemes using a microprocessor controlled, temperature-stabilized driver are used to determine resistance from drive current and drive voltage readings. That information shows that incidental resistances (temperature coefficients in leads and packages and shunt resistors, for instance) do not overwhelm the small resistance changes used as a measurement parameter.

A straightforward analog control circuit, the Wheatstone bridge is used to perform that function. It is very simple, very accurate, quite insensitive to power supply variations and relatively insensitive to temperature. The circuit is "resistor" programmable but depends for stability on matching the ratio of resistors. In one form, an adjacent "blind" pixel – an identical bolometer element filtered at some different waveband – is used as the resistor in the other leg of the bridge, allowing compensation for instrument and component temperatures and providing only a difference signal related to infrared absorption in the gas.

An optics test bed is used to evaluate different configurations and perform measurements of the device under benchtop conditions. For elevated ambient (automotive) temperature operation, the device is operated as instrumented tube furnaces and to calibrate the infrared readings against a conventional gas analyzer.

The Wheatstone bridge provides a simple computer interface and since it is implemented with relatively robust analog parts is not susceptible to radiation damage at high altitudes or in space.

For the Wheatstone bridge shown in FIG. 12, bridge is balanced when R1/R2 = R3/R4, and to first order, temperature coefficients of R1 and R2 can be neglected if resistors are matched. The temperature coefficient of R3 is important but should have negligible effect across delta T caused by the gas absorption. Preferably, the bridge is carefully balanced for the designed operating temperature. The estimated errors from an analog readout of this circuit come from the amplifier input offset and input bias currents which introduce offset voltage or error term. FIG. 13 shows a test configuration.

Turbulence detection and signal processing

In connection with industrial gas sensors, we have found that source-detector-electronics combinations can readily be stabilized to provide signal to noise performance of 1000:1 or better under conditions of stable temperature and steady state gas flow. Typical conditions are pulse frequencies of 1-10 Hz, well matched to the speed of available thermal detectors. However, high frequency transients associated with changes in gas flow provide a significant disruption. Ordinarily, in fact, detector preamplifier circuits are severely filtered to suppress these high frequency transients.

Most detectors have poor low frequency characteristics and are subject to 1/f or low frequency noise and drift. This is also true for most DC amplifiers where precision components are required for good low frequency response. This noise is avoided by selectively filtering and amplifying only those high frequency components present in a turbulent gas stream. In order to separate these high frequency components, a narrow, band pass filter is used; these filters are preferably constructed using low cost integrated circuits.

Emitter elements (narrow spectral band, high cold resistance) are used with filtered pyroelectric detectors. A/D converters are used to collect and analyze the data and optimize the signal processing sequence.

Although the high frequency components are difficult to see in the power spectral density plots, the thermopile detectors used have a poor high frequency response. Lead selenide and pyroelectric detectors have a much better high frequency response than the thermopile detector.

FIG. 14A shows a typical nondispersive infrared gas sensor test bed including infrared radiator and detector, suitable filters, and a small environmental chamber for performing thermal cycle and gas flow tests. FIG. 14B shows a typical signal processing stream for data reduction.

Automated data collection analysis software, or off-line data analysis software is used for signal processing, rapid prototyping of data collection and analysis systems. Real-time power spectral density plots and other signal processing techniques identify and isolate those frequency characteristics, that will enable this simple, yet effective gas detection approach.

FIG. 15 shows measured data from a pulsed-source and thermopile detector combination, illustrating the high (20 - 40 Hz) ripples associated with changes in gas flow. Long considered a problem for IR gas detectors, this characteristic is used to exploit this "noise" as the primary "signal" for a leak detector.

Multi-pixel sources for scene generators and FPA health check

Multi-pixel calibrator for hyperspectral imagers

A tiny, self-referencing band emitter is used for absolute radiometric calibration of infrared spectral channels. This simple, rugged device can be incorporated directly into a radiometric instrument, or into a field test kit. Microelectromechanical (MEMS) fabrication techniques are used to produce a photonic band gap infrared emitter surface with a narrow emission band tuned to the infrared spectral channel under test. A discrete single-channel (less than 1mm active area) radiometric calibration element is used. This configuration is stable, repeatable, and has high power conversion efficiency and out-of-channel rejection. The configuration can provide a transistor-sized multi-pixel, multi-channel hyperspectral calibration tool.

A simple built-in radiometric and wavelength calibration device is used for hyperspectral imaging systems. A silicon bridge emitter element has a photonic band gap (PBG) surface tuned to emit over a narrow infrared waveband. With very low thermal mass and high temperature coefficient of resistivity (TCR), this element acts as its own thermistor for self-referencing, electronic feedback control.

FIG. 16 shows a simple, built-in calibrator for hyperspectral imaging systems, using silicon micro bridges with a photonic band gap surface structure to achieve narrow band emission and absolute feedback temperature control in the infrared.

Hyperspectral imaging

Passive infrared spectra contain critical information about chemical make-up while broad-band infrared images provide information on the location, presence, and temperature of objects under observation. Hyperspectral imaging, the ability to gather and process infrared spectral information on each pixel of an image, can ultimately provide two dimensional composition maps of the scene under study and this data is

critical for ecosystem inventory and status monitoring. These studies routinely require data in the near- and mid- infrared spectral bands, over large areas, at a reasonably high resolution suited to ecological studies. Data goals include complementary surface moisture and surface (vegetation) temperature data taken in registration with the shorter wavelength data (allowing precise and straightforward correlation with LWIR data) for plant coverage, deforestation, and plant health monitoring studies. Variations in surface albedo within from frame to frame and even within a single frame make it difficult to infer accurate temperature measurements from bandpass flux at a single wavelength. This may be particularly acute for deforestation studies where sudden loss of vegetation coverage would be expected to produce surface humidity changes with simultaneous shifts in surface temperature and surface albedo.

A traditional solution is to measure infrared bandpass flux in adjacent spectral bands to allow extraction of accurate color temperatures. Hyperspectral imaging can provide surface temperature and humidity mapping, at a resolution compatible with the shorter wavelength systems, over inaccessible regions where this data is not available from ground monitoring stations or other sources.

Current hyperspectral imaging systems such as the NASA/JPL Airborne Visible Infrared Imaging Spectrometer (AVIRIS) and Kestrel's Fourier Transform Hyperspectral Imager (FTHSI) are bulky and expensive which renders widespread use of the technology impractical, especially for commercial applications. Rapidly evolving uncooled hyperspectral imaging systems, based on recent advances in infrared focal plane array technology, can provide simultaneous mid-wave (MWIR) and long-wave (LWIR) data for coastal ecology studies. These devices, which must operate under field and flight conditions over large temperature and humidity ranges, require periodic radiometric and spectral calibration to assure long term accuracy.

Radiometric calibration

Hyperspectral image measurements are difficult to make in the field since the instruments must operate unattended (or with minimal attention) in hostile environments, over extreme field temperature and humidity ranges. Much of the important irradiance information is in the 1-3 mm spectral band where low signal and drift in infrared sources

and infrared detectors make stability and calibration difficult. In fact, the standard NIST FAL, T-10 reference bulbs generally used for laboratory calibration have very low signal in this waveband. But the atmospheric research community has made steady progress in the accuracy and reliability of these measurements and there is now a broad consensus on absolute standards for bolometric radiometry established through bi-annual international inter-comparisons between instruments used by various groups and a gold triple point standard. In general terms, the state of the art for absolute accuracy in these measurements has progressed to around 0.3% (3s).

The most effective strategy for maximizing instrument sensitivity is calibration to identify and compensate for gain and offset variations. This is done with conventional blackbody sources which depend upon large size and thermal mass to achieve uniform temperature. These sources are not easily incorporated directly into the instrument. As a consequence, calibration is infrequent and, particularly for instruments stationed at inaccessible locations, very infrequent.

Accordingly, to one aspect of the invention, a miniature, electrically-modulated multispectral line source weighing a few grams and occupying a fraction of a cubic centimeter provides the solution to this problem. The heart of this source is an array of photonic band gap narrow band emitter pixels. Each pixel radiates only within its designated spectral band and achieves temperature stability by heating and cooling on a time scale much faster than thermal diffusion. Its low thermal mass, near-perfect in-band emissivity, and high temperature coefficient of resistivity cause it to precisely follow its drive current, permitting instantaneous feedback and precise temperature control. The source is readily packaged into radiometric instruments where its low power demand permits remote, battery-powered operation under computer control.

The stability of conventional, cavity-style blackbody sources depends on good thermal conductivity (to minimize spatial temperature gradients) and a large thermal inertia (to minimize temporal fluctuations). This determines their weight and power consumption, both of which are typically large. The IR source of this aspect of the invention, because it is based upon a few-micron-thick textured emitter element, does rely on its thermal mass for stability, but instead depends upon a stable electronic drive supply. This is an important advantage for the source of the invention because super-stable, precisely controlled

electronics are much easier to engineer than a highly stable thermomechanical system and, when built, respond orders of magnitude more quickly to programmed changes, weigh less, occupy less space, and are less expensive than massive radiators.

Conventional blackbody sources require long lead times for warm-up and stabilization and, during these times, they place a parasitic heat load on components in the optical train. For components at cryogenic temperature, the source-induced heat load is especially burdensome because it is continuous, and heats the optical train even when not in use as a reference or for calibration. Miniature IR sources of the invention, on the other hand, rely upon electrically heated filaments of such low thermal mass that their temperature at all times correlates precisely with the current flowing through them. They can be heated (and cooled) in milliseconds, delivering a current-following temperature profile exactly matching the drive pulse. Because they rely on electrical pulse shaping and current control rather than thermal mass for stability, these miniature sources have several important advantages. First, they need only be powered for a short time when required, thus eliminating parasitic heating. Second, their low thermal mass and high radiant output allow them to achieve a very high temperature-slew-rate with virtually no thermal hysteresis. This means that at any instant, filament output is directly related to electrical drive power. Effectively, this converts the [difficult] thermal stability problem into a [straightforward] matter of assuring electrical stability.

Portable MTF (modulation transfer function) tester

According to another aspect of the invention, an infrared resolution tester which is a thermal version of the familiar resolution test patterns for visible band optical systems. Based on the use of miniature textured metal radiators for flat-field correction of flight systems, the invention is based on lithographic techniques to build a postage-stamp sized device with alternating bands of polished (emissivity, $\epsilon \cong .01$) and textured ($\epsilon \cong .99$) metal to form the familiar USAF 1951 optical resolution test pattern. The integrated resolution tester based on this device is light-weight, low power, and responds rapidly to turn on/turn off commands. This device is mounted on a temperature controlled stage and demonstrates performance with collimating optics. This device is a flightworthy resolution tester for field and flight monitoring of infrared imaging systems.

For any imaging system, one of the most important figures of merit is resolution. This is typically expressed as a modulation transfer function (MTF), or contrast as a function of spatial frequency. For visible-band systems, MTF has historically been measured with standard resolution test charts; because no such devices are available in the infrared, designers typically rely on slits (often home-made) in a metal foil mounted in front of a large cavity-style blackbody to make the measurement. However, recent advances in ion-beam microtexturing now enable another aspect of the invention, namely the manufacture of adjacent regions of very high and very low emissivity in a complex pattern of very closely controlled characteristics.

FIG. 17A shows a resolution test pattern and FIG. 17B shows a resolution tester. By using ion beam lithography techniques, alternating bands of very high and very low emissivity are established on a lightweight, high conductivity metal foil surface. Using a tiny thermoelectric hot/cold stage to uniformly vary the temperature of this test pattern permits simultaneous radiometric and resolution tests.

Modern high-performance IR systems have narrow fields of view, consequently long focal lengths and very high resolution. This complicates the problem of designing a built-in resolution tester, since calibration objects must appear to be very far away. In a conventional test arrangement, a collimator is used to project the image of the blackbody source with a slit pattern onto the aperture of the system under test. In this arrangement, the collimator acts as one lens and the fore-optics as another; the magnification of this two lens system is the focal length ratio of the two lenses. This means that, to project very small test patterns onto the focal plane array under test, either the test target itself must be very small or the collimator must have a much longer focal length than the fore-optics of the system under test. A test object of the invention has extremely fine lines and spaces, as the key to calibrating high resolution systems with a device of modest size. In one form, the invention includes a three-element, germanium f/1 lens system adapted from the "IR microcam," to build a hand-held external test device.

FIGS. 18A and 18B shows the IR μcam lens as a 3-element germanium f/1 system. It has a 25mm aperture. It provides night vision capability for hand-launched unmanned aircraft (HL-UAV). This optical train is the basis of a hand-held resolution tester.

FPA Health Check Source

Like most infrared seekers, gain and offset in the AIT seeker depend on the local temperature (and pixel-to-pixel temperature variations) on the focal plane array. One way to compensate for gain and offset variations is to use a flat-field IR reference source to provide uniform illumination on all pixels before (or during) flight. Such a source would also be extremely useful for an FPA health check on a Dem-Val flight. The metal texturing technology developed by the M&S program makes it possible to build extremely compact, lightweight infrared reference sources. Another aspect of the invention is an MWIR reference source for the BMDO STRV-2 mission. The STRV-2 source is very small (6mm diameter x 3mm thick) since it was designed to go on the filter wheel very close to the FPA.

Changes in the STRV-2 orbital and mission profiles meant that its original cryocooler was replaced with a more robust, but vibrationally noisier, cooler. Although this solved some thermal problems for the MWIR telescope, it meant that the telescope had to take its images with the cooler switched off. The new orbit, inclined nearly 65 degrees, will allow the telescope to see the sun for nearly half of every orbit so that the telescope must be designed to operate accurately even when it is not in thermal equilibrium. This will require on-station calibration. But, because weight and space are at a premium within the MWIR payload, a conventional blackbody source was not practical.

FIG. 19A shows a prototype reference source for STRV-2, mounted in an existing filter wheel slot for minimum design and schedule impact. This source provides flat-fielding to correct pixel-to-pixel offset variations. FIG. 19B shows exemplary sources adjacent to a metric.

This simple modular device provides a flat field warm-body reference with no parasitic heating of the optical train and it will allow correction of pixel-to-pixel offset variations on the focal plane.

The invention may be embodied in other specific forms without departing from the spirit or essential characteristics thereof. The present embodiments are therefore to be considered in all respects as illustrative and not restrictive, the scope of the invention being indicated by the appended claims rather than by the foregoing description, and all changes which come within the meaning and range of equivalency of the claims are therefore intended to be embraced therein.

APPENDIX -- PCT APPLICATION NO. PCT/US99/07781

MONOLITHIC INFRARED SPECTROMETER APPARATUS AND METHODS

Background

Conventional Ebert and Czerny-Turner type spectrometers and spectrographs are known in the art and have been common optical instruments for most of this century. These instruments use free-space optical elements - mirrors, reflective gratings, and slits - to disperse incident light into component wavelengths. Recently, there has been some experimental work using waveguides made of plastic or silicon dioxide, rather than air, to transmit the light from one optical element to the next.

Most infrared spectrometers and spectrographs of the prior art use cooled infrared detectors as well as separately-aligned optical elements. Cooling the detectors requires added bulk and heavy equipment, such as closed cycle refrigerators, cryogenic liquid, and thermoelectric coolers with large power supplies. Maintaining optical alignment is also a challenge if the instrument is to be subjected to environmental stresses.

Infrared spectroscopy for chemical analysis has typically used laboratory grade spectrometers, spectrographs, or Fourier Transform Infrared (FTIR) instruments. These instruments can be as small as a cigar box and as large as a table top. They generally consist of entrance and exit slits, reflective mirrors and a reflective diffraction grating made of glass which may or may not be rotated to scan the wavelengths of interest. The FTIR, for example, generally uses a Michelson interferometer with a moving mirror in one interferometer leg and a fixed wavelength reference such as a laser to scan the wavelengths. In addition there is a host of external equipment, including power supplies, scan motors and associated control electronics, and of course a cooled infrared detector. For example, an infrared chemical analysis instrument developed by Foster-Miller uses an FTIR about the size of a breadbox with a liquid nitrogen-cooled mercury cadmium telluride (HgCdTe) detector.

There are a few spectrometers, in the prior art, that attempt to remedy the above-described problems of size, weight, complexity and power consumption. Zeiss manufactures a Monolithic Miniature-Spectrometer, or MMS 1, and distributes the MMS 1 through Hellma International, Inc., of Forest Hills, NY. The MMS 1 uses a

conventional silicon photodiode array and a cylinder of glass with an integral imaging grating. However, its operation is limited by the photodiode and the spectral limitations of the glass relative to ultraviolet (UV) and visible wavelengths. The detector is also positioned away from the waveguide, presenting certain optical alignment difficulties, particularly under environmental stresses.

Another instrument has been demonstrated by researchers at Kernforschungszentrum Karlsruhe GmbH (U.S. representative American Laubscher Corp., Farmingdale, NY). It uses a waveguide and grating fabricated in a multi-layer photoresist of polymethyl methacrylate (PMMA) to couple the output of an optical fiber to a linear detector array or array of fibers. This instrument is designed for demultiplexing applications. As above, because of the choice of materials, operation of this device is limited to visible and near-IR wavelengths of 6OOnm to l3OOnm. Specifically, fabrication of the waveguide and grating is done by a process called LIGA (which stands for the German words for Lithography, Galvanoformung and Abformung) which uses a three-layer photoresist and deep-etch X-ray lithography.

Yet another instrument has been developed by researchers at Oak Ridge National Laboratory. It is a microspectrometer based on a modified Czerny-Tumer configuration and machined from a block of PMMA also known as Acrylic or Plexiglas. It has a bandwidth of about 1μm centered at 980nm and uses an externally mounted linear photodiode array.

None of these prior art spectrometers permit fully monolithic operation and spectral sensitivity from 1.1μm - 12μm, or further, and with uncooled detectors.

It is, accordingly, an object of the invention to provide apparatus that solves or reduces the above-described problems in the prior art.

Another object of the invention is to provide a hand-held, monolithic, rugged IR spectrometer.

A further object of the invention is to provide methods of manufacturing uncooled IR spectrographs.

Yet another object of the invention is to provide a process of isolating chemical species over a large infrared band with a monolithicaily-constructed IR spectrometer.

These and other objects will become apparent in the description which follows.

Summary of the Invention

The spectrograph of the invention overcomes many of the problems in the prior art by using uncooled detectors, e.g., microbolometers, which eliminate the need for associated cooling equipment. Other detectors such as PbSe or PbS are also suitable. In addition, the spectrograph of the invention is monolithically constructed with a single piece of silicon, which eliminates the need for alignment and which makes the device inherently rugged and light weight. The use of standard silicon microelectronics technology also makes the invention low-cost, as compared to the prior art. By way of example, these costs can be orders of magnitude lower than the conventional spectrographs, i.e., hundreds of dollars instead of tens of thousands of dollars.

In one aspect, the invention includes a solid optical grade waveguide (similar to a slab of glass) coupled to a line array of detectors. Light from a source (e.g., earth emissions transmitted through gases) is focussed at a first surface of the waveguide, reflected from an internal mirror to a diffractive surface, which diffracts the light to a second reflector which focusses the light onto the array at a second surface of the waveguide. Accordingly, because of refraction, an f/1 light bundle entering the waveguide is translated to about an f/2 bundle within the waveguide, making it easier to cope with wavefronts therein.

In one aspect, the waveguide is silicon to transmit IR light; and the detector array is one of microbolometers, PbSe, PbS, or other IR sensitive detectors.

In another aspect, the waveguide is transmissive to visible light and the detectors are CCD elements.

In yet another aspect, the waveguide is ZnSe and the detectors are "dual band" so that visible and IR light energy are simultaneously captured at the detectors. For example, each pixel of the dual band detector can include a microbolometer and a CCD element.

The invention has several advantages over the prior art. First, it monolithically integrates all parts of the spectrometer, including the detector, thereby making the

instrument compact, rugged and alignment-free. Further, by fabricating the entire device on one piece of silicon, using silicon micromachining technology, we take advantage of the thirty years of silicon process development, and the emergence of silicon as a commodity item, to enable the fabrication of the instrument at a very low cost.

Other capabilities, features and advantages of a spectrometer constructed according to the invention include: (a) the ability to sense and identify chemicals i n a variety of applications and environments, (b) the ability to determine chemical concentrations, (c) operation with low-cost, low power, and long-term unattended operation or calibration, (d) uncooled operation, without expensive and unwieldy cooled detector elements, and (e) a rugged, alignment-free instrument.

The invention is next described further in connection with preferred embodiments, and it will become apparent that various additions, subtractions, and modifications can be made by those skilled in the art without departing from the scope of the invention.

Brief Description of the Drawings

Figure 1 shows a perspective view of a spectrometer system of the invention;

Figure 2 illustrates optical bench features of the waveguide, optical path, and detector of the system of Figure 1; and

Figure 3 shows a schematic layout of the optical trace of the system of Figure 1.

Detailed Description of the Drawings

As shown in Figure 1, one embodiment of the invention includes a spectrometer system 10 with the following elements: a silicon block waveguide 12, a cylindrical mirror 14 (e.g., gold-coated), a diffraction grating 16 (preferably gold-coated), and a linear detector array 18 (e.g., a microbolometer or microthermopile array). Electronics 20 can couple to the array 14 so as to collect electronic data representative of the spectral characteristics of the light 22 entering the system 10. Control of the system 10 is obtained through user interface 24. A battery 26 can be used to power the system 10.

APPENDIX -- PCT APPLICATION NO. PCT/US99/07781

The system of Figures 1 and 2 can further include detector preamps 30, a multiplexer 32, input focusing lenses 34, a microprocessor 36, an LCD display 38, keys 40 on the interface 24, and a protective housing 42.

Generally, these elements have the following function, as further described in the attached appendices and in the related provisional application.

1. Silicon block waveguide 12.

The silicon slab waveguide is the transmitting medium for the light before and after it is dispersed by the grating. Because it is a high index of refraction material (n=3.4), compared to the surrounding environment (n-l), light will be reflected from the polished top, bottom and sides of the waveguide without loss. The silicon block also acts as a fixed dimension frame upon which the grating, mirror, and detector array are fabricated thereby making the instrument compact, rugged, and alignment-free.

2. Reflective flat mirror 14.

The reflective flat mirror folds the path of the injected light so as to achieve a fiber-to-grating vs. grating-to-detector distance ratio of 2:1 or more. This is important if the input light comes from an infrared fiber with a typical core diameter of ²00~m yet we are focusing the light onto a detector array with 50~m wide pixels. To focus the light effectively with only one concave surface, fiber-to-grating vs. grating-to-detector distance ratio is directly proportional to the ratio of entrance and exit spot sizes.

3. Reflective diffraction grating 16.

The concave grating disperses the light into its component wavelengths (shown in Figure 3 as light path 40) and focuses it onto the detector plane18. In a normal grating with uniform line spacing, each wavelength has a different focal length. Therefore, the focal points for the various wavelengths will lie along the circumference of a circle that includes the grating. This circle is called the Rowland circle and is well-known by those skilled in the art of optics. However chirping the grating, i.e., varying the line spacing, flattens out the focal points for the various wavelengths almost completely.

APPENDIX - - PCT APPLICATION NO. PCT/US99/07781

4. Detector plane 19''.

The detector plane 19'' (Figure 3) is where the linear detector array 18 is located and the point at which the grating 16 focuses all wavelengths.

5. Linear detector array 18.

The linear detector array 18 converts the dispersed photons into electrical signals for each wavelength.

6. Anti-reflection coating(s).

Anti-reflection coatings should be used on either or both the input plane and the detector array plane. By suppressing reflection at the interface bekveen high index of refraction silicon and the ambient environment, we ensure that the maximum number of photons are available for detection.

The invention can be used in applications where infrared analysis for chemical identification and concentration measurement is desired, especially in applications which require low cost, expendable sensors; low power sensors; or uncooled sensors. Particular applications may include detection and measurement of hazardous and pollutant gases, polluted water, chemical analysis of core samples, rocket plumes, smokestacks, biologic and chemical warfare agents, etc.

Appendix A shows and describes other features, embodiments, aspects and advantages of the invention.

The invention thus attains the objects set forth above, among those apparent from preceding description. Since certain changes may be made in the above apparatus and methods without departing from the scope of the invention, it is intended that all matter contained in the above description or shown in the accompanying drawing be interpreted as illustrative and not in a limiting sense.

It is also to be understood that the following claims are to cover all generic and specific features of the invention described herein, and all statements of the scope of the invention which, as a matter of language, might be said to fall therebetween.

APPENDIX - - PCT APPLICATION NO. PCT/US99/07781

APPENDIX A

TO

Monolithic Infrared Spectrometer and Methods

APPENDIX -- PCT APPLICATION NO. PCT/US99/07781

TABLE OF CONTENTS

APPENDIX -- PCT APPLICATION NO. PCT/US99/07781

ABSTRACT

The next missions to Mars are targeted toward collecting surface samples and returning a representative subset of them to Earth. It is important that instrumentation placed on the surface be capable of rapidly differentiating the range of composition and aggregation of surface samples available, of characterizing the regimes from which they are collected, and of classifying the samples collected for later sample return. We propose to develop further and to validate an existing breadboard spectrometer that meets these characterization requirements. The resulting 3-12 μm instrument will be tiny, rugged, inexpensive to replicate, and will require very few resources, leaving significant system resources to support a range of complimentary instruments.

The proposed spectrometer is small, lightweight, low power, and can classify rocks on a large range of spatial scales. An integrated infrared illuminator will allow operation as a reflectance instrument for close inspection of small areas of rock or soil. Alternatively, larger areas can be analyzed from a distance. The signal-to-noise ratio will range from 200 to 4800, depending on the wavelength and mode of operation.

The existing breadboard instrument combines three key technologies: 1) a compact silicon waveguide spectrometer developed by Ion Optics, Inc., 2) high performance, broadband, uncooled thermopile detector linear arrays developed at JPL, and 3) a custom thermopile readout chip developed by Black Forest Engineering. Further improvements in all three areas, combined with compact packaging, will result in a small, rugged instrument having sufficient sensitivity to characterize rock and soil mineralogy and allow sample selection for subsequent return to Earth. The engineering model produced in this effort will be, with minor modifications, ready for flight qualification.

A strong Education/Public Outreach effort will make information about this program available to the public over the internet as well as provide opportunities for participation by minority college students.

1. RESEARCH OBJECTIVES

A. Science Objectives

It is the objective of this proposal to create a miniature instrument capable of classifying rocks, soils, and the surrounding terrain. We will accomplish this through modest modifications to an existing solid state spectrograph.

The next missions to Mars are targeted toward collecting surface samples and returning a representative subset of them to Earth. It is important that instrumentation placed on the surface be capable of differentiating the range of types of surface samples available, and characterizing the types of samples collected for later sample return. It is important that a range of in situ measurement techniques be used so that the strengths of each technique can be used to complement the strengths of others. For example, an x-ray diffraction measurement gives very precise estimates of the mineralogy, but is not ideally suited for examining large areas, many samples, or elemental composition. Alpha backscatter provides an excellent measurement of elemental composition. Infrared spectroscopy is suited for indicating the mineralogy of large areas and the large-scale variance of mineralogy in rocks, but can only provide precise measurements of composition and/or precise classification of mineral types in favorable mineral mixtures. Combining the techniques, however, provides a very powerful in-situ tool set ideal for selecting the few very precious samples returned to Earth. To allow several in situ measurement techniques on the same platform, it is necessary that each technique utilize a minimum amount of resources with respect to cost, mass, energy, volume, and data rate. We propose here a micro infrared spectrometer that meets these criteria.

Mars is known to have large ancient volcanic areas, polar regions having layered terrain and surrounded by permafrost, and extensive areas which are consistent with water or ice erosion. There is evidence for layering in rocks, ancient lacustrine environments, and active aeolian features (such as sand dunes). Most rock surfaces seem to have a substantial coating of desert varnish, though a range of rock coloration (including white) has been detected. The generally red appearance of the surface has been attributed to oxidized iron. The soil has an abnormally high CO_2 content, the result of exposure to a CO_2 environment, moisture, and solar radiation.

Samples that might provide evidence of life may be found in regions that were once water-rich, for example ancient lake beds The strongest indication of such an environment would be the

APPENDIX -- PCT APPLICATION NO. PCT/US99/07781

detection of evaporite deposits, rich in sulfates and carbonates, or confirmation of lacustrine sedimentary deposits, or the presence of highly altered materials (such as clays).

For volcanic regimes, the greatest interest lies in differentiating between basalt compositions, particularly with respect to silicon, iron, calcium and magnesium content. This information can be used to locate different sources, determine the degree of differentiation of magmas, and can be used to validate models equating flow form to magmatic viscosity.

Detection of metamorphic minerals would provide significant information on local tectonic activity on Mars. The location and size of ice deposits is also of extreme interest. Measurement of Mars dust is important for understanding Mars, and for implementing sample return and manned landing missions to Mars. Critical parameters include variation in composition, soil density, and variations in particle size.

Infrared spectroscopy provides a method for readily distinguishing between classes of rocks and mapping variations in mineralogy within rocks. This technique is most effective when used in association with techniques that provide definitive composition and mineralogy for individual grains in rocks. Depending on the wavelength region, infrared spectroscopy can provide estimates of the SiO_2 content, the degree of hydration of minerals, and can distinguish between various clays and evaporites. Infrared measurements also can provide very quantitative information in favorable circumstances, such a when a Christiansen peak is present. The technique is also suitable for estimating particle size both from scattering properties and from thermal emission measurements. Reflectance measurements penetrate to a few wavelengths of light, so are most diagnostic for freshly exposed surfaces. Thermal inertia measurements penetrate to the depth of the diurnal thermal wave.

Choice of the wavelength region to observe depends on the diagnostic features for expected minerals, on the observation conditions, and on the choice of detectors. The spectra in Fig. 1 (from the Aster catalog) illustrate that the spectral region this instrument spans is suited for discriminating between a wide range of geological samples which may be postulated for Mars. Note that the spectra in Fig. 1 are in reflectance units, and that some of the ordinal axes have been scaled differently. Fig. 1 shows, for instance, significant differences which can be used to differentiate (left to right, top to bottom) slate, horneblend schist, enstatite , andesite, clay, basalt, goethite, anorthosite, anorthite, gypsum, apatite, and halite - a range of evaporites, sedimentary and igneous minerals. These spectra are just illustrative, since the issue of which minerals can be distinguished in the presence of weathering is too complex to address here.

Requirements on the spectral range, spectral resolution, and signal-to-noise requirements for a spectrometer can be estimated from Fig. 1 (the figures are scaled). There is always a push for higher resolution and sensitivity, but it is clearly possible to distinguish between a wide variety of minerals, and, to a lesser extent, the composition within classes of minerals at a modest resolution of about 0.1 micron. Similarly, a signal-to-noise ratio of 30 is sufficient to discriminate between mineral classes in most cases. The proposed solid state spectrograph has a spectral resolution ranging from 0.05 to 0.1 microns, and signal-to-noise ratios ranging from 200 to 4800.

Our miniature solid state spectrograph has several modes of operation. These include 1) a self-illuminated contact mode, suitable for classifying grains in rocks as small as 1x0.1 mm 2) a distant mode suited for characterizing large rock and locations by measuring spectra integrated over areas up to 1-2 meters in diameter.

Reflectance and emissivity measurements sample surfaces to a depth which is at best a few wavelengths of the light being measured. The measurements are best performed on fresh rock or soil surfaces, such as those exposed by trenching, scraping, or drilling. The interpretation of measurements made in this wavelength region are complicated by the crossover between reflected and emitted light (for Mars surface temperatures). There are a multitude of ways to address this issue for ground measurements including measuring samples at different temperatures (different times of day), measuring samples in shadow (though scattered light complicates this), and by measuring radiation from a sample with and without illumination.

Infrared measurements can be made quickly, using few resources, and are ideally suited for determination of the crystal field and the type of molecules contributing to an absorption. Quantitative measurements of elemental composition are better obtained using other techniques. The small size and cost of the proposed infrared spectrograph leave sufficient mass, power, space and budget to include complementary techniques.

APPENDIX -- PCT APPLICATION NO. PCT/US99/07781

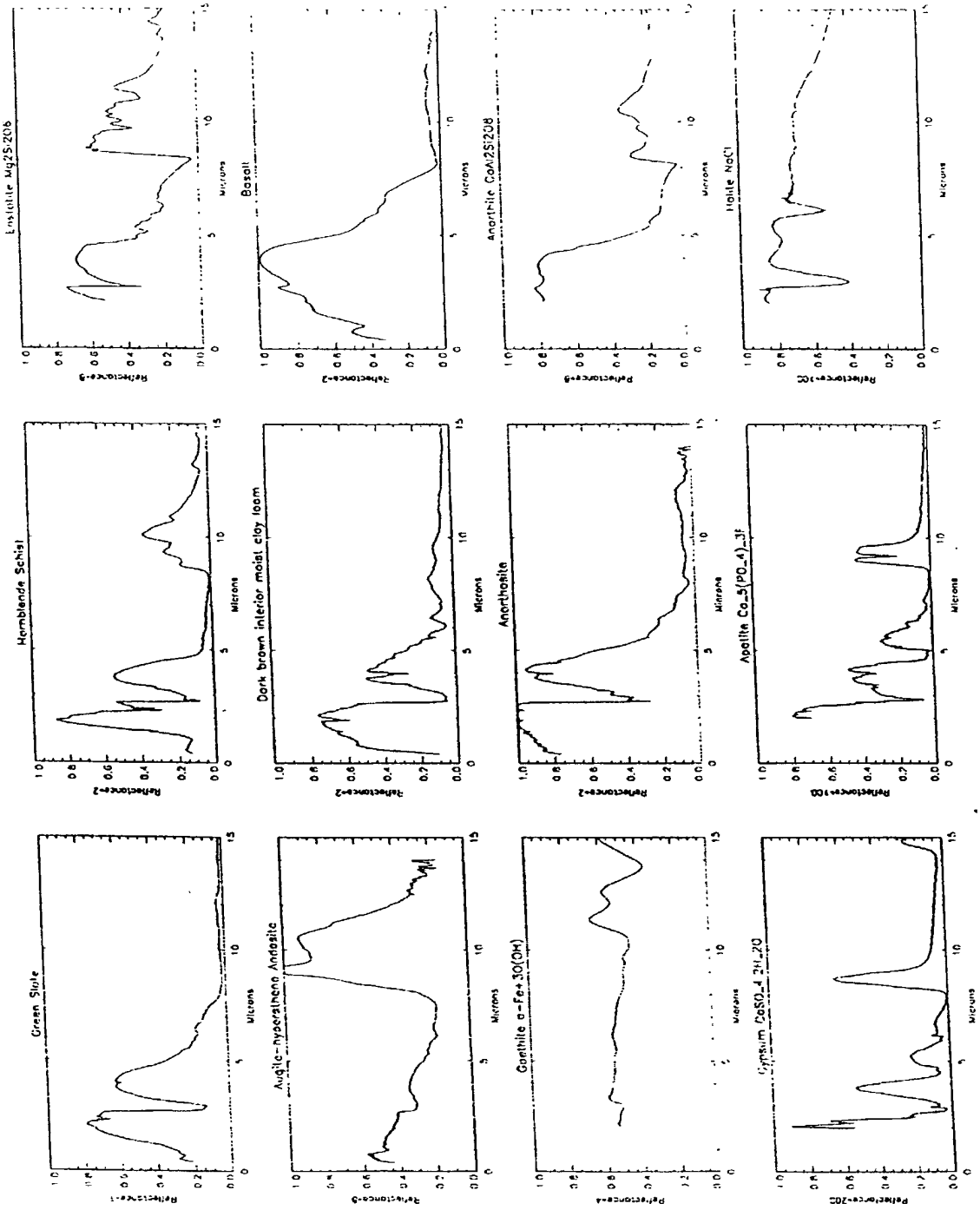

Figure 1. Spectra of a variety of minerals related to petrographic types.

APPENDIX -- PCT APPLICATION NO. PCT/US99/07781

B. Engineering Objectives

We will further develop and validate an existing breadboard spectrometer. The instrument will be compact, lightweight, and low power and will cover the spectral range 3-12 μm. The complete unit will be roughly 4 cm by 3 cm by 2 cm in size, weigh roughly 100 g, and consume about 200 mW of power. The spectral resolution will be 0.05 μm in the 3-6 μm range, and 0.1 μm in the 6-12 μm range. The device can operate as a reflectance instrument (contact mode) for close inspection of small areas of rock or soil, with a signal-to-noise ratio ranging from 600 to 4800. Alternatively, the spectrometer can operate in survey mode, passively measuring rock and soil spectra in both the solar reflectance and thermal emission spectral regions. In survey mode it will look from a distance at a large area and will have a signal-to-noise ratio ranging from 200 to over 1000.

An existing breadboard instrument, shown in Fig. 2, combines three key technologies: 1) a compact silicon waveguide spectrometer developed by Ion Optics, Inc., 2) high performance, broadband, uncooled thermopile detector linear arrays developed at JPL, and 3) a custom thermopile readout chip developed by Black Forest Engineering. A spectrum taken with the silicon waveguide is shown in Fig. 3. Further improvements in all three areas, combined with compact packaging, will result in a small, rugged instrument with sensitivity sufficient to characterize and select samples for subsequent return to Earth. The engineering model produced in this effort will be, with minor modifications, ready for flight qualification.

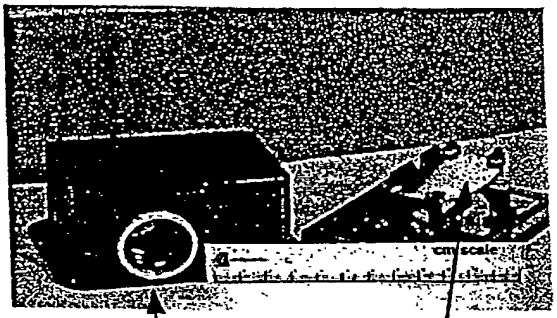

Fig. 2. Silicon waveguide spectrometer and housing developed by Ion Optics with NASA SBIR funding.

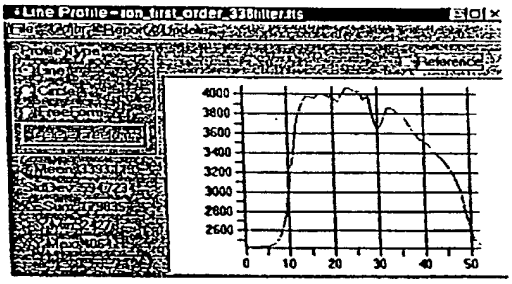

Fig. 3 Uncalibrated spectrum from prototype silicon waveguide. Radiation from the source passes through air and a 3.38 μm cut-on filter. The midpoint of the filter is at channel 11. Channel 30 shows a CO_2 absorption at 4.26 μm.

The existing breadboard instrument, which operates in the 3-5.5 μm range, is shown schematically in Fig. 4. It was developed by Ion Optics with funding from NASA SBIR phase II contract NAS7-1389. At the heart of this breadboard is a D-shaped silicon waveguide 1 mm thick and roughly 5 cm by 3 cm across. The unit uses a conventional Ebert layout, with the optical elements on the edges of the silicon waveguide. Infrared radiation is focused by an external lens onto an entrance slit defined by gold coatings on the silicon edge. Radiation traverses the silicon to a curved mirror on the opposite face, then the light is dispersed by an ion milled diffraction grating and focused by a second concave mirror. After exiting the silicon waveguide on the flat edge, the spectrum is detected by a linear array of thermopile infrared detectors. Each component of the spectrometer: the slab waveguide, the fold mirror, and the reflective diffraction grating, is made of silicon and fabricated into a seamless, permanently aligned unit with no moving parts.

APPENDIX -- PCT APPLICATION NO. PCT/US99/07781

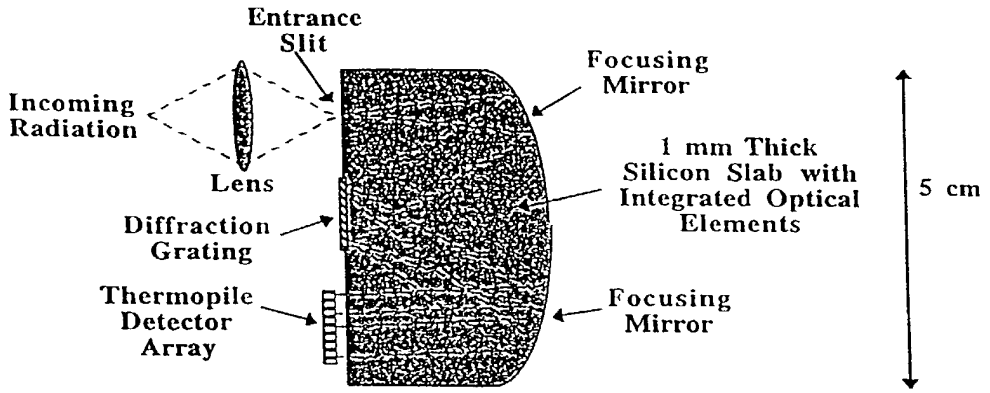

Figure 4. Schematic drawing of breadboard 3 to 5.5 μm spectrometer. Infrared light from the target is focused onto a slit by an external lens. As the light enters the silicon waveguide, the angular spread is reduced due to the high index of refraction of silicon. Inside the silicon slab, light is reflected from a concave mirror, dispersed by a diffraction grating, and imaged with a second mirror. The dispersed light is detected by an external linear detector array.

The components themselves incorporate a number of advanced design features. The slab waveguide is formed to include the other components (stops, mirrors, and grating), including A/R coated beam dump facets for unwanted diffraction orders. Because silicon is opaque to photons above its band gap, the slab excludes visible light from the detector. Silicon's high refractive index provides lossless reflections at the polished top and bottom faces of the device, acting as a waveguide to keep the radiation in the plane of the slab. Because of the high index of silicon, the cone of incident illumination is dramatically reduced upon entering the waveguide. This effect provides better optical throughput than can be achieved with an open-air spectrometer and overcomes many of the astigmatism issues associated with conventional designs.

For the proposed instrument, we will improve the performance and further miniaturize the current MWIR silicon waveguide with a Littrow mount design (described in section 3A). We will make a companion waveguide for the 6-12 μm range. The two silicon waveguides, together spanning the range 3-12 μm, will be mounted close together so they can share the same external lens. An infrared illuminator will be mounted on the assembly to provide a radiation source for reflectance measurements. A bi-linear array of thermopile detectors will detect the resulting spectra. The proposed instrument configuration is shown in Fig. 5.

The modes of operation for this spectrometer, contact mode and survey mode, are shown in Figs. 6a and 6b. In contact mode, illustrated in Figs. 5 and 6a, the rover arm presses the spectrometer against a rock or section of soil. The frame holds the spectrometer at a fixed distance from the sample. The sample is illuminated, and the reflected spectrum recorded. The 3-6 μm and 6-12 μm waveguides view different rectangular areas roughly 1.5 mm apart. Each rectangular area is about 1 mm long and 0.1 mm wide, matching the spectrometer entrance slit. In survey mode, illustrated in Fig. 6b, the spectrometer is pointed down or away from the rover, passively sensing reflected solar and thermally emitted radiation. Survey mode analyzes large areas and can help to select interesting areas for further analysis. Long term drifts can be nulled by pointing the spectrometer into space.

APPENDIX -- PCT APPLICATION NO. PCT/US99/07781

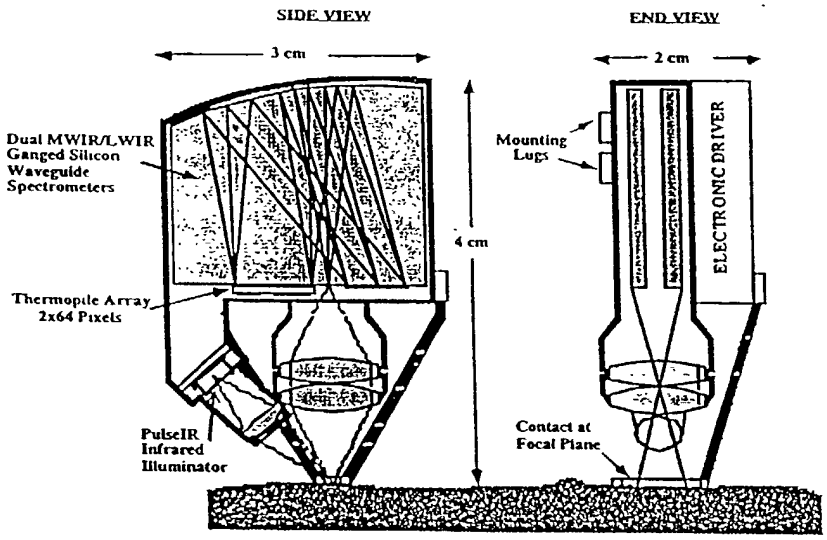

Figure 5. Proposed instrument configuration shows infrared radiator with lens integrated into the instrument package. Two silicon waveguides, with a bilinear thermopile array, cover the spectral range 3-12 μm. The package will be smaller and more robust, with lower power consumption than the existing breadboard spectrometer.

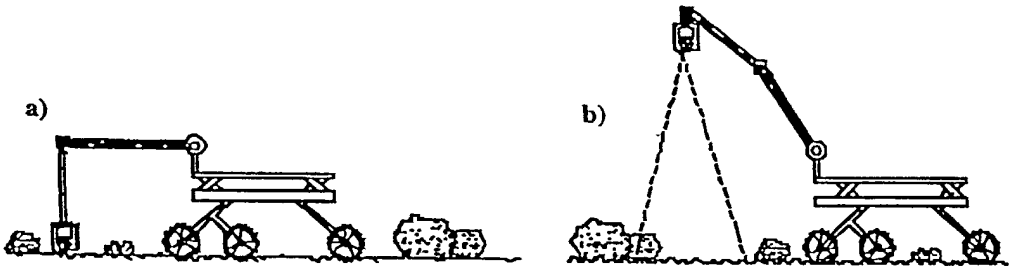

Figure 6. Modes of spectrometer operation. In contact spectrometer mode (a) the rover arm presses the spectrometer against a rock or section of soil. The sample is illuminated, and the reflected spectrum is recorded. The 3-6 μm and 6-12 μm spectrometer waveguides see different rectangular areas on the sample roughly 1.5 mm apart. Each rectangular area is about 1.0 mm long and 0.1 mm wide, matching the spectrometer entrance slit. In survey mode (b) the spectrometer is pointed down or away from the rover, passively sensing reflected solar and thermally emitted radiation. Survey mode analyzes large areas and can help to select interesting areas for further analysis.

The spectrometer can be configured in other ways. The lens can be positioned to provide a fixed focus at longer distances, say 1 meter away. Then the spectrometer will be operated in survey mode while looking at fairly small areas of rock or soil. Because of its compact size, this spectrometer can also be configured to fit down a bore hole to analyze composition at various depths, thus eliminating the problem of removing and analyzing intact core samples.

APPENDIX -- PCT APPLICATION NO. PCT/US99/07781

2. DESCRIPTION OF EXISTING BREADBOARD INSTRUMENT

A prototype silicon waveguide spectrometer has been developed by Ion Optics, Inc. with phase II funding from NASA/JPL SBIR NAS7-1389. This waveguide has been integrated with 1) a thermopile array developed at JPL and funded by NASA Code S UPN 632-20, and 2) a readout chip developed by Black Forest Engineering as a subcontract to NASA SBIR phase II contract NAS7-1899. Test results for each component are described below.

A. Silicon Waveguide

Fig. 2 shows the D shaped silicon waveguide mounted in a prototype spectrometer housing. This waveguide, with its f/1 input lens, was tested independently of the thermopile detector array by mounting an infrared imaging camera at its output port. Initial tests with a broadband source were very promising. The zero order diffraction spot is roughly the size of the 80 μm input slit, showing that the imaging components of the spectrometer are optimized. Very little stray light is seen between the zero order spot and the first order diffraction spectrum. Comparison of total light in the first order spectrum to the zero order spot yields a 47% grating efficiency. An uncalibrated spectrum is shown in Fig. 3. Radiation from the source passes through air and a 3.38 μm cut-on filter. The midpoint of the filter can be seen at channel 11; channel 30 shows a CO_2 absorption at 4.26 μm. Thus the spectral dispersion is 0.46 μm per pixel, as predicted. The total throughput of the silicon waveguide with input lens is estimated to be 15%.

B. Detector Array

Thermopiles are broadband, uncooled infrared detectors in the same class as bolometers and pyroelectric detectors. A thermopile consists of several series-connected thermocouples running from the substrate to a thermally isolated infrared absorbing structure. Incident infrared radiation creates a temperature difference between the absorber and the substrate, which is measured as a voltage across the thermocouples. Thermopiles offer a simplicity of system requirements that make them ideal for some applications; they typically operate over a broad temperature range and are insensitive to drifts in substrate temperature, requiring no temperature stabilization. They are passive devices, generating a voltage output without bias. They do not require a chopper. Thus, for some applications thermopile detectors can be supported by more simple, lower power, more reliable systems than either bolometers, pyroelectric or ferroelectric detectors. If thermopiles are read out with high input impedance amplifiers they exhibit negligible *1/f* noise since there is no current flow. They typically have high linearity over many orders of magnitude in incident infrared power.

A NASA funded development effort at JPL (Code S UPN 632-20) has produced 64 element linear arrays of thermopile detectors on silicon substrates. These detectors are 1.5 mm long with a pixel pitch of 75 μm, matching the geometry of the current Ion Optics spectrometer. Each micromachined detector consists of a 0.6 μm thick suspended-silicon-nitride membrane with 11 thermocouples composed of Bi-Te and Bi-Sb-Te. A schematic diagram of a single pixel is shown in Fig. 7, while a photograph of the complete array is given in Fig. 8. At room temperature these devices exhibit D* values of 1.4×10^9 $cmHz^{1/2}/W$ over the full range of wavelengths proposed for this instrument (3-12 μm), significantly better than that reported for other thermopile arrays. Detector responsivity is typically 1100 V/W at dc, and response times are 100 ms. Detector noise has been measured at frequencies as low as 20 mHz, and the only noise source is Johnson noise from the 40 kΩ detector resistance. Responsivity and response time have been measured as a function of temperature from room temperature down to 100 K. The total change in these quantities over this temperature range is roughly 20%, indicating that the detectors perform well over the entire range of Martian temperatures.

APPENDIX -- PCT APPLICATION NO. PCT/US99/07781

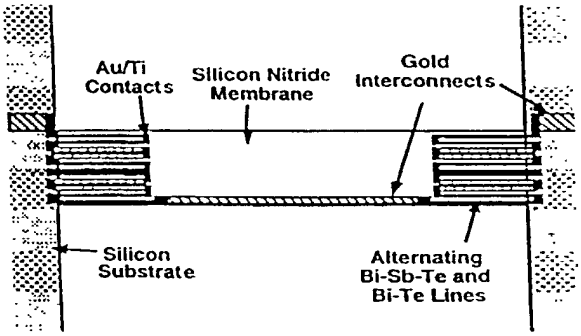

Figure 7. Schematic diagram of a single thermopile detector pixel. The detector is a 0.6 μm thick membrane composed of silicon nitride and metal lines and connected to the substrate at the left and right side of the figure. Infrared radiation heats the thermally isolated membrane. The temperature difference between the membrane and substrate generates a voltage in the 11 series connected Bi-Te / Bi-Sb-Te thermocouples.

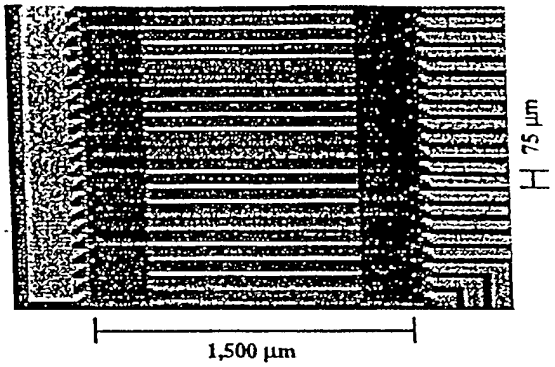

Figure 8. Photograph of a section of 64 element thermopile detector array fabricated at JPL. Each pixel is 1500 μm long, with a pixel pitch of 75 μm.

C. Detector Readout Electronics

To take full advantage of the thermopile array D* values, the signal readout must have a low noise figure for the given detector resistance and at the slowest measurement frequency of interest. In other words, the total input-referred noise after amplification must be only slightly higher than the detector Johnson noise. Typically this goal is difficult to achieve at low frequency for low resistance detectors.

In the current spectrometer, the thermopile array is read out with a custom integrated circuit chip designed by Steve Galeema of Black Forest Engineering. This sixty four channel device includes a preamplifier and filter for each channel, a multiplexer and a 12 bit A/D converter. Power draw is 55 mW. The input uses a chopping scheme to dramatically reduce low frequency noise and drift. The output is easily interfaced with a commercial processor chip. Black Forest's chip was originally designed for use with a thermopile array having a detector resistance of 1300 Ω. Initial tests indicate that the completed chips increase the noise of a 1300 Ω source by a factor of two over the range 0.1-10 Hz. This performance is excellent for a CMOS circuit with such a low source impedance. In the current spectrometer, this readout chip is mated to the 40 kΩ JPL detectors. The mismatch between detector and readout resistance causes some degradation in the system noise performance.

D. Radiation Source

Ion Optics' core product is the *pulsIR*® radiator, shown in Fig. 9. Ion Optics supplies infrared radiator components, first demonstrated in a 1994 DOE SBIR program, for the commercial gas sensor OEM industry. By the end of 1998, Ion Optics *pulsIR*® is expected to be in nearly 10% of all non-dispersive infrared gas sensors built in the United States. The key to the operation of the *pulsIR*® radiator is an extremely thin metal ribbon with a proprietary surface treatment to improve the conversion efficiency of radiator thermal energy to in-band radiation. The *pulsIR*® sources, with efficient, low thermal mass radiators and appropriate infrared windows (or windowless) convert significantly more electrical energy into useful, in band radiation than standard tungsten filament bulbs.

APPENDIX -- PCT APPLICATION NO. PCT/US99/07781

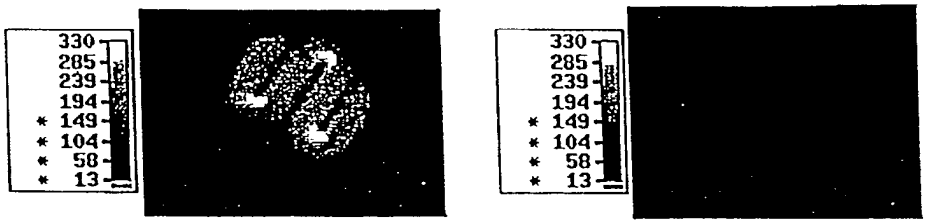

Figure 9. Thermal images of a *pulsIR*® source with power applied and 300 ms after power is turned off.

3. WORK PLAN

A. Silicon Waveguide Development

This task will be performed by Ion Optics, Inc.

The objectives of this task are to substantially increase performance of the existing MWIR waveguide, and to make a similar waveguide in the 6-12 μm range. A simultaneous improvement in the resolution and signal-to-noise performance of the existing spectrograph can be made by making the silicon waveguide less than one-half its present size. These improvements can be achieved with a Littrow mount for the grating, folding the spectrometer optical path on itself and significantly reducing the size of the silicon waveguide (Fig. 10). This design disposes of unwanted diffraction orders; dumps for unwanted diffraction orders occupy much of the flat facet space in the breadboard spectrometer. The shorter optical path in the Littrow mount design results in smaller losses due to absorption of light in the silicon and its escape from silicon faces. Lessons learned during fabrication of the current waveguide will lead to a more efficient grating with fewer stray reflections. Combining a Littrow mount design with an improved grating fabrication process is expected to result in a factor of three improvement in both throughput and stray light rejection.

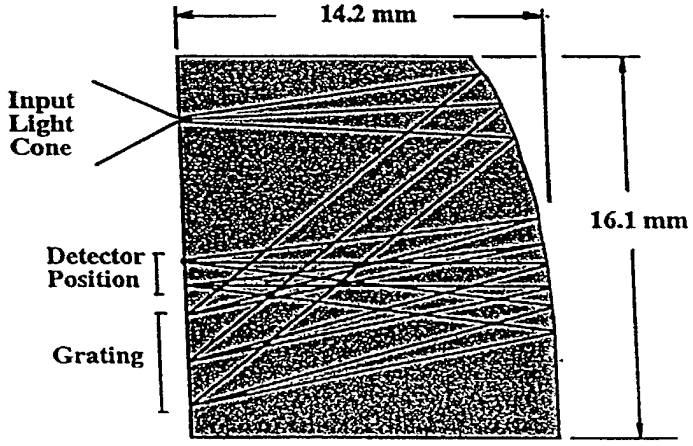

Figure 10. Preliminary modeling of a Littrow mount design of the grating. Optical models indicate the size of the silicon waveguide can be substantially reduced. This innovation is the key to the proposed level of miniaturization and performance enhancement

The design and fabrication of the 6-12 μm grating will benefit from NASA SBIR phase I funding recently awarded to Ion Optics, substantially reducing cost to this proposal of developing the two waveguides.

APPENDIX - - PCT APPLICATION NO. PCT/US99/07781

B. Detector Array Development

This task will be performed at JPL.

To measure spectra from the 3-6 μm and 6-12 μm waveguides simultaneously, the current linear thermopile detector array will have to be redesigned and fabricated as a bi-linear array with the appropriate geometry for the proposed instrument. In addition, we will strive to achieve a factor of two improvement in D* through three changes in the fabrication process.

1) First, properties of the Bi-Te and Be-Sb-Te thermoelectric films can be improved. Film composition can be optimized by changing the sputter target composition in an iterative fashion. Depositing the films on warm (100° C) substrates may improve the thermoelectric properties without overheating the photoresist used in lift-off. Optimization of the post-fabrication annealing procedure may also improve material properties.
2) Thickness of the silicon nitride membrane will be reduced from its current value of 6300 Å to about 4500 Å, decreasing thermal conduction paths to the substrate and improving responsivity and D* values. Response time will not increase because heat capacity is also reduced.
3) The device absorptivity will be increased from its current value of 50-60%. In the 3-6 μm range, this improvement can be achieved by depositing a reflecting layer of platinum on the underside of the membrane and a platinum layer with about 377 Ω/square on the top of the membrane. These metal layers, combined with the 4500 Å silicon nitride layer between them, form an optical cavity with high absorption in the 3-6 μm range. To increase absorption in both the MWIR and LWIR ranges, a gold or carbon black may be used. Alternatively, a metallized surface in close proximity behind the array will increase absorption by allowing some of the lost light to reflect back onto the detectors.

C. Readout Electronics Development

This task will be subcontracted to Black Forest Engineering.

To optimize system signal-to-noise ratio, it is critical to implement a readout that does not significantly add to detector noise. In the current system, noise performance suffers in two ways, first, the readout doubles the noise of the 1300 Ω source resistance, second, the 40 kΩ JPL detector resistance differs from that used in the readout design. The second issue could easily be resolved by redesigning the JPL detectors such that their resistance is optimal for the current readout circuitry. However, there is a potentially large advantage in redesigning the readout instead. Redesigning the readout for the higher source impedance of the JPL detectors should result in a lower noise figure and lower power draw. Typically CMOS amplifiers achieve better noise figures as source impedance is increased; the lower power draw results from lower current needed in the input transistors for higher resistance sources.

Black Forest Engineering will design and test the readout circuits as a subcontract. Fabrication will be performed on multiproject wafers at a commercial foundry.

D. Spectrometer Integration

This task will be performed by Ion Optics, Inc.

Thermopile detectors require vacuum for maximum sensitivity. Therefore, a hermetic package with an infrared window will be designed and fabricated to hold the silicon waveguides, detector array, and readout. The cover will be laser welded under vacuum. A surrounding dust-resistant case will enclose this package in addition to the radiation source, lenses and electronics. Within the dust-resistant case will be a commercial digital signal processor (DSP) chip and associated electronics for controlling the array readout chip. Packaging components will be designed with eventual flight qualification in mind.

The output from the miniature solid state spectrometer will probably consist of an asynchronous serial interface conforming to the EIA-RS-232 standard. The data format is still to be determined, but the RS-232 standard allows the electrical interface between the instrument and its host to be specified independent of the data format. It will consist of a half-duplex, bi-directional, two wire interface. Power consumption can be minimized by reducing the data rate and terminating the lines with high impedance loads.

The ultimate field test is to mount the resulting spectrometer engineering model on the arm of a rover and collect field data remotely. The most likely vehicle for such a demonstration is the JPL FIDO rover, which replaces the Rocky 7 rover. A small interface box will be constructed to supply power to the instrument and allow it to communicate with the rover via a serial RS232/422 bus. In addition, a mounting bracket will be made to provide a mechanical interface between

APPENDIX -- PCT APPLICATION NO. PCT/US99/07781

spectrometer and rover. The spectrometer's power requirements are well within the rover's capability. Alternatively, if a different field test platform is available, an appropriate interface will be supplied.

E. Laboratory and Field Testing

This task will be performed both by JPL and Ion Optics, Inc. Prior to system integration, each component will be tested in the laboratory. The following performance parameters will be measured:

1) Silicon waveguide (all parameters characterized as a function of wavelength)
   - Grating efficiency
   - Spectral resolution
   - Throughput with f/1 input lens
   - Optical cross talk
2) Thermopile detector array
   - Resistance
   - Responsivity versus wavelength
   - D* versus wavelength
   - Temperature dependence of responsivity
   - Response time
3) Thermopile readout chip
   - Power draw
   - Noise versus frequency for source resistance of thermopile detectors
   - System D* for thermopile array plus readout chip

The complete system will be carefully characterized and calibrated in the laboratory. The instrument response function and signal-to-noise performance will be characterized with blackbody sources in vacuum. Wavelength characterization and calibration will utilize a second spectrometer to provide monochromatic light as well as calibration standards (such as indene and polystyrene) to verify band positions. Stability of the calibration will be tested over the range of temperature conditions expected on Mars (200-300K).

Prior to testing on the rover, instrument performance will be validated on mineral and petrologic suites consistent with candidate surface materials expected on Mars. These samples will be measured in Mars-like conditions (CO_2 atmosphere, night and day temperature range) in the laboratory with artificial illumination. They will also be measured in ambient earth conditions with natural illumination. Furthermore, the instrument will be demonstrated in a variety of field sites which have good exposure of a range of petrographic types (such as evaporites, basalts, carbonates). In order to ensure that the instrument is available for rover integration, two or more spectrometers will be fabricated, permitting laboratory characterization and calibration to continue while one spectrometer is used in rover field tests. Making multiple copies of the instrument is expected to be straightforward.

4. EXPECTED RESULTS

A. Performance Goals

The program's performance goals are (a) detector-readout assemblies with a system D* value of 2×10^9 $cmHz^{1/2}/W$ and (b) a total spectrometer throughput of 65% with an f/1 input lens. Section 2 describes performance of the existing instrument, while section 3 describes the tasks required to reach these much more aggressive performance goals.

B. Noise Equivalent Radiance

In order to calculate the instrument signal-to-noise ratios for various conditions, we first calculate noise equivalent radiance on the target within a spectral band equivalent to one detector (0.05 μm for 3-6 μm and 0.1 μm for 6-12 μm). With a detector area of 75 μm by 1.5 mm, and a system D* for the detectors plus readout of 2×10^9 $cmHz^{1/2}/W$, the noise equivalent in-band power at the detectors, normalized to frequency bandwidth, is 1.68×10^{-11} $W/Hz^{1/2}$. Assuming an integration time of 10 seconds, noise equivalent in-band power at the detectors is 5.30×10^{-12} W. With a 65% throughput for the input lens and silicon waveguide, the noise equivalent in-band input power to the spectrometer is 8.16×10^{-12} W. Two f/1 optics will image the target onto the slit with no magnification. Thus the target size is the same as the slit (75 μm by 1 mm), and the lens acceptance cone is 0.84 steradians, resulting in a noise equivalent in-band radiance from the target of 1.29×10^{-8} $W/(cm^2 ster)$.

APPENDIX -- PCT APPLICATION NO. PCT/US99/07781

C. Survey Mode Signal-to-Noise Ratio

Using the resulting value for noise equivalent in-band radiance at the target, one can predict signal-to-noise ratios for survey mode. Survey mode is illustrated in Fig. 6b, while the projected signal-to-noise ratios for this mode of operation are shown in Fig. 11 Normally incident sunlight is assumed. For reflected radiation, the target is assumed to have unit reflectivity, while for emitted radiation, unit emissivity is assumed. While these two assumptions are inconsistent, the resulting signal-to-noise values allow one to easily determine sensitivities to given changes in surface emissivity/reflectivity. Over most of the wavelength range, even for a cold surface, the signal-to-noise ratio is more than adequate for mineralogical surveys (signal-to-noise requirements are described in section 1A). Higher signal-to-noise ratios can be obtained at the expense of spectral resolution by adding signals from groups of consecutive pixels. Increasing the integration time is another technique for increasing the signal-to-noise ratio.

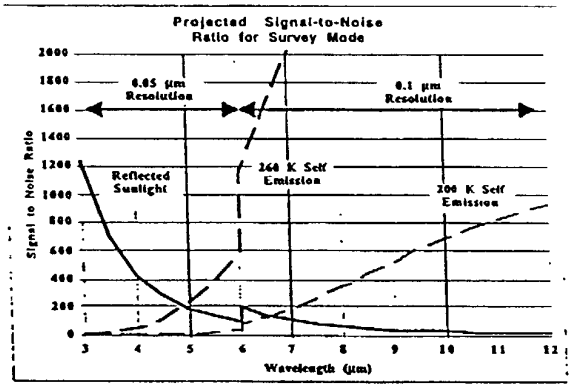

Figure 11. Projected signal-to-noise ratios for survey mode, showing sensitivity to reflected sunlight and thermal emission for typical day and night Mars temperatures. Integration time is 10 s.

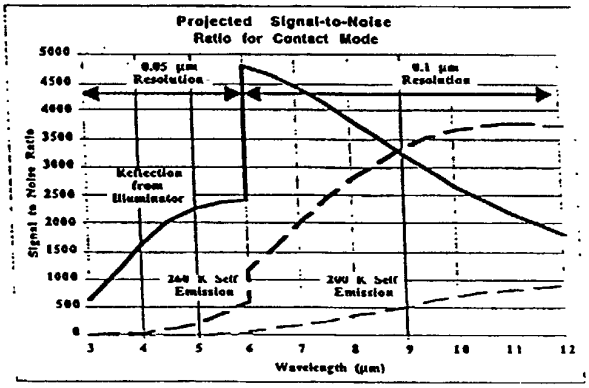

Fig. 12. Projected signal-to-noise ratios for contact mode (Figs. 5 and 6a) with a source electrical power of 60 mW. Integration time is 10 s. The signal-to-noise ratios for thermally emitted radiation are also shown for comparison.

D. Contact Mode Signal-to-Noise Ratio

To calculate signal-to-noise ratios in contact mode (Figs. 5 and 6a), a measure of the reflected illuminator radiance on the target is needed. The illuminator is a filament source produced by Ion Optics, which can be made with high emissivity over the entire wavelength range. Assuming 60 mW of electrical power to the illuminator, 60% efficiency in conversion from electrical power to

APPENDIX -- PCT APPLICATION NO. PCT/US99/07781

filament heat, and a filament emissivity of 0 9, the filament temperature will be 500 K. The 2 mm by 5 mm filament is imaged onto the target with no magnification by an f/1 lens with 90% transmission Combining these numbers with the noise equivalent in-band radiance on target calculated above (1.29×10^{-4} W/(cm^{2}ster)), results in the signal-to-noise ratios shown in Fig. 12. In this mode of operation the signal-to-noise ratio far exceeds the level required to meet the mission science goals (described in section 1A). A higher input power to the source or a longer integration time can increase these values significantly.

An upper limit to the instrument mass can be easily calculated. The predicted volume is 24 cm^3. If we assume that the entire volume is aluminum, at 2.7 g/cm^3, the total mass will be about 65 g. A solid Kovar block, with a density of about 8 g/cm^3, would weigh about 192 g. Since much of the volume is occupied empty space, the mass will be significantly less than these values.

The power budget for this instrument is:

reflectance source	60 mW
thermopile readout chips	100 mW
commercial DSP chip for controlling readout chip	50 mW
Total power	210 mW

5. RELEVANCE OF PROPOSED WORK TO NASA

Sample collection for future sample return is a major focus of the Mars 2003 mission. These samples are slated for return on the Mars 2005 mission. This spectrometer is explicitly designed to provide rapid classification of samples together with the areas from which they are obtained. The instrument is also designed to be inexpensive to duplicate and easy to accommodate on successive missions, so that samples collected on each mission can be readily compared.

The search for evidence of life on Mars is a second significant goal of the missions to Mars. It has been postulated that the best places to search for evidence of life are in areas that were once water rich. This instrument operates in a wavelength region that is suited for detecting evidence of lacustrine environments, including evaporites, clays, and carbonates. It can also detect organic molecules, should they be present.

Understanding the environment on Mars for future manned missions is another major NASA goal. Thermal emission and scattering measurements are suited for characterizing soil size properties down to 2-3 microns. This spectrometer is capable of detecting a wide range of mineralogic and organic biohazards, as well as surface ice deposits, should they be present.

Characterizing the mineralogy and geology of Mars is important for understanding the processes that have shaped Mars. This instrument can be used to differentiate between the mineralogy characteristic of igneous, metamorphic, and sedimentary regimes. The silica content of basalts can be estimated and used to validate viscosities estimated from the morphology of flows. Soil types and aggregations, as well as CO_2 content of the soil can be estimated using a combination of scattering, thermal, and spectral techniques. Soil layers can be measured (using all three techniques) in trenches carved by a rover arm and in modest size boreholes.

In short, the many applications of this miniature spectrograph are relevant for a large number of NASA's objectives for missions to Mars. Many of the measurements that can be performed with this instrument are of fundamental importance for understanding Mars. In addition, these measurements can provide confirmation and redundancy for measurements performed by other instruments that may have higher specificity and risk. This instrument is particularly ideal because it is rugged enough to survive a range of landing techniques and consumes a small fraction of the resources available to a rover.

6. SCHEDULE AND COST

We propose a three year effort costing $919.5k. The schedule is designed to maximize the possibility of having an instrument ready for the Mars '03 launch. Before the Mars '03 proposal deadline, improvements in the three key spectrometer components - silicon waveguide, thermopile array, and readout chip - will be complete and test results will be available. Thus the risk of placing this instrument on the Mars '03 rover or lander will be low. Integration, laboratory and field tests will be performed before the Mars '05 proposal deadline.

The requested funding is $365.9k for FY '98, $356.5k for FY '99, and $197.1k for FY '00. The approximate cost breakdown for each task is: silicon waveguide development - $310k, detector

APPENDIX - - PCT APPLICATION NO. PCT/US99/07781

1. Introduction

In this successful phase 2 SBIR program with JPL, Ion Optics, Inc. is developing a tiny, integrated infrared reflection probe. This device will provide fundamental chemical composition and density information which is important in satellite-based exo-biology and ecological studies. Perhaps the most striking application of this instrument is to extract composition information from soil and rock samples, which is critical to the search for evidence of planetary life on the Mars Pathfinder 2003 mission. The phase 2 SBIR program will produce working prototype instruments, as an intermediate step towards developing and demonstrating a fully miniaturized, extremely low power flight instrument for the Mars 2003 mission.

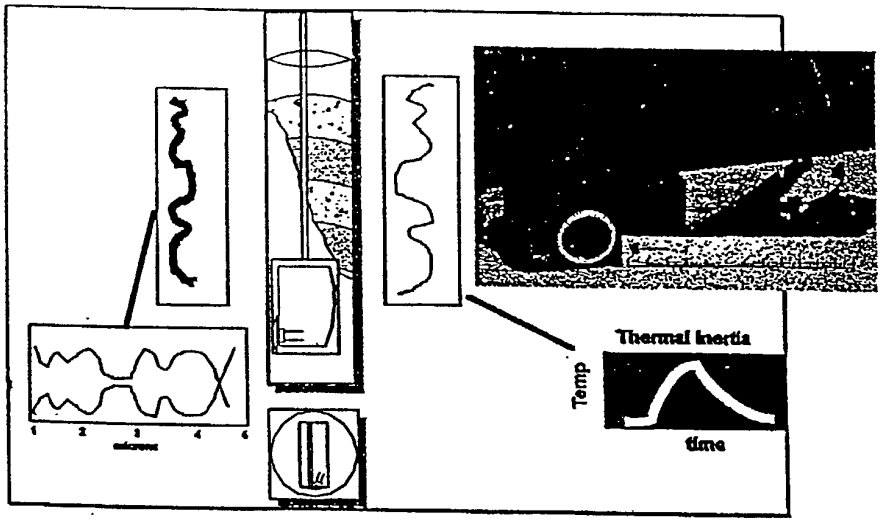

Figure 1 *Schematic of tiny infrared micro-probe arrangement for subsurface exploration on Mars. The miniature solid-state spectrograph and pulsed infrared source allows spectroscopic measurement of spectral lines of specific contaminants as well as local measurements of thermal inertia and soil density. Phase II prototype (inset) is now undergoing final integration and test for delivery in the first quarter of 1998.*

The ultimate purpose of this project is to develop and demonstrate an infrared spectrometer suitable for integration in packages for both Mars Lander and Mars Rover. This instrument is intended to be sufficiently rugged to survive hard landings, small enough to fit in boreholes, light enough to have little impact on the mass budget of landed packages, inexpensive enough to permit a diverse set of instruments on a landed package, and to have sufficient resolution and performance to identify the mineralogy of rocks and soils, to help select a suitable range of materials for sample return and to search for evidence historic environments which may have been capable of supporting life.

APPENDIX -- PCT APPLICATION NO. PCT/US99/07781

IOI/Sensor Development Corp.
Solid State Infrared Spectrograph

Infrared spectral information is critical to understanding Martian geology and evidence of conditions for life. Infrared spectrometers are particularly suitable for rapidly characterizing differences in mineralogy of a large number of rocks and extensive areas of soil. They are most powerful, in the in-situ environment, when used in combination with instruments which can unequivocally (though at a slower pace) identify elemental compositions and crystal structures. IR spectrometers are also very useful for micro-thermometry and micro-calorimetry (powerful techniques for differentiating rocks) because a color temperature can be obtained. In the search for environments which may have supported life on Mars, the infrared region from 1 to 10 microns is particularly useful for detecting evidence of past aqueous environments. This is due to the multitude of bands in this wavelength region related to clays, evaporites, and carbonates.

2. Technical Accomplishments

Most of the effort this month has focused on the fabrication of the silicon waveguides. In particular, we have had to work closely with the vendor etching the grating in order to work through design and processing issues. We have now received the etched gratings and the waveguides are being AR and gold coated. In parallel with this activity we continue to work on the signal processing software and electronics. We have slowed the effort on the neural network software pending collection of test data from the unit under development.

2.1 Spectral Analysis

One of the unresolved issues concerned the required dynamic range required when making our spectral measurements. That is, what the resolution of the analog to digital conversion needed to be when measuring spectral peaks, in order to differentiate between different concentration levels. The result of the calculations showed that a 16 bit analog to digital (A/D) should provide the necessary accuracy to resolve absorption's from 200K ppm (water) to 5-10 ppm of No_x. If we examine the range provided by a 16 bit A/D, we get 2^{16} bits available to represent a range from 200K (signal intensity (linear extrapolated) to 60 specs) to 5 ppm resolution (signal intensity (linear extrapolated) to 0.0009 specs).

$2^{16} = 65{,}536$

$60/65{,}536 = 0.000915$ Spec/ppm

$0.000915/0.00018$specs $= 5.08$ ppm-resolution

Where 0.00018 specs is the intensity for 1 ppm of No_x using MIDAC measurements and 0.000915 is the minimum resolution provided over a range from 0 to 60 for a 16 bit A/D with all 16 bits used to represent data. These calculations indicate that the minimum resolution of No_x will be 5.08 ppm.

2.2 Optical Front End Fabrication

As reported, we placed orders for the fabrication and processing of the silicon waveguides. Because of the uniqueness of the design, our vendors have had some difficulty in processing the parts. However the parts have now been machined to there desired shape and the diffraction gratings applied. The parts have been inspected and ship to the last vendor for AR and gold coating.

APPENDIX -- PCT APPLICATION NO. PCT/US99/07781

IOI/Sensor Development Corp.
Solid State Infrared Spectrograph

2.2.1 Silicon Waveguide Processing

Computer Optics was contracted to machine the silicon blanks to their final shape before the diffraction grating was applied. They were also tasked with developing a fixture that would facilitate polishing and handling, and also applying the diffraction grating to twenty blanks simultaneously. A picture of this fixture and the waveguides appears in Figure 2.1 Using this fixture, and scrap waveguide blanks, they refined the polishing process and delivered finished pieces in early October.

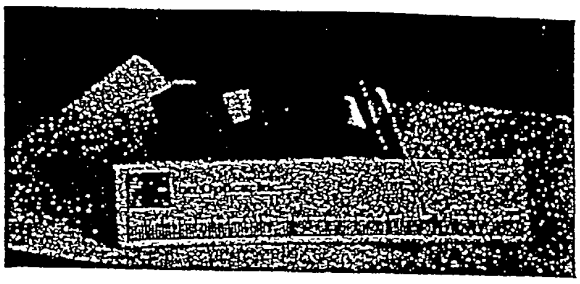

Figure 2.1 *Silicon waveguides mounted in polishing fixture.*

2..2.2 Grating Application

The fabrication of the gratings required three steps, spin coating the photoresist onto the blocked up benches, exposing the hologram into the resist, and then transferring the hologram into the silicon via ion beam etching. All three of these steps required very careful preparation, testing and finally execution.

The photoresist spin required the fabrication of a special spin rig to handle the heavy and cumbersome silicon block. The block was carefully cleaned to remove surface contaminant from the edges of the pieces. Special adaptations were made to the blocking fixture to allow for the differential expansion of the silicon and the aluminum block.

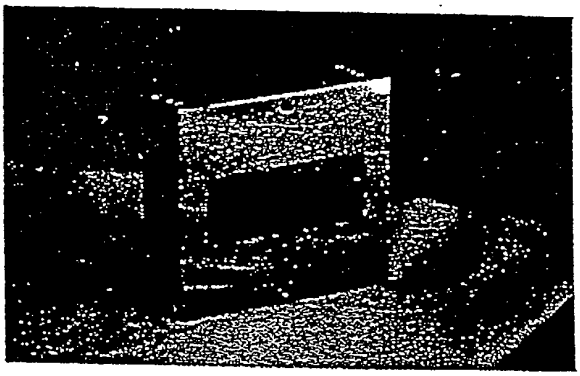

Figure 2.2 *Contaminants from the small spaces or "cracks" between adjacent waveguides destroyed the original grating mask.*

The hologram required extensive exposure testing and precise alignment on the optical table. Numerous test were made on trial pieces and ion etch rates determined. Finally the exposure was made and the hologram processed. The block was then baked to set the resist. At this point, contaminants that had been contained between the slab layers migrated from between the slabs and destroyed the hologram. It is hypothesized that the extra thirty degrees of baking temperature caused the appearance of these contaminants.

It was decided to remove the hologram, re-clean the surface and then re-coat and reprint the hologram. Because of the set up time required to re-shoot original holograms, the second hologram was done as a reprint from a master. This lowered its fidelity, therefore we expect a reduced efficiency in the grating, from 70% down to 45%.

APPENDIX -- PCT APPLICATION NO. PCT/US99/07781

IOI/Sensor Development Corp.
Solid State Infrared Spectrograph

The second hologram was successfully etched into the surface measured and delivered to Computer Optics for final coatings.

The finished pieces with the machined gratings appears in figure 2.3. It appears that at least 10 of the waveguides look very good and that there are another 6 or so that are usable. In order to minimize risk, we have decided to coat only 10 of the devices and hold the others in reserve. The coating process involves applying an anti-reflection coating to the flat surface to allow scattered light to easily escape, and to gold coat the diffraction grating and back cylindrical surface. We expect to received finished pieces before the end of the year.

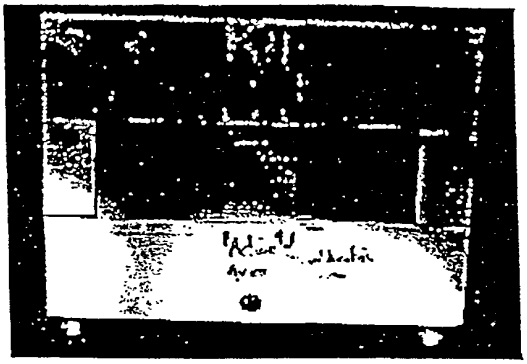

Figure 2.3 *Photograph of silicon waveguides with the diffraction grating applied. The grating can be seen in the center of the waveguides.*

APPENDIX -- PCT APPLICATION NO. PCT/US99/07781

IOI/Sensor Development Corp.
Solid State Infrared Spectrograph

2.3 Detectors

We've received the first PbSe detector array with the multiplexer. Although there were some minor mechanical alignment problems, these have been resolved. However we were not able to successfully test the finished assembly, it appears that the problem lies in the drive electronics. We have returned the assembly back to the vendor for additional testing.

We also received a 64 element micro-thermopile detector developed by JPL under another program. We plan to integrate this detector into our unit and evaluate its performance. There are many advantages to using the micro-thermopile: it is sensitive over a wide range of wavelengths, it does not suffer from 1/f noise and so does not require a chopper, and it does not have to be cooled. Conventional thermopiles are not as sensitive as a PbSe detector, however this device has a measured D* of 1.4 x 10^9. We are also investigating using a custom multiplexer/readout circuit being designed at Hypress (Stanford Conn.) for a micro-thermopile under development at Hypress. We have built a breadboard circuit and installed the micro-thermopile array in our optics housing. However at this time we are only using a small number of channels, for test purposes, until the multiplexer becomes available.

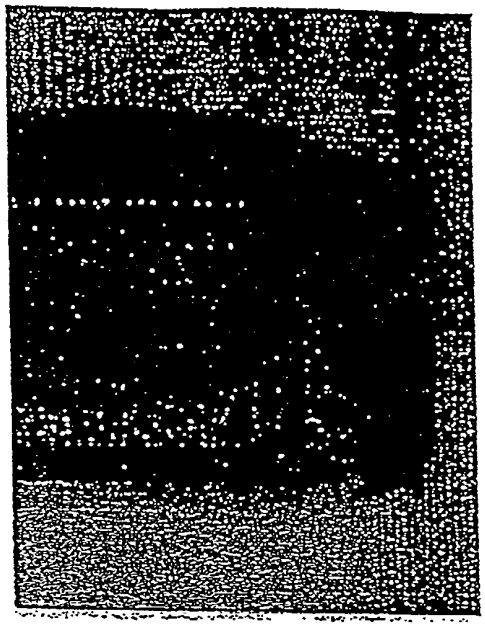

Figure 2.4 ***This photograph shows a portion of the PbSe detector array. The long thin rectangular shape of each pixel is clearly visible.***

2.4 Processing

Significant progress has been made in the development of the signal processing software. As discussed last quarter, we plan to use digital signal processing (DSP) techniques in order to extract the modulated signal from each detector element. The neural network software being developed for determining chemical concentrations based on the spectral content is also most efficiently processed on a DSP. We are using an evaluation board for the Motorola DSP56L811 from Motorola as a development platform. This processor will perform the signal processing necessary for signal extraction and chemical detection and can also control a display and keypad; a serial interface will be used for communication with an external computer. This processor was only recently introduced; software development has been hampered because of the immaturity of the development tools. However, these problems have been addressed, and various algorithms implemented and tested.

APPENDIX - - PCT APPLICATION NO. PCT/US99/07781

IOI/Sensor Development Corp.
Solid State Infrared Spectrograph

2.5 Mechanical

The design of the optical housing and associated components has been finalized and the parts have been received. We are currently in the process of assembling an optics housing using a spare unpolished waveguide (see 2.5). The optical housing has a removable cover that will permit the components to be aligned prior to the cover being applied. The cover contains the entrance window with a replaceable cutoff filter. This filter can be replaced accommodating different spectral bands. The package also incorporates a mount to hold the input lens or a fiber optic input.

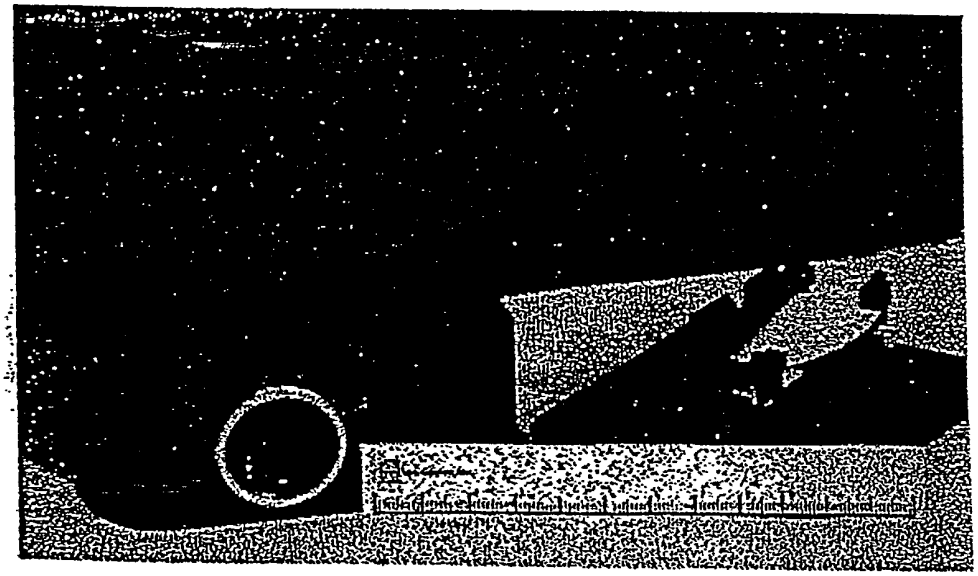

Figure 2.5 ***Photograph of the completed optical housing and base. A silicon waveguide has been mounted to the base with the chopper and beam dump. The I/O connector is visible mounted to the base under the waveguide.***

2.6 Commercial Development Marketing

We have recently hired a consultant to assist in the marketing of our micro-spectrometer. We are researching who our potential customers may be (beyond those we have already identified) and what features they would like to see. We have also held discussions with a potential partner in the manufacture and marketing of a micro-spectrometer. Textron Systems, Wilmington Ma., has expressed considerable interest in our product. This partnership could be particularly significant in that Textron/Opto, a sister division, is a potential source for the PbSe detector array. This partnership may help us procure a detector/multiplexer assembly at a significantly reduced cost.

APPENDIX -- PCT APPLICATION NO. PCT/US99/07781

IOI/Sensor Development Corp.
Solid State Infrared Spectrograph

3. WORK PLANNED FOR NEXT QUARTER

3.1 Silicon Waveguide Fabrication

We expect to receive the finished silicon waveguides the last week in December. They will be characterized for spectral resolution, through-put, and scattered light.

3.2 Optical Chopper

We have received the chopper assembly. We shall be testing and integrating them shortly.

3.3 Detector Assembly

We have received the 64 element PbSe array and multiplexer from NEP however it was returned for repair. When the assembly arrives we will characterize the performance of the detector and readout electronics including D*, responsivity, pixel to pixel uniformity, and frequency response.

3.4 Assembly Test and Integration

We have started the assembly of the optical housing. As new components arrive, they will be integrated into the housing. We expect to have a fully assembled optical housing by the third week in January. At that time, data will be collected for data processing and system characterization.

APPENDIX -- PCT APPLICATION NO. PCT/US99/07781

1. Introduction

There is considerable topical interest in the content of Martian soils and sub-soil composition and particularly in establishing the presence or evidence of past water, carbonate minerals, or organic matter. Because of the problems of oxidation leaching in the near surface and the constant surface recovering by dust storms, it is extremely desirable to obtain composition and structure data at some depth below the surface. Typical procedures include sampling soil or core via drilling, extracting these samples and performing some sort of ex-situ analysis on the intact core samples. This requires specialized drills to extract the core samples, and even then, it is difficult to keep the core samples intact and to establish the sample orientation for measurement. We propose to enable downhole measurements which will extend the capability of these remote Martian probes with a tiny, rugged reflection analyzer instrument so small that it can make measurements from inside typical boreholes from soil and core sampling drills.

Phase I demonstrated the feasibility of a compact, rugged, lightweight spectrograph operating at room temperature in the 2-to-5 μm wavelength range. The critical innovation is the spectrometer's completely solid state construction – it can be assembled entirely from micro-machined silicon components (even the MWIR detector arrays can be made of silicon). The resulting instrument has the advantages that it can be made very small and very light (about an inch in diameter and weighing a few grams), is permanently aligned for operation over a broad spectral range, and is extremely resistant to damage resulting from harsh environments (launch vibration, aggressive chemicals, radiation). The Phase II instrument will be approximately ¼ the size of the Phase I instrument with higher spectral resolution, lower noise , and more sophisticated signal processing and control.

We have continued to make good progress this quarter on the fabrication of the phase II instrument. Orders have been placed for the fabrication and processing of the micro-machined silicon waveguide, the detectors, the housings and mechanical mounting hardware. We have procured the computer processing board and software development is well under way. However the micro-machining of the silicon waveguide has proved more difficult than anticipated. Although our vendors are confident that these manufacturing difficulties can be overcome, it has caused a small slip in schedule.

2 System Design

From the analysis of the Phase I device and the results of our system models we have developed an improved design that will greatly increase the utility of the spectrometer. We previously completed the baseline silicon block spectrometer optic design. It uses a modified 'Ebert' layout fabricated from micro-machined silicon, with an F/1 input design (Figure 2.1)

In the 'D' shaped optic, IR light enters the entrance slit, a thin film deposited A/R coated area, and illuminates a cylinder mirror which collimates light. The high refractive index of silicon greatly reduces the angle of the cone of light, this permits the use of an F/1 lens at the entrance aperture. It also reduces the size of the cylinder mirror and permits the spectrograph to operate near the diffraction limit. The collimated beam is reflected off a gold coated diffraction grating.

The grating disperses the IR spectrum which is re-imaged after a second reflection off the cylinder mirror. The light exits the block through an AR coated surface and is imaged onto the detector plane. The detector plane is at a slight angle in order to flatten the field across the image. The air gap permits the detector plane location to be adjusted, allowing for manual focusing. As the rays exit the block, the large cone angle of the rays is restored, fully filling the acceptance angle of the detector.

APPENDIX -- PCT APPLICATION NO. PCT/US99/07781

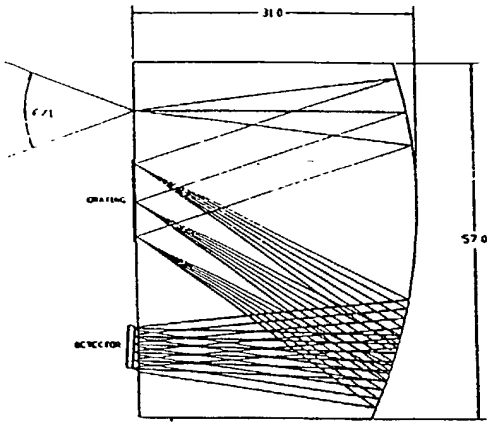

Figure 2.1 *Phase 2 optical bench raytrace. This layout has only two optical surfaces, greatly simplifying fabrication and increasing reliability by eliminating tolerance stack up inaccuracies. The flat grating design increases grating efficiency and makes the device easier to manufacture. Its F/1 design allows for twice the through put of the Phase 1 design, and its air gap at the detectors provide for focusing and permit the use of conventional AR coats.*

The grating produces a number of lower energy unwanted diffraction orders. In our earlier design these orders were trapped in the block and were scattered and added to unwanted background signal on the detector. The new design permits the exit of these unwanted orders out of the flat surface where they will be captured by a light trap. The components themselves incorporate a number of advanced design features. In particular the diffraction grating is made with a variable line density or "chirp" to flatten the Rowland circle and provide a flat focal plane for the array. The slab waveguide is formed to include mounting surfaces for other components and includes baffling and beam dumps. Since the silicon is opaque to photons above its bandgap, the slab excludes visible light from the detector. Silicon's high refractive index provides lossless reflections at the polished top and bottom faces of the device, waveguiding the radiation in the plane of the device. However, more important, because of the high index of the silicon, the cone of incident illumination is dramatically smaller inside the device. This provides better optical throughput than can be achieved with an open-air design. In addition, for measurements at longer wavelengths, the entire spectrograph can readily be cooled on a single cold-finger, in much the same way that focal plane arrays are now cooled in conventional instruments.

APPENDIX -- PCT APPLICATION NO. PCT/US99/07781

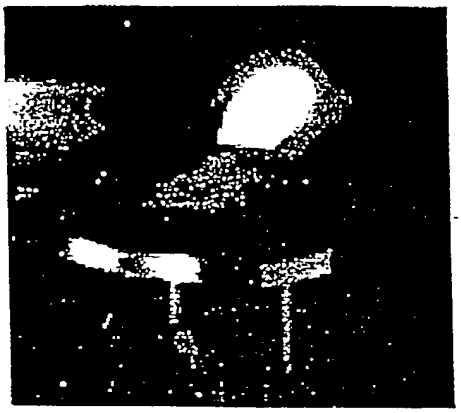

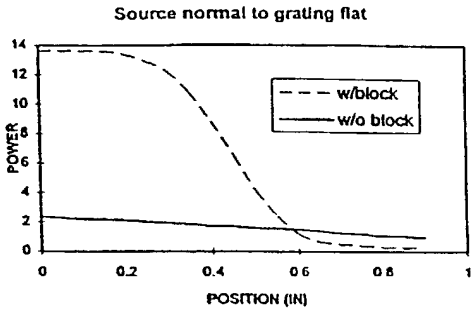

Figure 2.2 *The central innovation which makes the design of the instrument possible is the high-index slab waveguide. Refraction at the entrance slit sharpens the entrance cone and improved throughput, as shown in the thermal image and line scan data.*

3. Technical Accomplishments

This quarter, the major effort for the program shifted from the analysis and design of the instrument to the fabrication of the optical components and detectors and development of the signal processing and interface software. In parallel with this effort, our subcontractor NeuroDyne has continued with its efforts extracting chemical compositions from measured spectra. A detailed discussion of our accomplishments follow.

3.1 Spectral Analysis

The mid infrared waveband operating range of the phase 2 instrument should reveal the presence of many of the scientifically important CO_2 and H_2O along with Fe^{3+} minerals, distinguished by Cpx - Opx, and Olivine. Observations of the C-H stretch band at 3.4 micron wavelength and bound water in the 2.5-3.5 micron band should also confirm the likely presence of organic materials and/or hydrated minerals. The ability to resolve characteristic carbonate absorption bands in the 3.2-4.4 micron waveband and sulfates in the 1.3-3.6 micron region should provide the ability to distinguish various clays and micas. This is illustrated in 3.1 by an FTIR spectrum obtained in our laboratory from a calcite sample furnished by JPL.

APPENDIX -- PCT APPLICATION NO. PCT/US99/07781

IOI/Sensor Development Corp.
Solid State Infrared Spectrograph

Figure 3.1 *FTIR reflection spectrum of a representative calcite rock furnished by JPL. In this figure the high resolution spectra obtained from FTIR spectrograph indicate that the fundamental absorption bands are quite broad and may be resolved by the 64 channel spectrograph.*

For the instrument under development, a spectral range of 3.17 to 5.5 microns has been selected with a resolution of 0.034 microns. This range is acceptable for measuring hydrocarbons, CO, CO_2,and NO. Experimental spectral measurements have been made for NO, CO, and CO_2 at different concentration levels. These measurements were made independently and as such, the spectra had to be assembled to resemble measurements with all three constituents present. In the initial processing, the CO, CO_2, and NO data were added together uncorrelated and then treated independently. Thus NO could increase or decrease independent of CO or CO_2 levels.

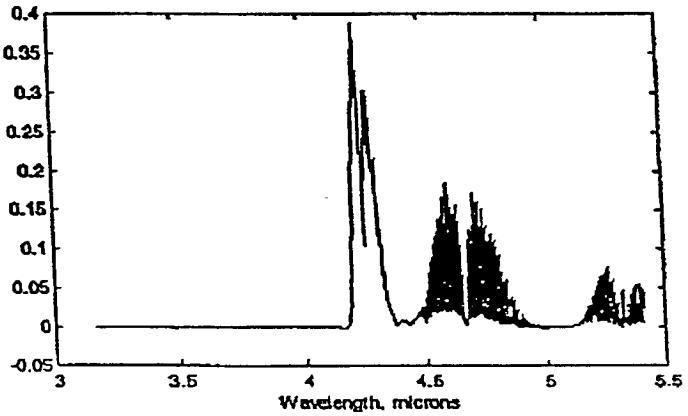

Figure 3.2 *Mean of spectral intensities over 4560 samples of absorption measurements. Note the characteristic peaks corresponding from left to right for CO_2, CO, and NO.*

APPENDIX -- PCT APPLICATION NO. PCT/US99/07781

IOI/Sensor Development Corp.
Solid State Infrared Spectrograph

3.2 Optical Front End Fabrication

Due to the uniqueness of the design we have worked closely with our vendors to develop a fabrication plan that is consistent with the inexpensive mass production of the front end. This process was discussed in the last report. A brief summary follows:

Optical blanks. "D" shaped optical blanks are purchased from VA Optical, a silicon supplier. The near net shape will include all the polished flats but not the cylindrical surface.

Cylinder. The blanks will be sent to Digital Optics Corporation who will stack twenty parts into a monolithic block then shape the block into a cylinder lens. They possessed the interferometric equipment necessary to measure and produce the necessary surface on the cylinder mirror. They will gold coat the mirror and AR coat the flat.

Grating. The gratings will be built by Diffraction Limited. They will produce a grating in photoresist on the surface and etch it into the silicon. They will also work with the elements assembled in a stack. Once the grating is made they will add gold reflector overcoat and deposit the entrance slit.

Assembly. The part will be returned to Ion Optics where its performance will be measured. This is done by feeding the block with a lab spectrometer and measuring the quality of the output image with an IR camera. Once its performance is verified the device will be integrated into the housing with the detector and focused.

We have now placed orders with all three vendors. Although we had to rejected the first optical blanks supplied by VA optical due to surface defects, they have now delivered new devices that are much higher quality. Any remaining defects will be removed during the polishing phase of the processing. Computer Optics has fabricated a jig for holding the devices during processing. Using this jig, and scrap waveguide blanks, they are refining the polishing process. In the meantime, Diffraction Limited has been modeling the grating design and testing their etch process, again using scrap waveguide components. Successful processing of these the optical waveguide requires a close coordination between Ion Optics, Computer Optics, and Diffraction Limited. Communication between Diffraction Limited and Computer Optics has been hampered because of Diffraction's location in Waitsfield Vt. We are closely monitoring the progress of both vendors and have facilitated communication between them. However this issue, and problems Computer Optics has had in refining the machining process has caused a delay in the delivery date of the machined waveguides. While communicating frequently with our vendors, we have been working to both reduce the delay in the delivery of these components and its effect on the program.

3.3 Mechanical

The spectrometer design requires the precise alignment of the optical bench, the chopper, the detector array, filter, and input lens. This is all accomplished with a precision sealed package. The package holds the chopper, filter and detector in position and provides for a vacuum seal.

APPENDIX -- PCT APPLICATION NO. PCT/US99/07781

IOI/Sensor Development Corp.
Solid State Infrared Spectrograph

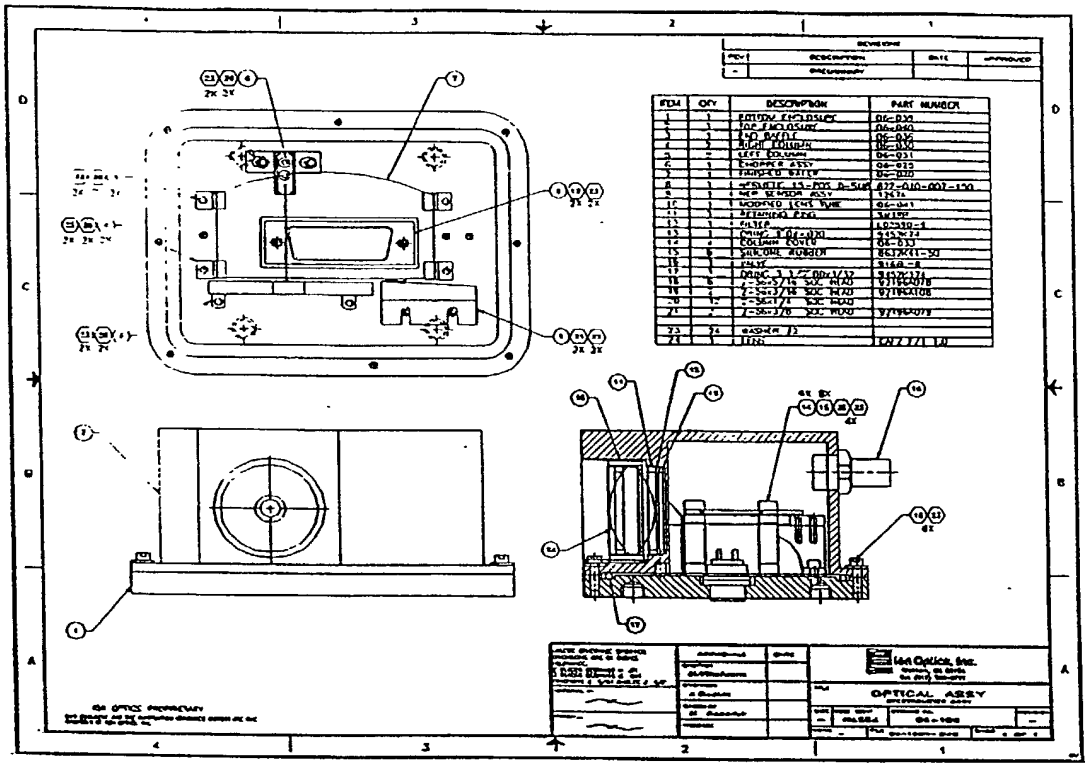

Figure 3.3 *The design of the optical housing and mounts is essentially complete. This drawing shows the assembly drawing for the optical housing.*

The design of the optical housing and associated components has been finalized and the parts sent out for quotation. We have also completed the detail design on most of the other mechanical components and have started to receive fabricated components. The spectrometer tree below details the components necessary to build the instrument and their relationship.

Now that a plan is in place for the detector readout electronics, the layout and packaging of these elements has been completed. Cooling the PbSe array and providing an interface to the readout electronics within a small volume complicates the mechanical design. Because we want to cool the detector assembly itself, not the readout electronics, we must mount the PbSe array directly on the TE cooler with the multiplexor circuit close by. The detector assembly must be adjusted relative to the optical waveguide in order to optimize the detection of the refracted radiation. While working closely with the detector vendor, we optimized the design for both optical and electrical performance while striving for a design that is easy to assemble and adjust while being small and cost effective.

APPENDIX -- PCT APPLICATION NO. PCT/US99/07781

IOI/Sensor Development Corp.
Solid State Infrared Spectrograph

Spectrometer Tree
Ion-Optics

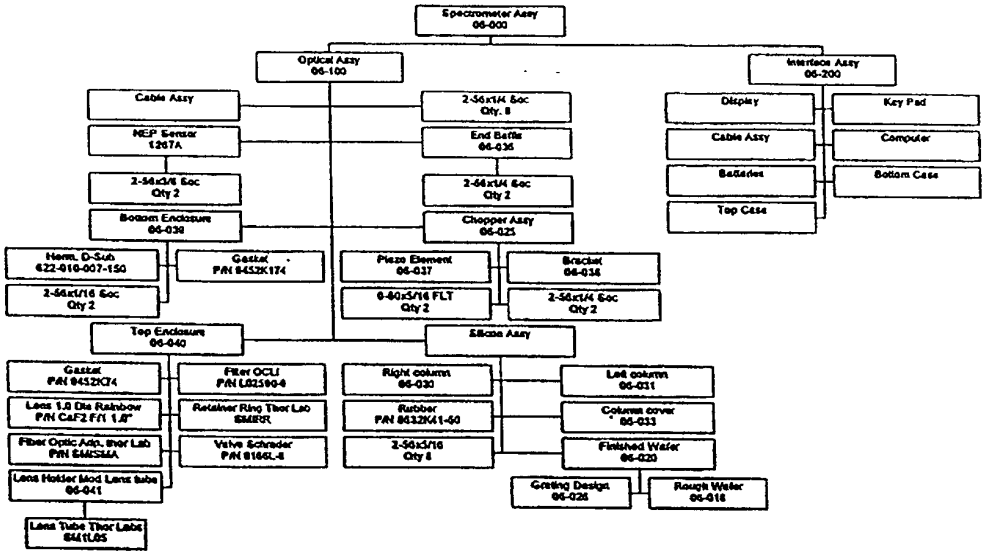

Figure 3.4 *The spectrometer tree identifies all the subassemblies of the miniature spectrometer and their relationships.*

The optical housing has a removable cover that will permit the components to be aligned prior to the cover being applied. The cover contains the entrance window with a replaceable cutoff filter. This filter can be replaced accommodating different spectral bands. The package also incorporates a mount to hold the input lens or a fiber optic input.

3.4 Optical Chopper

The chopper consists of a two layer piezo-electric modulator. The deflection at the tip of the device depends on the bias voltage applied. By applying a time varying waveform to the device, a flag at the tip of the device alternately opens and blocks the entrance slit of the silicon waveguide. We have designed the device to operate from 200 to 350 Hz. A vendor has been selected and the element ordered. After fabrication it will be mounted on a base and tested.

APPENDIX -- PCT APPLICATION NO. PCT/US99/07781

IOI/Sensor Development Corp.
Solid State Infrared Spectrograph

3.5 Detectors/Readout Electronics

As discussed last quarter, we have selected a PbSe detector and selected a linear detector array vendor. However, we have spent considerable time evaluating a new custom multiplexor designed by our vendor. In order to optimize the performance of the PbSe detector it is customary to modulate or chop the optical signal in order to avoid 1/f noise in the detector. A

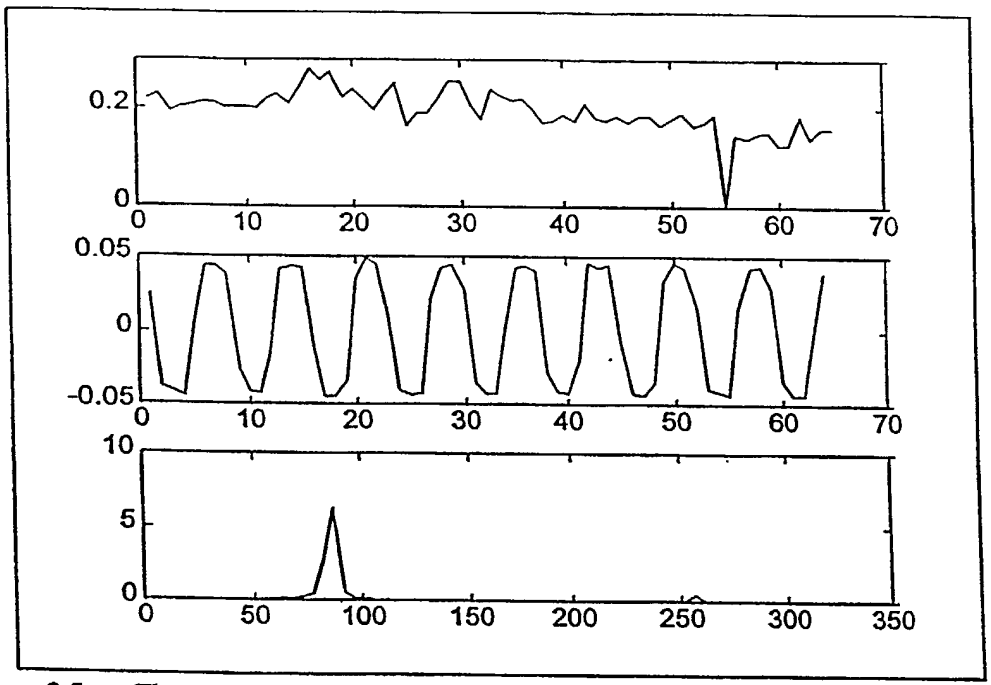

Figure 3.5 *The top trace shows the raw multiplexed data from all pixels during a single frame. The middle trace corresponds to the signal on a single pixels over many frames after the data has been unpacked. The modulated input signal is clearly evident. The bottom trace is the power spectral density for the modulated signal.*

lock-in amplifier is then used to recover the modulation and narrow band the signal. This process is greatly complicated by the use of the multiplexor. We proposed last quarter that we would use a digital detection scheme to accomplish the same result. This involves directly digitizing the multiplexor output and then using digital signal processing techniques to narrowband the signal. Figure 3 illustrates the process. Synchronizing the A/D clock with the pixel clock, the serial data output of the multiplexor is sampled. Consecutive samples in time for each pixel are assembled to form a sampled waveform for each and every pixel. The modulation signal can then be identified and measured using Fourier transform analysis techniques.

In performing our measurements, we found that we could not accurately calculate D* due to the limited performance of our data acquisition system. The noise contributed by the data acquisition system dominated the D* calculation. The calculated D* was only $5*10^7$, orders of magnitude less than our expected value for an un-cooled PbSe detector. (In order to simplify the measurements, the initial tests were performed with an un-cooled array.) However, recognizing

APPENDIX -- PCT APPLICATION NO. PCT/US99/07781

IOI/Sensor Development Corp.
Solid State Infrared Spectrograph

the limitations of the data acquisition equipment, we were nonetheless encouraged enough by the performance of the multiplexed array to proceed with the procurement of the detector array with the custom multiplexor. We will work closely with the detector vendor in the design and layout of the multiplexor circuit and design data acquisition for the instrument compatible with its expected performance.

There is a large DC offset associated with each pixel due to dark current and background radiation. We will subtract this bias on a pixel by pixel basis, multiply the resulting signal by a fixed gain, and then digitize the signal. This will greatly reduce the dynamic range requirements on the A/D and allow the detection of low level signals in the presence of large background offsets.

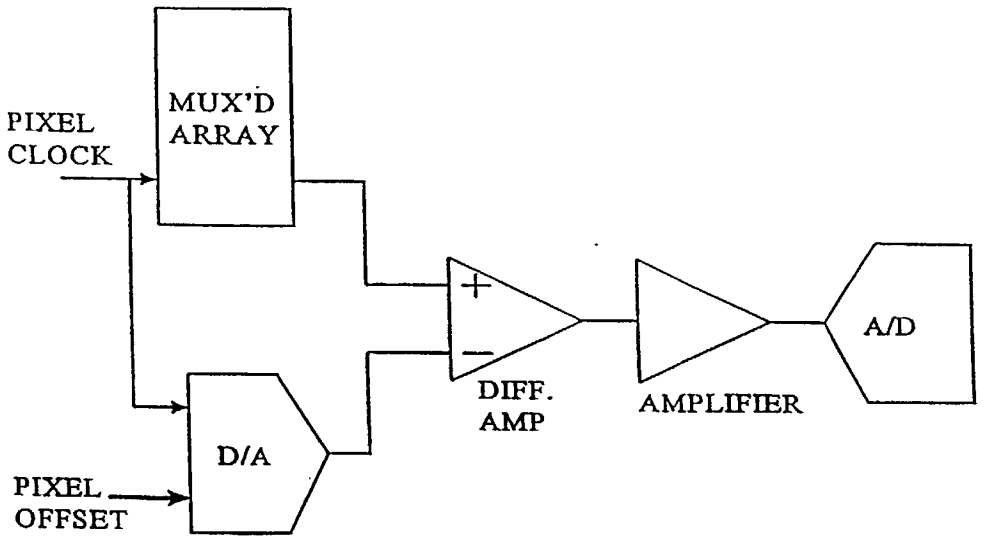

Figure 3.6 *Pixel to pixel offsets can be extracted and the signal amplified improving the dynamic range of the measurement.*

We continued to monitor the development of a 64 element micro-thermopile detector under development in a separate JPL-sponsored effort. There are many advantages to using the micro-thermopile: it is sensitive over a wide range of wavelengths, it does not suffer from 1/f noise and so does not require a chopper, and it does not have to be cooled. Conventional thermopiles are not as sensitive as a PbSe detector, however scientists at JPL believe that they can produce a micro machined thermopile, in the configuration we desire, with a D* of 10^9, equivalent to un-cooled PbSe. Although this device is experimental, we hope to incorporate this device into a prototype spectrometer and evaluate its performance. Although we believe we need the sensitivity of a PbSe detector at this time, the micro-thermopile is a very attractive alternative, that could be used in spectrographs that range from 1 - 20 μm (the full IR spectrum).

APPENDIX -- PCT APPLICATION NO. PCT/US99/07781

IOI/Sensor Development Corp.
Solid State Infrared Spectrograph

3.6 Processing

The continued growth of the digital signal processing market has resulted in a number of low cost DSP processors for embedded applications. After examining the requirements for the signal processing and concentration extraction algorithms, we have chosen the DSP56L811 from Motorola. This processor is a cost-effective solution that combines the prodigious number crunching of a digital signal processor with the versatile functionality of a microcontroller. This processor will perform the signal processing necessary for signal extraction and chemical detection and can also control a display and keypad; a serial interface will be used for communication with an external computer. An off-the-shelf development board has been acquired which will facilitate the rapid development of the spectrometer processing unit. A compiler has also been acquired for software development in 'C'. Benchmark tests performed on the processor at Ion Optics have verified the performance of the processor in our application.

4. WORK PLANNED FOR NEXT QUARTER

4.1 Silicon Waveguide Fabrication

We expect to receive the finished silicon waveguides by the end of Oct. They will be characterized for spectral resolution, through-put, and scattered light.

4.2 Optical Chopper

A vendor has been selected and the piezo-electric element ordered. We expect to receive and test the chopper assembly shortly.

4.3 Detector Assembly

We are awaiting delivery of the 64 element PbSe array and multiplexor from NEP which is due the end of September. At that point we can characterize the performance of the detector and readout electronics including D*, responsivity, pixel to pixel uniformity, and frequency response.

4.4 Assembly Test and Integration

With the delivery of the silicon waveguides, PbSe detectors, optical housing and mounts expected in October, the optical front end will be assembled and tested. Data will be collected for data processing and system characterization.

4.5 Phase III Product Evaluation

To investigate commercial markets for this spectrographs we have contacted several spectrograph vendors, and started a market survey of users. To assist in this we have produced a preliminary spec sheet showing two embodiments of the device. The first is the handheld spectrometer and the second is the OEM bench. In the coming months we hope to refine these specs by contacting various potential end users and OEM customers.

APPENDIX - - PCT APPLICATION NO. PCT/US99/07781

1. Introduction

NASA has a need for low-cost, low-power, low-mass, highly integrated spectral data acquisition instruments that enable space science observations from small and micro-spacecraft Phase I demonstrated the feasibility of a compact, rugged, lightweight spectrograph operating at room temperature in the 2-to-5 μm wavelength range. The critical innovation is the spectrometer's completely solid state construction – it can be assembled entirely from micro-machined silicon components (even the MWIR detector arrays can be made of silicon). The resulting instrument has the advantages that it can be made very small and very light (about an inch in diameter and weighing a few grams), is permanently aligned for operation over a broad spectral range, and is extremely resistant to damage resulting from harsh environments (launch vibration, aggressive chemicals, radiation).

This past quarter we have made considerable progress in the design and fabrication of the next generation instrument. This instrument is about ¼ the size of the device currently operating in our laboratory. A detailed system analysis has been performed and validated the basic design. In some cases we have modified our design based on this analysis and our experience fabricating the phase 1 instrument. We are now beginning to place orders for the optics, detectors, and other long lead items. We anticipate beginning test and integration of the next generation device early next quarter.

2. Technical Accomplishments

Significant progress has been made this quarter. System modeling and concept design for the new instrument have been completed. A detailed discussion of our accomplishments follow.

2.1 Reevaluation of Phase 1 Spectrometer

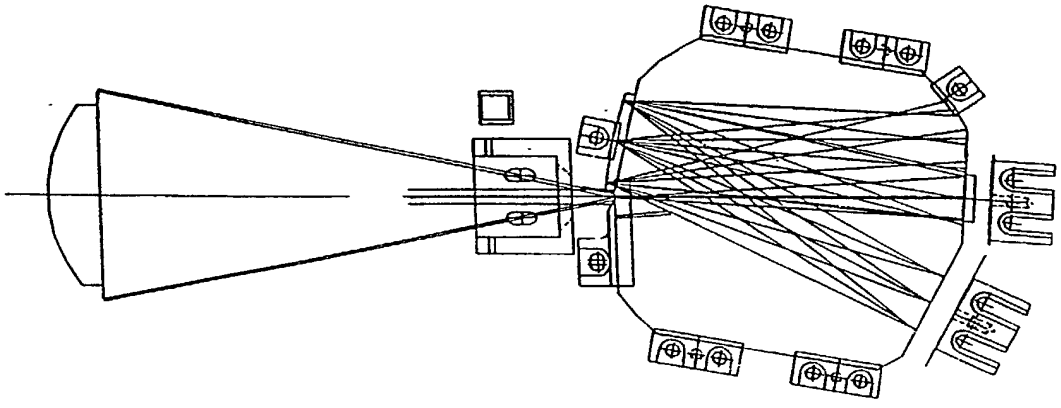

Figure 2.1 Phase one optical bench and lay out showing grating, detector plane, chopper, and filter.

APPENDIX -- PCT APPLICATION NO. PCT/US99/07781

The components themselves incorporate a number of advanced design features. In particular the diffraction grating is made with a variable line density or "chirp" to flatten the Rowland circle and provide a flat focal plane for the array. The slab waveguide is formed to include mounting surfaces for other components and includes baffling and beam dumps. Since the silicon is opaque to photons above its bandgap, the slab excludes visible light from the detector. Silicon's high refractive index provides lossless reflections at the polished top and bottom faces of the device, waveguiding the radiation in the plane of the device. However, more important, because of the high index of the silicon, the cone of incident illumination is dramatically smaller inside the device. This provides better optical throughput then can be achieved with an open-air design. In addition, for measurements at longer wavelengths, the entire spectrograph can readily be cooled on a single cold-finger, in much the same way that focal plane arrays are now cooled in conventional instruments.

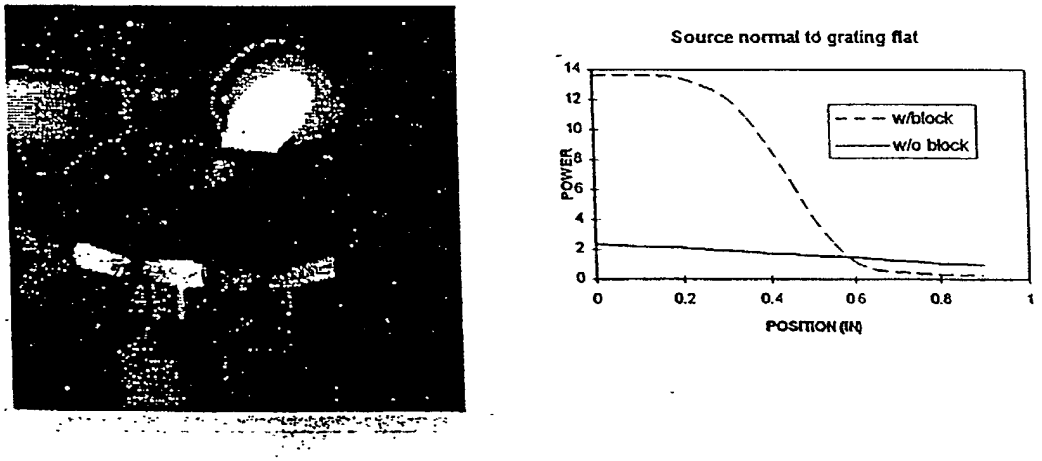

Figure 2.2 *The central innovation which makes this possible is the high-index slab waveguide. Refraction at the entrance slit sharpens the entrance cone and improved throughput, as shown in the thermal image and line scan data.*

The phase 1 block spectrograph was reevaluated to uncover the lessons learned and to find areas of improvement for the phase two miniaturization redesign. The following lists some of the key points:

•*Size* - The Phase 1 design is too large, does not provide an advantage over more conventional designs, and is relatively complex and expensive to manufacture.

•*Facets* - The Phase 1 block had 4 active facets, which were at precise odd angles to one another, two of which require AR coating.

•*Fabrication* - The Phase 1 design called for the grating to be fabricated onto a cylindrical surface whose radius was smaller than the block. This proved impossible to fabricate, since it would require acute inside corners in the silicon block. In the Phase 1 design we solved this problem by applying the curvature to an external piece and contact coupling it to the block. This functioned correctly but proved to be lossy and provided reflection ghosts in the system.

APPENDIX -- PCT APPLICATION NO. PCT/US99/07781

IOI/Sensor Development Corp.
Solid State Infrared Spectrograph

•*Grating Design* - The design utilized a chirped grating to flatten the image field of the Rowland circle optical design. This required an expensive holographic setup. The curvature of the grating substrate made it difficult to etch the grating into the silicon uniformly, resulting in uneven optical efficiency across the grating.

•*Readout Electronics* - The 16 channel lock-in amplifier of the Phase 1 device was superior in performance to the digital lock-in initially used. However it required two 4" x 6" PC boards, much too bulky for the Phase 2 miniature device.

•*Chopper Design* - The tuning fork chopper used in the Phase 1 device has magnetic coil drivers, which radiate EM interference. This interference is at the chopping frequency and can not be filtered from the signal. This is an intrinsic short coming of the tuning fork design.

•*Light baffle* - The internal baffle cut in the block proved to be a tremendous scattering sight, greatly increasing the background radiation reaching the detector and reducing the optical signal discrimination.

•*Entrance Slit* - The entrance slit, built from a separate piece of machined aluminum, caused scattering from its edges, contributing to the background noise.

•*AR Coatings* - The system requires anti reflection coatings on its entrance and exit facets, this will reduce the losses by 50%. However since the facets are at odd angles this could be difficult and expensive to accomplish. Since the detectors are contact coupled to the silicon, special matching AR coatings must be devised to match the detector to the silicon index. This is a development task of its own.

These factors along with the discoveries we made from the system model were used to design a new spectrometer lay out and detection system.

2.2 System Modeling

A system model was created to determine the detectivity of the system. The basic question to be answered was how much radiance must the target provide in order to be detected by the spectrographic system. The intuitive answer is to make the system with the highest detectivity. However within the limitation of the detectors and spectrometer throughput what can we reasonably expect to see, and is that sufficient to make measurements to detect the chemicals of interest. Two aspects of this question have been explored, the first is to determine what temperature of the target (a measure of radiance) is required to get a signal to noise of 1 out of the detectors at each wavelength. This assumes that the sample radiates like a black body. The second aspect is what spectral features are we looking for in the sample gasses, what resolution is required to resolve them, and are they within our spectral sensitivity.

We developed a system model that took into account temperature of the target, spectral throughput of the lens and optical bench, efficiency of the grating, spectral separation, and detectivity of the detector array. The model produced the following results

APPENDIX -- PCT APPLICATION NO. PCT/US99/07781

IOI/Sensor Development Corp.
Solid State Infrared Spectrograph

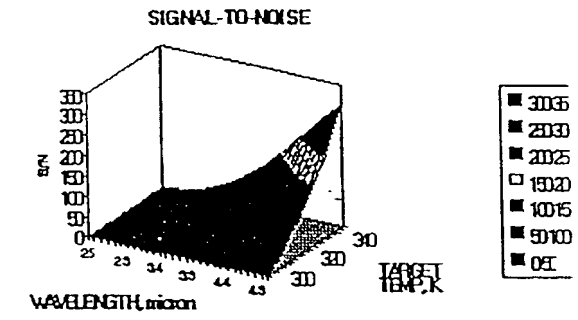

FIGURE 2.3 *This figure shows the detectivity of the spectrometer system, as modeled. The horizontal axes indicate the spectral band and the thermal temperature (radiant intensity) the vertical axis indicates the signal to noise ratio. Not surprisingly, this analysis shows that at longer wavelengths the signal to noise is higher (system will detect better).*

2.3 Spectral Analysis

There is considerable topical interest in the content of Martian soils and sub-soil composition and particularly in establishing the presence or evidence of past water, carbonate minerals, or organic matter. Because of the problems of oxidation leaching in the near surface and the constant surface recovering by dust storms, it is extremely desirable to obtain composition and structure data at some depth below the surface. Typical procedures include sampling soil or core via drilling, extracting these samples and performing some sort of ex-situ analysis on the intact core samples. This requires specialized drills to extract the core samples, and even then, it is difficult to keep the core samples intact and to establish the sample orientation for measurement. We propose to enable downhole measurements which will extend the capability of these remote Martian probes with a tiny, rugged reflection analyzer instrument so small that it can make measurements from inside typical boreholes from soil and core sampling drills.

The mid infrared waveband operating range of the phase 2 instrument should reveal the presence of many of the scientifically important CO_2 and H_2O along with Fe^{3+} minerals, distinguished by Cpx - Opx, and Olivine. Observations of the C-H stretch band at 3.4 micron wavelength and bound water in the 2.5-3.5 micron band should also confirm the likely presence of organic materials and/or hydrated minerals. The ability to resolve characteristic carbonate absorption bands in the 3.2-4.4 micron waveband and sulfates in the 1.3-3.6 micron region should provide the ability to distinguish various clays and micas. This is illustrated in Figure 2.4 by an FTIR spectrum obtained in our laboratory from a calcite sample furnished by JPL.

APPENDIX -- PCT APPLICATION NO. PCT/US99/07781

IOI/Sensor Development Corp.
Solid State Infrared Spectrograph

Figure 2.4 *FTIR reflection spectrum of a representative calcite rock furnished by JPL. In this figure the high resolution spectra obtained from FTIR spectrograph indicate that the fundamental absorption bands are quite broad and may be resolved by the 64 channel spectrograph.*

2.4 Optical Front End Design

From the analysis of the phase 1 device and the results of our system models we have developed an improved design that will greatly increase the utility of the spectrometer. We have completed the baseline silicon block spectrometer optic design. It uses a modified 'Ebert' layout fabricated from micro-machined silicon, with an F/1 input design (Figure 2.5)

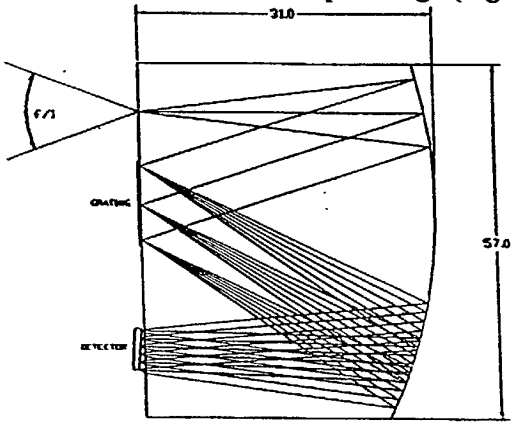

Figure 2.5 *Phase 2 optical bench raytrace. This layout has only two optical surfaces, greatly simplifying fabrication and increasing reliability by eliminating tolerance stack up inaccuracies. The flat grating design increases grating efficiency and makes the device easier to manufacture. Its F/1 design allows for twice the through put of the Phase 1 design, and its air gap at the detectors provide for focusing and permit the use of conventional AR coats.*

APPENDIX -- PCT APPLICATION NO. PCT/US99/07781

IOI/Sensor Development Corp.
Solid State Infrared Spectrograph

In the 'D' shaped optic, IR light enters the entrance slit, a thin film deposited A/R coated area, and illuminates a cylinder mirror which collimates light. The high refractive index of silicon greatly reduces the angle of the cone of light, this permits the use of an F/1 lens at the entrance apearature. It also reduces the size of the cylinder mirror and permits the spectrograph to operate near the diffraction limit. The collimated beam is reflected off a gold coated diffraction grating. The grating disperses the IR spectrum which is re-imaged after a second reflection off the cylinder mirror. The light exits the block through an AR coated surface and is imaged onto the detector plane. The detector plane is at a slight angle in order to flatten the field across the image. The airgap permits the detector plane location to be adjusted, allowing for manual focusing. As the rays exit the block, the large cone angle of the rays is restored, fully filling the acceptance angle of the detector.

The grating produces a number of lower energy unwanted diffraction orders. In our earlier design these orders were trapped in the block and were scatterred and added to unwanted background signal on the detector. The new design permits the exit of these unwanted orders out of the flat surface where they will be captured by a light trap. The following table addresses all the pros and cons of this new "D" shaped design.

Requirement	Phase 1Design	Phase 2 Design	Pro / Con
Size/weight/volume	3" dia. x .25" thk 1.75 cu. in.	1" x 1.5" x .040" thk 0.06 cu .in.	Provides a 30x decrease in optical bench weight
Number of Facets	6 - 4 on block and 2 on contact coupled grating	2 - each facet used multple times	4 reflection design significantly decreases size
Grating	Chirped grating on seperate curved surface	Conventional flat grating	Easier to manufacture, and maintain uniform efficiency, etched into block prohibits the exchange of gratings
Chopper	Tuning fork	PZT bimorph	No radiated fields, chopper not required with micro thermopile detector
Scattering	No exit for higher diffracted order, no beam dump, scattering internal baffle	AR coated exit for higher orders, external beam dumps, no internal baffles,	Decreases signal noise by eliminating scattered light to detector
AR coating	AR coating on two odd angle surfaces	AR coating on 1 surface	Cheaper to manufacture
Spectral band	2.5 - 5 um	3.13 - 5.5	Better spetral features, but requires TE cooling of the PbSe detecotr
Spectral Resolution	0.15 um	0.039 um	Higher resolution required for gas identification
Detector	PbSe 16 element	TE cooled PbSe 64 element or micro thermopile	Required to find spectral features, PbSe cooling improves SNR
Read out electronics	16 channel lock-in amplifier	64 Channel multiplexed w/ digital lock-in; or w/ 64 hybrid lock-in amplifiers	Greatly reduces space, Hybrid has fewer noise sources in system but is more bulky
Filter	External	Used as window on vacuum package	Dual use saves components
Package	Open air, large	Sealed, for dry gas or vacuum	Needed to keep condensate of TE cooled detector, more expnsive
Detector/block interface	Contact coupled	Air gap	Provides for focusing, eases exchange of detectors.
Slit	Free standing to provide focus	Deposited on block	Deposited slit is finer, less scattering and ghosts

APPENDIX -- PCT APPLICATION NO. PCT/US99/07781

IOI/Sensor Development Corp.
Solid State Infrared Spectrograph

2.5 Optical Front End Fabrication

Due to to the uniqueness of the design we have worked closely with our vendors to develop a fabrication plan that is consistent with the inexpensive mass production of the front end. This consists of the following:

Optical blanks. "D" shaped optical blanks are purchased from VA Optical, a silicon supplier. Their main business is to produce substrates for the micro-chip industry. For this reason they can produce superior flat polish on both sides of the optic. The near net shape will include all the polished flats but not the cylindrical surface.

Cylinder. The blanks will be sent to Digital Optics Corporation who will stack twenty parts into a monolithic block than shape the block into a cylinder lens. They possessed the interferometric equipment necessary to measure and produce the necessary surface on the cylinder mirror. They will gold coat the mirror and AR coat the flat.

Grating. The gratings will be built by Diffraction Limited. They will produce a grating in photoresist on the surface and etch it into the silicon. They will also work with the elements assembled in a stack. Once the grating is made they will add gold reflector overcoat and deposit the entrance slit.

Assembly. The part will be returned to Ion Optics where its performance will be measured. This is done by feeding the block with a lab spectrometer and measuring the quality of the output image with an IR camera. Once its performance is verified the device will be integrated into the housing with the detector and focused.

2.6 Mechanical

The design requires the precise alignment of the optical bench, the chopper, the detector array, and the filter. This is all accomplished with a precision sealed package. The package holds the chopper, filter and detector in position and provides for a vacuum seal.

The miniature chopper we developed consists of a piezo-electric (PZT) bi-morph strip with a flag on the end. The bi-morph strip is a sandwich of PZT and stainless steel bonded together. The bi-morph curls like a bi-metallic as a voltage is applied across the PZT causing it to change length. This provides very fast chopping of the optical beam within a minimum volume and with less EMI.

The electronic read-out will fit into the vacuum package so the signals are amplified and multiplexed before leaving the package. This provides for the minimum number of electrical feed throughs. It also provides a modularity of the design so the spectrometer optics package can be traded out with little effort.

The detector mount will hold the backside of the TE cooler to which the detector array is bonded. The mount will allow the detector to be precisely positioned with micrometer screw adjusts and then locked into place. Heat from the TE cooler will be conducted through the mount and into the base of the package.

APPENDIX -- PCT APPLICATION NO. PCT/US99/07781

IOI/Sensor Development Corp.
Solid State Infrared Spectrograph

The package will have a removable cover that will permit the components to be aligned prior to the cover being applied. The cover will contain the entrance window that will be coated to act as a cutoff filter in the system The package will also incorporate a mount to hold the input lens or a fiber optic input.

2.7 Detectors

When it comes to determining system performance, no other component will have as much effect perhaps than the detector. For this reason, we have extensively researched detectors applicable for our requirements. However criteria other than performance must be considered when evaluating detector systems for our portable, handheld spectrometer. These include cost, size, complexity and flexibility. For example, photoconductive devices typically suffer from low frequency or 1/f noise which can be reduced by chopping the input signal and AC coupling the output from the detector. However this adds a level of complexity to the optical system and the read out electronics.

After considering the wide range of detector arrays available, we have narrowed our options to two choices: a PbSe photoconductive array and a micro-thermopile linear array. A thermoelectrically cooled PbSe array provides the best performance with moderate cooling requirements in our region of interest. When cooled to approximately 145 to 250 K, low NEP performance extends well beyond 5.5 micrometers. Thermoelectric coolers are rugged low cost devices that can provide adequate cooling for the PbSe device. We anticipate a requirement for a two stage TE cooler.

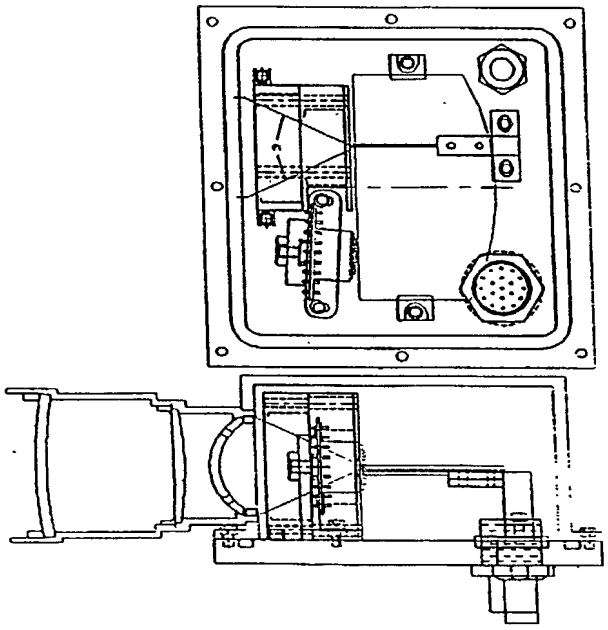

Figure 2.7 *This is the package design that utilized the Optoelectronics/Textron integrated multiplexer and PbSe detector array.*

APPENDIX -- PCT APPLICATION NO. PCT/US99/07781

IOI/Sensor Development Corp.
Solid State Infrared Spectrograph

We have completed an extensive survey and contacted all the PbSe array detector vendors in the U.S. Out of this survey we located only one, Optoelectronics Texton, with an operating multiplexed PbSe array. We spent several months in good faith effort, developing an array design operating parameters, and package. However when it came time to formalize our Purchase Order, Opto provided a price 3 times that of the ball park figures we had been working to (approaching $100k). This cost is well outside our budget, and the episode has been a major schedule set back to the program. We have now developed an alternative detector plan, and have begun to carry it out

After investigating a number of other PbSe detector array sources, we have selected New England Photoconductor (NEP) as the detector array vendor. NEP is a local manufacturer of photoconductive arrays that supplied the array used in the phase I system. Their performance under that contract was very favorable. NEP quoted the lowest price for a custom 64 element linear array and will integrate their array with a newly developed custom integrated multiplexor circuit. We are in the process of evaluating the technical risk and system performance of this developmental multiplexor and its possible impact on system performance. Its major disadvantage is that it adds significant technical and schedule risk. However an integrated multiplexor will significantly reduce the size, cost, and complexity of the readout electronics.

We have also investigated the use of a 64 element micro-thermopile detector under development in a separate JPL-sponsored effort. There are many advantages to using the micro-thermopile: it is sensitive over a wide range of wavelengths, it does not suffer from 1/f noise and so does not require a chopper, and it does not have to be cooled. Conventional thermopiles are not as sensitive as a PbSe detector, however scientists at JPL believe that they can produce a micro machined thermopile, in the configuration we desire with a D* of 10^9, equivalent to uncooled PbSe. Although this device is experimental, we hope to incorporate this device into a prototype spectrometer and evaluate its performance. Although we believe we need the sensitivity of a PbSe detector at this time, the micro-thermopile is a very attractive alternative, that could be used in spectrographs that range from 1 - 20 um (the full IR spectrum).

2.8 Readout Electronics

Typically, a modulated or chopped detector signal is recovered using a lock-in amplifier or synchronous detection scheme. The large number of pixels and the use of a multiplexor complicates the extraction of the modulated signal from our PbSe detector. We are currently investigating extracting the modulated output digitally. The serial output of the multiplexor will be digitized with a high speed, high resolution A/D converter. The sampled outputs from each pixel will be collected from multiple scans and processed digitally. For example, by performing a Fast Fourier Transform (FFT) on the data collected for each one pixel, the energy content at the modulation frequency can be determined. The FFT acts as a narrowband filter at the modulation frequency. This energy can be averaged over time to further increase signal to noise. We plan to evaluate this approach using an off-the-shelf A/D board and a standard analysis package running on a personal computer. This allows us to rapidly prototype and test different processing techniques.

In order to reduce our technical risk, we have also specified and received a proposal for a hybrid multi-channel lock-in amplifier. This device will replace the multiplexor. It is assembled from un-packaged die and mounted on a thick film circuit; an eight channel device occupies 2.56 square inches. Although this approach is fairly large and costly, it has a low technical risk and guaranties maximum performance.

APPENDIX - - PCT APPLICATION NO. PCT/US99/07781

IOI/Sensor Development Corp.
Solid State Infrared Spectrograph

2.9 Processing

The continued growth of the digital signal processing market has resulted in a number of low cost DSP processors for embedded applications. We are currently investigating several processors for our application. In particular, we are evaluating the DSP56L811 from Motorola. This processor is a cost-effective solution that combines the prodigious number crunching of a digital signal processor with the versatile functionality of a microcontroller. This processor could perform the signal processing necessary for signal extraction and chemical detection and also control a display and keypad; a serial interface will be used for communication with an external computer. An off-the-shelf development board will facilitate the rapid prototyping of the final spectrometer unit.

3. WORK PLANNED FOR NEXT QUARTER

3.1 Fabrication of the Silicon Spectrometer Optic.

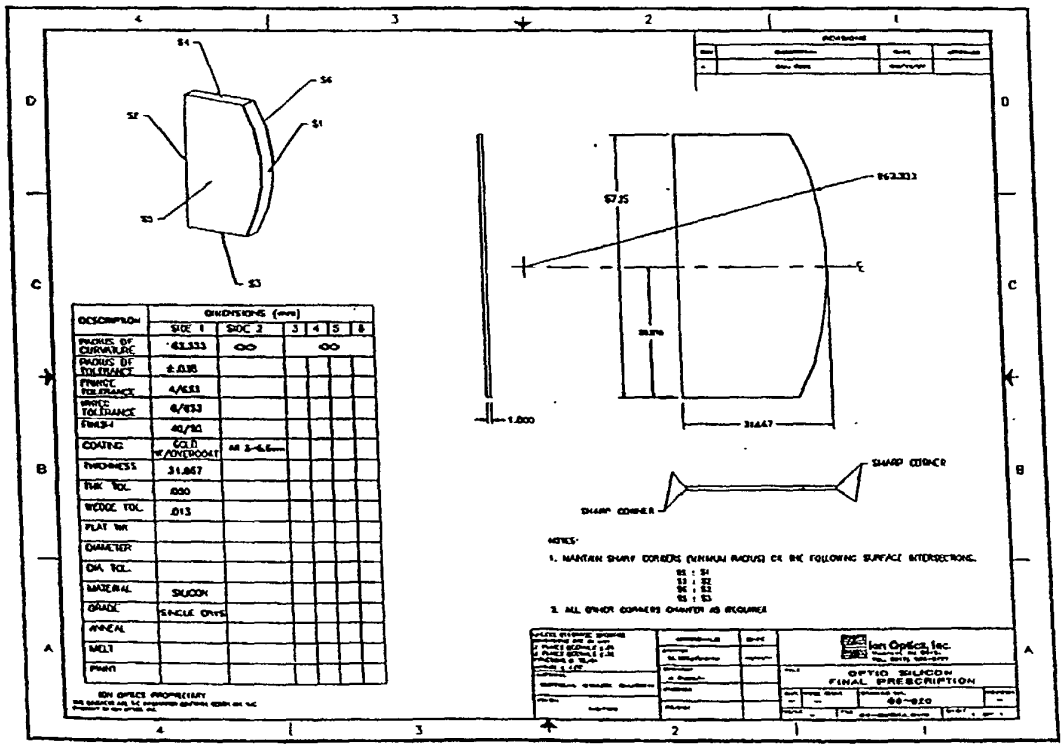

Figure 31 *Detailed drawing of optical bench ready for fabrication.*

APPENDIX -- PCT APPLICATION NO. PCT/US99/07781

IOI/Sensor Development Corp.
Solid State Infrared Spectrograph

The drawing package has been sent out for quotation. We intend to contract three vendors to build the assembly in stages.

1.) The silicon wafer and optical substrate fabricator will produce the silicon optic without the cylindrical optical surface and optical coatings.
2.) The lens fabricator will finish the cylindrical surface and AR coat the opposite flat.
3.) The grating fabricator will etch and gold coat the grating

At this point the Silicon Spectrometer Slab is complete and will be characterized for spectral resolution, through-put, and scattered light.

The goal of these three steps is to define a manufacturing process to maximize yield and operating characteristics.

3.2 Optical Chopper

A vendor has been selected and a quote obtained for five chopper assemblies based on the proof of concept prototype. The purchase order will be executed as soon as the final drawing package for the optical bench is released. This is anticipated to occur in June, 1997.

3.3 Detector Assembly

We have ordered a 64 element PbSe array from NEP and are currently evaluating the multiplexor. The characterization will be completed shortly. We can then place the order for the multiplexor and complete the packaging design. At that point, we will also begin the design of the data acquisition and signal processing circuitry. Delivery of the array will be in about 8-10 weeks.

3.4 Packing

The next major mechanical design task will be the case for the instrument. Particular emphasis will be placed on designing a low cost package that is easy to assemble.

3.5 Phase III Product Evaluation

To investigate commercial markets for this spectrographs we have contacted several spectrograph vendors, and started a market survey of users. To assist in this we have produced a preliminary spec sheet showing two embodiments of the device. The first is the handheld spectrometer and the second is the OEM bench. In the coming months we hope to refine these specs by contacting various potential end users and OEM customers.

4. CUMULATIVE COSTS

The cumulative costs for this PHASE 2 project is shown in the accompanying graph. Current expenditures are in line with projected cost to complete.

APPENDIX -- PCT APPLICATION NO. PCT/US99/07781

Introduction

Phase I demonstrated the feasibility of a compact, rugged, lightweight spectrograph operating at room temperature in the 2-to-5 μm wavelength range. The critical innovation is the spectrometer's completely solid state construction -- it can be assembled entirely from micromachined silicon components (even the MWIR detector arrays can be made of silicon) The resulting instrument has the advantages that it can be made very small and very light (about an inch in diameter and weighing a few grams), is permanently aligned for operation over a broad spectral range, and is extremely resistant to damage resulting from harsh environments (launch vibration, aggressive chemicals, radiation).

All critical spectrometer components were designed, built, and integrated into a working spectrograph in Phase I, producing an instrument which exceeded efficiency projections and confirmed the resolution predicted by ray-tracing models. Phase II's objective is to extrapolate this prototype to a rugged, lightweight, uncooled MWIR spectrograph applicable to ongoing and upcoming NASA/JPL program needs. These needs include remote sensing from airborne and satellite platforms, and planetary programs to measure water vapor (H_2O) and carbon dioxide (CO_2) in clouds, sulfur dioxide (SO_2) and hydrogen sulfide (H_2S) in volcano plumes, and frozen gases and organic compounds in borehole cores. The Phase II focus will be upon (1) improving the Phase I spectrometer design for better resolution, sensitivity, manufacturability, and smaller size, and (2) extensive testing and evaluation in cooperation with scientists at JPL, yielding a miniature, mass-producible device with better resolution and lower noise than its Phase I parent. Beyond its usefulness to NASA, the fully developed spectrometer is expected to excite extensive commercial interest for applications requiring a low-cost, compact chemical sensor.

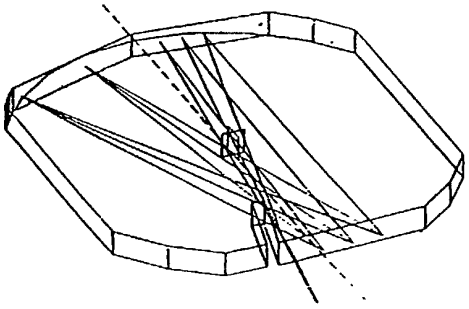

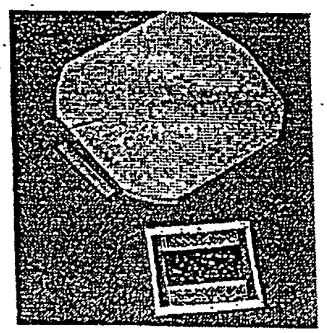

Figure 1 *In the Phase I proof-of-concept device, light enters the block, reflects off a flat fold mirror and is dispersed (and focused) onto the detector plane by a diffraction grating. The holographic grating (lying next to the block in this picture) is built on the surface of a silicon plano-convex lens. It has a variable line density, or chirp, to overcome the Rowland circle problem and flatten the focal plane.*

APPENDIX -- PCT APPLICATION NO. PCT/US99/07781

The silicon micro-spectrograph is a slab of high purity, optical grade silicon, with a holographic IR grating and linear detector array. This system will be lightweight, compact, rugged, alignment-free, calibration-free, and low-cost. During the third quarter of this project, we completed integration and test of a 3" prototype device with a 16-channel PbSe linear detector array. We were able to demonstrate clear resolution of molecular absorption/emission bands in the mid infrared.

Efforts to integrate the spectrometer test bed into a single package are underway. The package includes an optical bench, detector array, chopper and chopper driver, input optics and filter, 16 channel lock-in amplifier, high voltage drive batteries, and stand alone bar graph display. Detector output, previously fed into a PC via an A/D card, the digitally demodulated and displayed, is now demodulated via a dedicated 16 channel analog lock-in circuit and viewed on a stand alone bar graph display. The total spectrograph runs on two batteries and occupies the volume of a shoe box. Its compactness allows it to be easily carried and used in the field. This is emphasized by Ion Optics' recent demonstration of the spectrometer for Exxon/Chemical in Houston Texas, and its exhibition at the Boston SPIE conference.

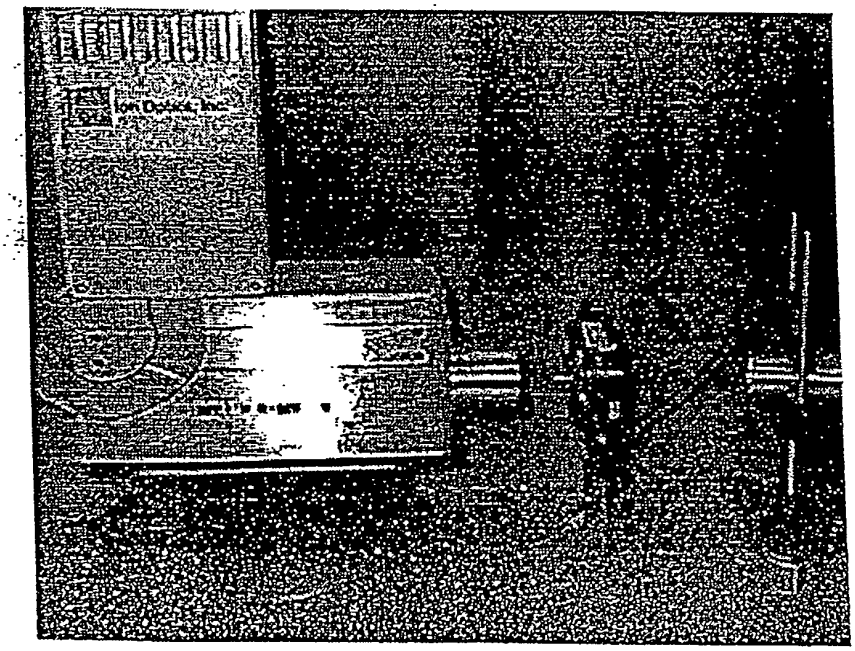

Figure 9 *A major internal milestone for the phase 2 program is an optimized 3" system to address stray-light and throughput issues identified in the phase I test results. In the 3rd quarter, we built a room temperature benchtop demonstration with an integrated 16 channel linear detector array, signal processing electronics, and an LED bar graph display.*

Already at this stage of integration, we have shown that a micromachined silicon device can achieve resolution and throughput comparable to off-the-shelf 1/8 meter monochromators which are

APPENDIX -- PCT APPLICATION NO. PCT/US99/07781

several times larger and heavier Work this quarter has concentrated on design and component fabrication for the next generation prototype, about 1/4 the size of the device currently operating in our laboratory. An additional major activity this quarter has been the identification and quantitative evaluation of NASA mission requirements for a potential MARS rover instrument based on our infrared spectrograph.

2. Technical Accomplishments

We have completed the baseline one inch microspectrograph design and we are presently involved in detailed negotiations with vendors for specifications and deliveries of components required for this. We expect to place orders for these components during April and begin integration and test of the final phase 2 deliverable spectrograph. This superior design uses only two milled facets, with reduced size electronics and detectors.

The heart of the system is the all solid-state spectrometer-on-a-chip. (Figure 2) It uses a modified "Ebert" layout , fabricated entirely from micromachined silicon. It consists of a roughly "D" shaped silicon die with an entrance slit defined by thin film coatings. IR light crosses the slab (with the silicon acting as a waveguide) and is focused toward a diffraction grating by the cylindrical edge of the die. The chirped (variable line spacing), grating disperses the spectrum and images the source onto a flat focal plane where it is detected by a linear infrared detector array.

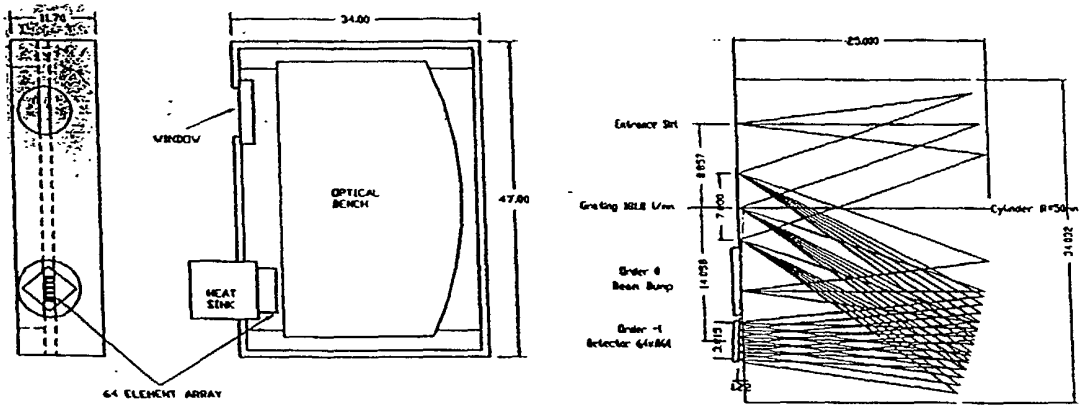

Figure 3 *Mechanical layout (left) and (CODE-V) ray trace (right) illustrate the operation of the miniature solid state optical bench. The entire assembly will be small enough to fit in a standard microprocessor chip carrier. The new design has fewer milled facets and incorporates built-in beam dumps for disposal of unwanted diffraction orders. The importance of these beam dumps was confirmed by our test results with the 3" prototype. They are implemented as AR-coated exit windows on the flat spectrometer entrance/exit facet. Dimensions are in mm.*

Applications for Mars Exploration

APPENDIX -- PCT APPLICATION NO. PCT/US99/07781

There is considerable topical interest in the content of Martian soils and sub-soil composition and particularly in establishing the presence or evidence of past water, carbonate minerals, or organic matter. Because of the problems of oxidation leaching in the near surface and the constant surface recovering by dust storms, it is extremely desirable to obtain composition and structure data at some depth below the surface. Typical procedures include sampling soil or core via drilling, extracting these samples and performing some sort of ex-situ analysis on the intact core samples. This requires specialized drills to extract the core samples, and even then, it is difficult to keep the core samples intact and to establish the sample orientation for measurement. We propose to enable downhole measurements which will extend the capability of these remote Martian probes with a tiny, rugged reflection analyzer instrument so small that it can make measurements from inside typical boreholes from soil and core sampling drills. The mid infrared waveband operating range of the phase 2 instrument should reveal the presence of many of the scientifically important CO_2 and H_2O along with Fe^{3+} minerals. This should also confirm the likely presence of hydrated minerals, anhydrites, and carbonates.

There are two critical innovations – a tiny (cm size) all solid state optical bench, and an electronically controlled, self stabilized blackbody radiator. (Figure 1) This instrument will provide complete spectral characterization of the surrounding soil media by allowing stratigraphic traces of specific infrared lines as a function of depth down the borehole. The combination of a pulsed blackbody source with the spectrometer has the advantage that, in addition to making reflection mode measurements of contaminant composition and concentration, it can also be used to measure thermal inertia of the surrounding media. Thermal inertia, the rate of heating and cooling following a measured thermal pulse, provides an important measure of the density of the surrounding media

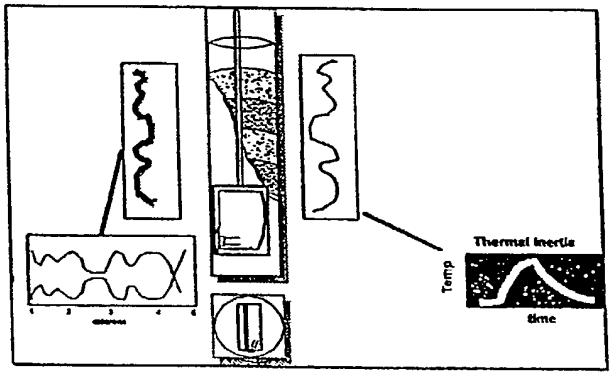

Figure 1 *Schematic of tiny infrared micro spectrophotometer arrangement for contaminant monitoring in boreholes. The miniature solid-state FTIR and pulsed infrared source allows spectroscopic measurement of spectral lines from specific contaminants as well as local measurements of thermal inertia and soil density.*

APPENDIX - - PCT APPLICATION NO. PCT/US99/07781

3. Layout and Component Selection for Final Phase II Deliverable Instrument

The manufacturing technique for the 1 inch spectrograph is being developed to facilitate quantity production. We are working with three vendors to develop a simultaneous multi element fabrication technique. Under this approach each vendor's contribution is optimized to effectively utilize their capital equipment, thus reducing fabrication cost. Under this approach, the raw silicon is purchased as silicon wafers from an electronic chip supplier; the advantage is that their standard electronic product is to a much higher surface finish then is normally available from optical manufacturers. Special optical grade silicon is used to meet our requirements (micro chip grade silicon is opaque in our wavebands). They will slice the wafers to near net shape with all the flat sides polished to the required finish. The wafers are shipped to the lens grinder, (who owns a cylinder generating machine). There they are stacked and clamped into a single monolithic block, to be shaped as if it were a solid lens. This finishes the entire block of 15 wafers at once. The gold coats and AR coats are applied and the block is forwarded to the gating vendor. The grating is etched into the monolithic block using a holographic transfer process. Finally the slit is applied, and the grating gold coated. The block is returned to Ion Optics for separation and integration with the detector array in the optics package.

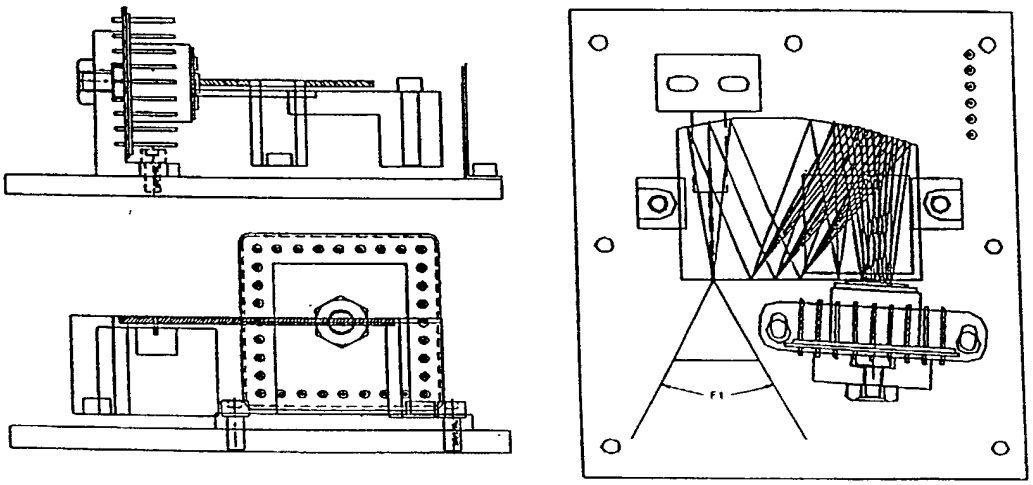

Figure 4 *Baseline mechanical layout for 1" spectrometer demo including focus, alignment and preliminary package and hermetic sealing details..*

APPENDIX -- PCT APPLICATION NO. PCT/US99/07781

4 Results of the Phase 1 project

We are developing a hand-held infrared spectrometer to measure the spectral emission of rocket plumes during test firings. This rugged, uncooled, field-instrument will fill an important need by providing laboratory-quality data on rocket plumes in the infrared emission bands. It will be useful not only as a diagnostic tool for engine performance but also for assessing the environmental impact (compliance) of new engine designs or different operating conditions. By measuring a complete spectrum and using neural net processing to reduce the data in real time, the finished instrument will be able to measure the concentration of NO_x constituents in a plume, despite the presence of water emission in the same spectral band. In Phase 1 we demonstrated the concept and showed that the optical measurement works. In phase 2 we will develop signal processing, analysis, and packaging required to build our sensor into a fieldable instrument. We expect that it will become a standard tool for propulsion research, not only for rockets but for high performance aircraft engines and for industrial process monitoring.

The new instrument will be about the size of a video palmcorder, containing a miniature infrared spectrograph, simple sighting and focusing optics, a control panel, and a flat panel display. A visible spotting scope boresighted with the spectrogaph is used to train light from the plume onto the entrance window of the block spectrograph. The spectrum is dispersed onto a linear detector array covering the mid infrared gas emission band (2.5 - 5 μm wavelength). Signals from the array are preamplified, conditioned, and digitized so that a microprocessor with embedded data reduction software can convert the signal into a spectrum and extract concentrations of compounds in the plume. The result is then displayed on the instrument's LCD flat panel display.

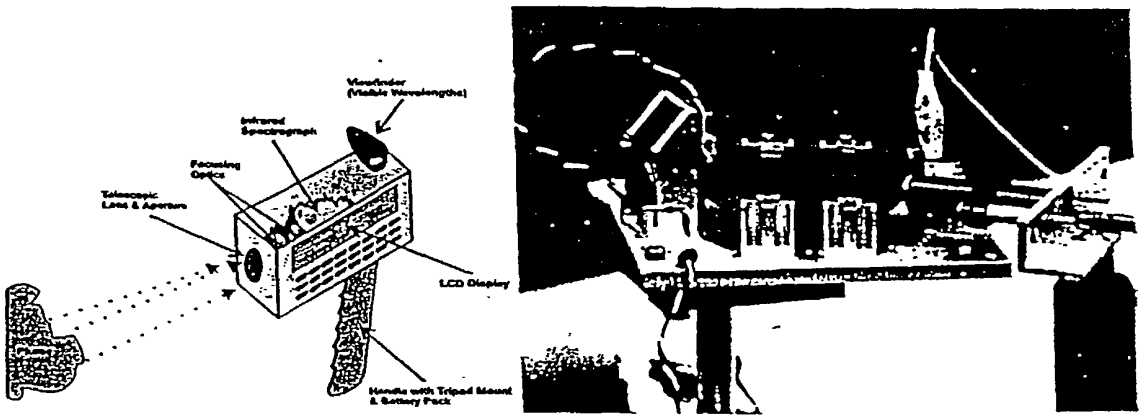

Figure 1 *Schematic illustration of compact, IR plume spectrometer (left). The phase 1 breadboard device (right) exceeded our performance predictions and successfully measured spectral lines from a 1 cm flame in our laboratory testing.*

APPENDIX -- PCT APPLICATION NO. PCT/US99/07781

As described in the phase I project summary, performance of the breadboard prototype has met or exceeded our design expectations and successfully measured spectral emission from test flames in our laboratory The phase 2 brassboard prototype will, itself, be a useful diagnostic tool for engine work at SSC It will also lead to a revolutionary new product for propulsion research and for on-line monitoring of industrial combustion and chemical processes.

At the heart of the system is the solid-state block spectrograph, fabricated entirely from micromachined silicon, which we demonstrated in Phase I. It consists of a roughly square silicon slab. The entrance slit is defined by the gold coated grating and a baffle slot. IR light crosses the slab (with the silicon acting as a waveguide) and is reflected toward a diffraction grating by a flat-fold mirror. The chirped (variable line spacing), concave diffraction grating disperses the spectrum and images the source onto a flat focal plane where it is detected by a room temperature linear infrared detector array. Each component of the spectrometer: the slab waveguide, the fold mirror, and the reflective diffraction grating are made out of silicon and fabricated separately using standard microelectronics processing methods.

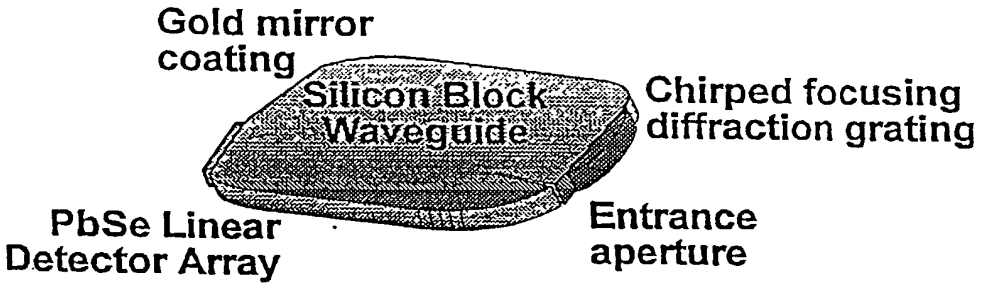

Figure 4.2 *Modular fabrication allows straightforward adaptation of this simple design to different wavebands and resolution requirements. The resulting sensor is rugged, permanently aligned, all solid-state; opaque to visible light and other interferences.*

The components themselves incorporate a number of advanced design features. In particular the diffraction grating is made with a variable line density or "chirp" to flatten the Rowland circle and provide a flat focal plane for the array. The slab waveguide is formed to include mounting surfaces for other components and includes baffling and beam dumps. Since the silicon is opaque to photons above its bandgap, the slab excludes visible light from the detector. Silicon's high refractive index provides lossless reflections at the polished top and bottom faces of the device, waveguiding the radiation in the plane of the device. However, more important, because of the high index of the silicon, the cone of incident illumination is dramatically smaller inside the device. This provides better optical throughput then can be achieved with an open-air design. In addition, for measurements at longer wavelengths, the entire spectrograph can readily be cooled on a single cold-finger, in much the same way that focal plane arrays are now cooled in conventional instruments.

APPENDIX -- PCT APPLICATION NO. PCT/US99/07781

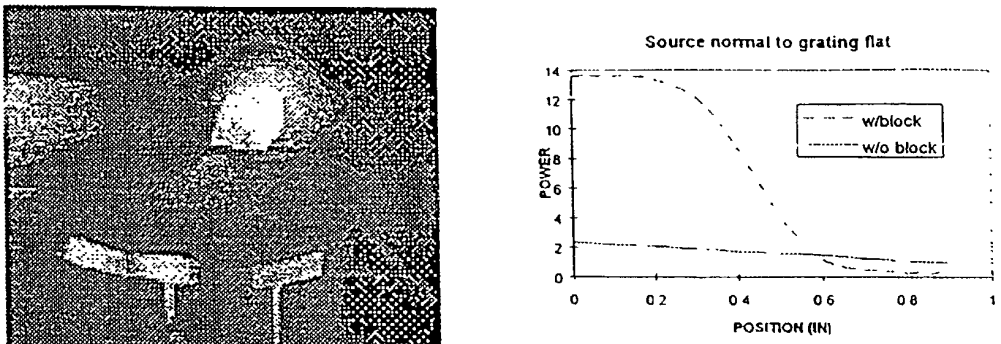

Figure 4.2 *The central innovation which makes this possible is the high-index slab waveguide. Refraction at the entrance slit sharpens the entrance cone and improved throuput, as shown in the thermal image and line scan data.*

4.1 Importance of this development for NASA

This instrument fills a gap in available field instrumentation for plume measurements -- a hand-held spectrometer capable of measuring the concentration of chemical species (CO_2, hydrocarbons, NO_2, N_2O, and HCl) present in rocket engine exhaust plumes. This is important to assure environmental compliance during test firings (for example, the Space Shuttle Main Engine (SSME)). Because the combustible mixtures in rocket engines are typically fuel rich, most of the active IR signature is caused by afterburning of the plume in the atmosphere.

In an era of increasing environmental consciousness, reducing greenhouse gas emissions and combustion by-products is an important part of engine design and optimization. In particular nitrogen oxides (NOx -- N_2O, NO_2, NO) are a natural by-product of high temperature combustion in rockets and in high performance jet engines. These compounds can be harmful to the ozone layer, so minimizing their presence in engine exhausts is a concern in the design of new engines for high altitude aircraft. The nitrogen oxides have strong infrared emission lines, but unfortunately, these are coincident with other prominent infrared emission bands, notably water and hydrocarbons.

APPENDIX -- PCT APPLICATION NO. PCT/US99/07781

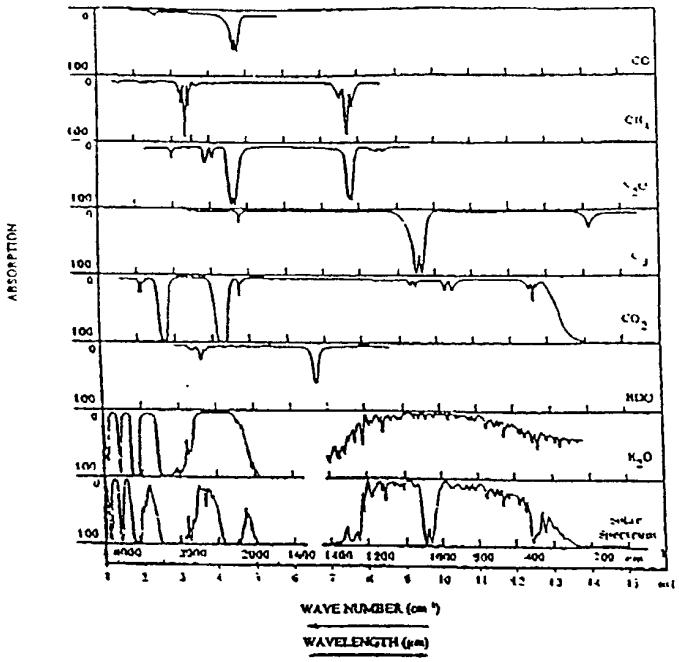

Figure 4.4 *The N_2O absorption/emission band, centered around 4.5μm, is near the edge of a water band. The harmonic band at 7.8μm is near a hydrocarbon line.*

The spectrometer will also be useful for engine performance testing (and environmental monitoring) of liquid propellant engines and hybrid motors burning hydrocarbon fuels. Typical fuel/oxidizer combinations of interest to SSC include RP1-JP/liquid oxygen (LOX) and polybutadiene hybrid engines. The resulting exhaust plumes have blackbody-like characteristics and contain CH_x, CO_x, and NO_x. These species are readily detectable by emission spectroscopy in the 2 to 8 micron range, thus the proposed spectrometer will function as a performance diagnostic for next-generation engines and motors employed on NASA's orbital and interplanetary flight vehicles, and perhaps for high performance air-breathing aircraft as well.

4.2 Phase 1 achievements and current project status

The phase I project consisted of three major related activities -- spectrograph optimization, spectrograph modeling/performance predictions, and breadboard device integration and test. Because of the possibility of detecting nitrogen oxides in the presence of interferences from other engine plume constituents, we have paid special attention to the stray light and optical signal-to-noise performance of the spectrograph in Phase 1. Stray light analysis and testing is important because a critical design feature of the plume spectrometer is its reliability and accuracy. To quantify the likely errors and evaluate potential self-referencing schemes, it is vital to understand the stray light performance of the instrument itself. To study the light budget,

APPENDIX -- PCT APPLICATION NO. PCT/US99/07781

Table 1 summarizes the results of stray light calculations. To realize a signal-to-noise (S/N) ratio of eighty, all the improvements indicated must be made to our basic spectrometer block By far the most important, however, is adding a beam dump to reduce scattered background and zero-order light diffracted from the block. Ray tracing suggested that beveling and polishing the block between the mirror and detector facets will accomplish this without major rework of the basic design

Table 1 *Summary of signal-to-noise ratio calculations*

Block Configuration	S/N ratio	Improvement in S/N ratio
Basic block configuration of phase 1 proposal	0.03	-----
Polish and clad top and bottom surfaces, resulting in efficient total internal reflection and eliminating surface scattering	0.38	0.35
Blaze the grating	1.24	0.86
Apply antireflection coatings to eliminate reflections at the spectrometer input and detector facets	3.42	2.18
Add a zero order beam dump	78.41	76.23

In addition to projecting signal-to-noise ratios, ray traces were performed to study zero order diffraction and to locate the system focus. Paraxial calculation and ray tracing indicates a need to increase the optical power of the dispersing grating/mirror to improve system throughput.

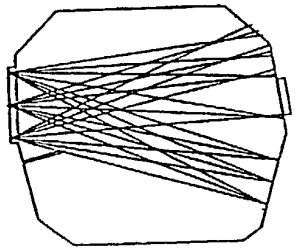

Figure 4.5 *One of the improvements suggested by the paraxial ray trace exercise was the addition of beam dumps. The sinusoidal grating diffracts unwanted orders into the top half of the block and are absorbed to eliminate scatter.*

APPENDIX -- PCT APPLICATION NO. PCT/US99/07781

An analysis was completed to determine the magnitude of the signal to noise ratio (SNR) for the PbSe detector for various temperture sources (where the noise refers to the intrinsic electronic noise of the detector). The signal analysis considered the source as a black body with temperature ranging from 300K to 350K This was multiplied by the NA of the spectrometer, after conversion to effective FOV, and then by the smaller of the line width of the emissions of interest or the detector element size, to determine the spectral power available to the detector We assumed a detector $D^*(\lambda)$ which is linear with wavelength (λ), and peaks at λ_{cutoff} of D^*_{max} We used a λ_{cutoff} of 5μm, a chop frequency of 1 khz, and a D^*_{max} of $1x10^9$ cm-√hz / watt. From this, Noise Equivalent Power (NEP) is computed for the 2π field-of-view (FOV) and 300K background for which the D* is valid. Then SNR is the ratio of the signal computed in the first analysis to the NEP. A "correction" term is then applied to account for the transmittances of the optics and the fact that internal scattering and stray light from the entire range of wavelengths to which the detector is sensitive will also be impinging on the detector.

Finally, the SNR is plotted on a 3-D surface plot to show SNR as a function of both wavelength and source temperature, and the projection of the surface on the temperature wavelength plane, with color used to show the regions within the SNR is within specific bounds.

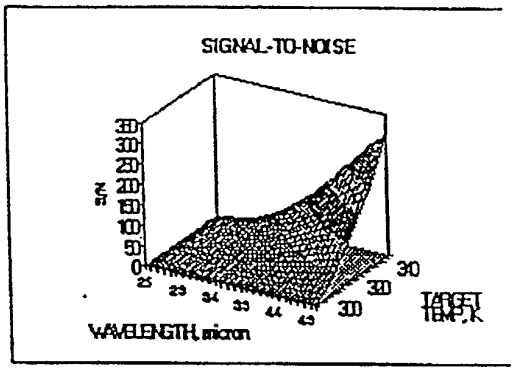

Figure 4.6 *Computed signal-to-noise achievable with the phase I breadboard device.*

Flame temperatures and corresponding emitted energy in the region of 4.45 μm are shown in the following plot. As may be seen, relative energy (at 4.45 μm) rises with flame temperature faster than as the square of the temperature (energy rise 2 orders of magnitude as temperature rises less than 1 order of magnitude), and faster still at the "lower" temperatures. At 3.5 μm, the rate of rise will be greater still. Hence, to get the equivalent signal from a 1-cm thick flame as from a black body of 315K, the flame temperature need be no higher than 1000-1200K. This is certainly on the low side of typical flame temperatures, and sufficient energy should be available for detecting the No_X emissions from a test flame.

APPENDIX -- PCT APPLICATION NO. PCT/US99/07781

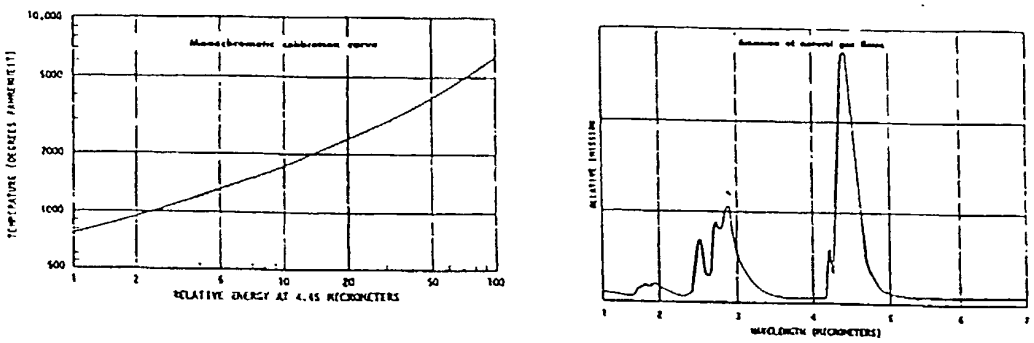

Figure 4.7 *Dependence of emission on flame temperature, and a representative spectrum. (From Bernard, Burton, abc's of Infrared, 1970, p.123)*

After building the solid state spectrograph components according to designs suggested by the ray-tracing and stray light analysis, we tested each of the components individually. The plot of transmitted power through the silicon slab (Figure 4.3) is an example of these measurements made to ring out individual components. In particular, we used an Agema ThermaVision camera to verify grating performance before the gratings were mounted on the spectrograph. The basic test setup is illustrated in Figure 4.8.

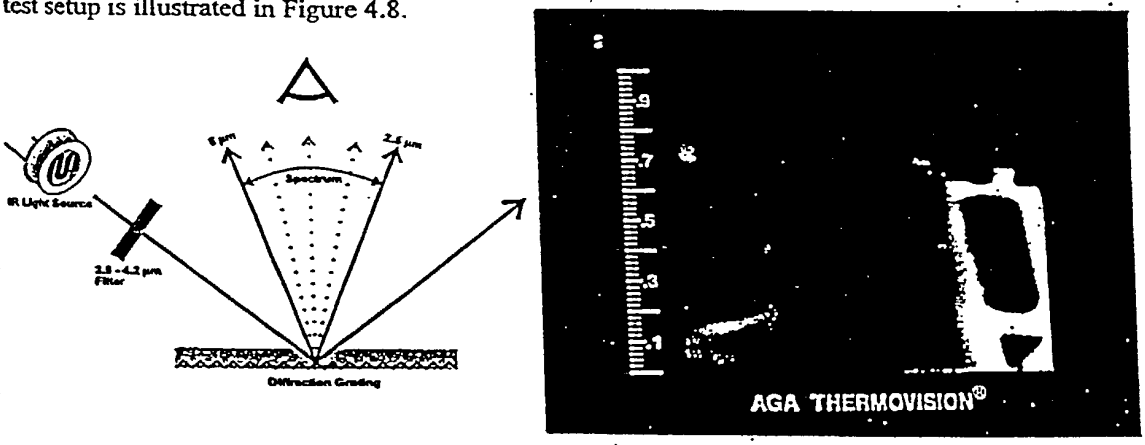

Figure 4.8 *A thermal imaging camera was used to check out the gratings under back illumination.*

For maximum sensitivity, a PbSe detector array was chosen. For initial testing before delivery of the PbSe array, thermal images of the detector plane were capturedand as well as manually scanned single pixel PbSe traces. The single pixel detector used a a micrometer drive and a single channel prototype of the final readout electronics. To extract maximum sensitivity from the PbSe detectors, both DC illumination from blackbody sources, and test flames from a

torches were collected through an external optical train with a 400 Hz tuning fork chopper. Preamplified signals were brought off the device on a ribbon cable to a computer A/D card. A simple synchronous detection scheme in software, for direct digital lock-in analysis of the PbSe signals was developed. Data acquisition software will command the board to sample each channel at roughly 20 kHz (depending on the number of channels configured for a given measurement.) Monitoring the trigger signal from the tuning fork chopper (which, itself, has a programmable phase delay), the software computes the HI and LOW integrals at pre-set delay times and average these over a pre-set integration time (currently baselined as 1 sec).

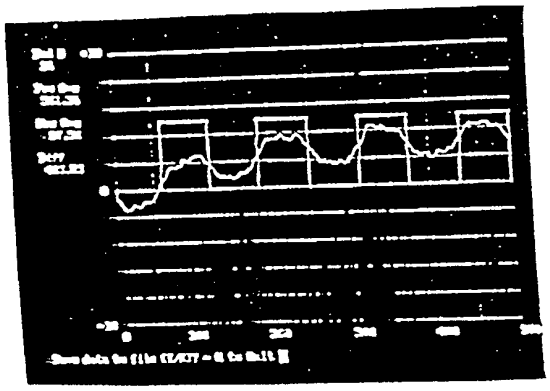

Figure 4.9 *Computer screen shows a typical image and signal-to-noise acheived from the digital lock-in program. Notice that the digital lock-in technique is rejecting both low-frequency (60 Hz pickup) and high frequency (1.5 kHz ringing) noise from the 400 Hz chopped signal.*

To facilitate stray light and efficiency measurements, individual modular components were mechanically clamped into position in the phase 1 test bed. A particular concern was the ability to move the mirror surface in order to avoid reflecting either the zero order or the -1 order beam from the diffraction grating. Actual integration of the optical components was done using laser alignment and infrared imaging techniques. Radiation was launched from a pulsIR black body source through the objective lens, chopper, filter and entrance aperture.

APPENDIX -- PCT APPLICATION NO. PCT/US99/07781

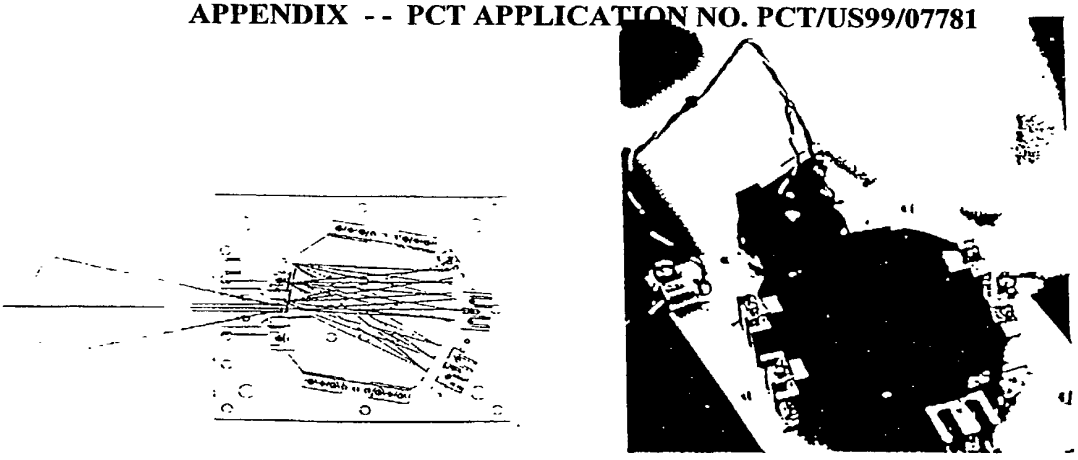

Figure 4.10 *Breadboard spectrograph test-bed constructed for phase I studies.*

An IR imaging camera behind the mirror location was used to align entrance radiation with the mirror. The mirror was installed and butt coupled to the block with an aluminum clamp. The grating was installed and the zero order reflection was seen at the beam dump location adjacent to the mirror. Imagery of the detector plane showed the spectrally dispersed image (test 4). Installation of the 4 um peak filter shows the image at location center left of the open spectrum. (test 7). We mapped the position of these peaks by scanning the PbSe detector across the detector face with a micrometer stage and calibrating the micrometer positions to the known (from corresponding FTIR traces) transmission wavelengths of these filters.

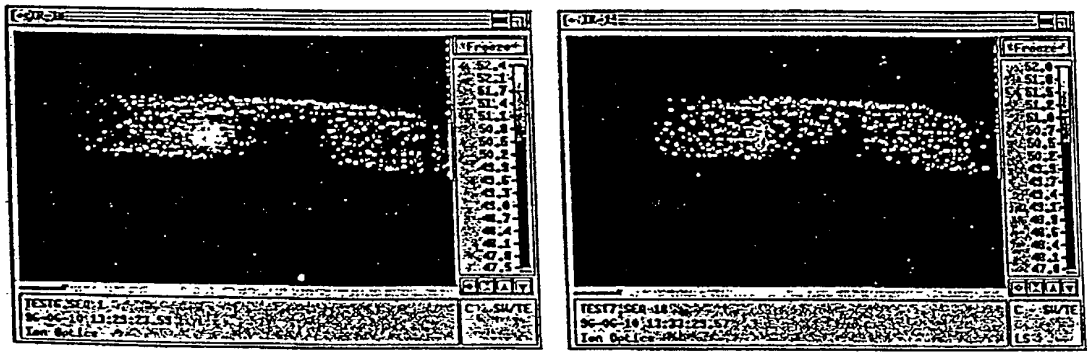

Figure 4.10 *Thermal images from IR camera show a blackbody spectrum dispersed across the focal plane facet (left) and the single spectral line through a 4.0 micron filter. The filter clearly curtails the transmission on the short wavelength side of the focal plane array.*

APPENDIX -- PCT APPLICATION NO. PCT/US99/07781

spectrograph itself and imaged into the spectrometer Test 8 shows imagery of the output on the IR camera. In addition, we quantified these measurements with a single element PbSe detector positioned at the output plane. The 5 mm square detector was slid across the detector plane and the output amplified and fed into the A/D converter. Coherent detection was used to isolate the chopped frequency. Plots were created of a hot nichrome filament (black body), the same filament filtered through a 4 um peak filter, and a 2.7 um filter.

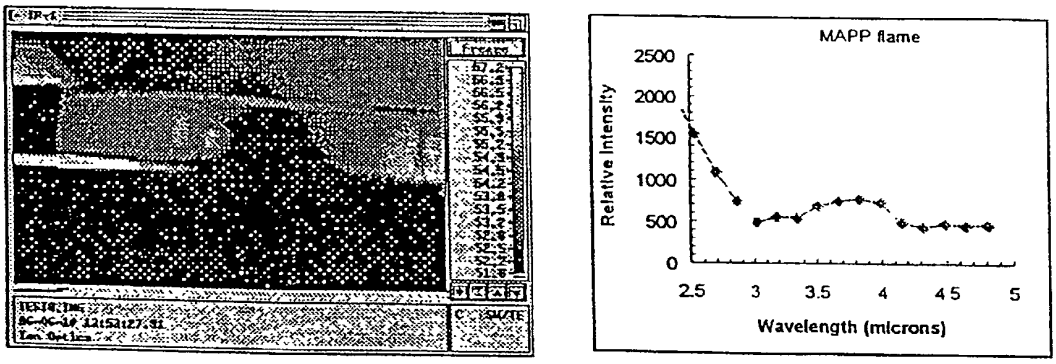

Figure 4.11 *Thermal image from IR camera shows a flame spectrum dispersed across the focal plane (left) and a micrometer scan from our PbSe detector (right). Two bright dots in the image correspond to the broad peaks in the discrete detector scan. At this resolution, water and hydrocarbon bands are clearly resolved.*

This test demonstrates that the phase 1 breadboard device met its signal to noise and spectral resolution goals. This clearly illustrates that the basic optical measurement design works and that this spectrograph can be the basis of a practical plume monitoring instrument for NASA. We believe it is also the basis of an exciting new commercial product.

5. Phase 2 Project Description

5.1 Technical Objectives

The goal of the phase 2 project is to make the successful phase 1 sensor into a successful plume monitoring instrument and ultimately into Ion Optics' next commercial product.

- Develop and test an "actual size" prototype spectrometer of approximately 1".
- Incorporate advanced neural network signal processing capability.
- Conduct extensive calibration and field tests in cooperation with SSC.
- Develop a marketing plan and commercialization strategy for the instrument.

5.2 Technical Approach

APPENDIX - - PCT APPLICATION NO. PCT/US99/07781

Ion Optics' approach to the Phase II program is ambitious but straightforward We must address three major areas: miniaturization, spectral deconvolution, and field demonstrations. The phase I effort demonstrated that the basic optical measurement works. In phase 2, we must add signal processing and analysis to make useful plume measurements with this innovative device

As described earlier, nitrogen oxides: N_2O, NO, NO_2 have absorption peaks which may overlap those of water vapor, carbon dioxide, and hydrocarbons. Water vapor in particular presents problems because its absorption peaks are broad and because it dominates the composition of the exhaust plume from the SSME. However since the spectrum for each of these compounds is known, we can use digital processing to **deconvolute** the spectrum by fitting the measured absorption spectrum with an iterative superposition of the **individual** spectra for each specie. We can increase accuracy by performing the fit for both the fundamental and first overtone absorptions. The spectrum we calculate from this superposition (of known spectra) method will give the best fit when the ratio of constituents is nearly identical to the actual composition in the plume. In order to perform the fit and subtract out the interfering spectra of water, CO_2 and hydrocarbons, we will team with experienced neural net processing experts at Neurodyne and at the MIT artificial intelligence laboratory.

For example, both NO and NO_2 have strong multiple absorptions in the range 1200-1800 cm^{-1}, a region of strong water vapor absorption. Each also has a weak overtone absorption in the 2900 cm^{-1} region where water vapor has no absorption. By fitting water vapor's known spectrum to the measured plume spectrum and adjusting the concentration and absorption strength to obtain the best fit, we can subtract out the water and fit the NO and NO_2 spectra to what remains of the measured spectrum. Because of water vapor's strong absorption in the 1200-1800 cm^{-1} range, there will be relatively little signal left after removing water and the fit may have much more uncertainty here than at 2900 cm^{-1}, even though the 2900 cm^{-1} absorption peak is relatively weak. In the phase 2 project, we will approach this problem with a combination of design improvements to improve the optical signal-to-noise performance and advanced signal processing to extract useful emission lines in the presence of interferences from other compounds.

5.3 Work Plan

5.3.1 Miniaturization

Compactness and light weight are, of course desirable in a hand-held field instrument. The phase 2 project will explore the practical lower limit of size for the silicon block waveguide spectrograph. The first consideration is the size of the detector array or, more accurately, the size of the detector pixels. We have seen that a typical lower limit on pixel size is 50 μm for the silicon microthermopile arrays. If we want to spread the wavelengths 3-5 μm over the detector array with a resolution of 0.01 μm, (10 nm) then we need 200 array elements. At 50 μm per element, the array would be at least 1 cm long. If instead of the silicon microthermopile array we were to use PbSe or InSb, then we might imagine a minimum pixel size of 5-10 μm, in which case the length of the detector array could be as little as 2 mm. This represents the minimal length of the detector plane facet of the block. So if we were to specify that the detector array occupy no

more than one quadrant of the block, then the block diameter must be at least 1 4 times the length of the detector array, which is just over $\frac{1}{2}$ -inch for a 1 cm long array.

The limits on the size of the focusing grating depend very much on the method of light injection into the waveguide. If we use a typical IR fiber as in the original design, then the fiber has a diameter of 250-400 μm, with a numerical aperture NA of ~0.2. This means that light exiting the fiber and entering the waveguide diverges very slowly, expanding from 250 μm to about 1 mm in a distance of ~6.4 mm. The grating should be large enough to intercept the entire beam at whatever distance from the fiber it is placed. For example, if the block is reduced to one-inch diameter and we maintain the 2:1 entrance path length to exit path length ratio, then the beam will expand to approximately 6 mm and the grating must be at least this large. However, we should remember that the focusing power of the grating is limited to ×2 by aberration and that therefore the focused spot size for a 250 μm fiber will be ~130 μm, covering several pixels and limiting resolution to about 0.03 μm for 3-5 μm spread over 200 pixels.

If light is coupled into the block waveguide using, then we can make the entrance slit any size suitable to our needs. Keeping in mind the 2:1 focusing power and the 50 μm pixel size, this would suggest an entrance slit of 100 μm in order to achieve 0.01 μm resolution for 3-5 μm with a 1 cm long, 200 pixel array.

We must also keep in mind the question of total internal reflection at the exit facet (detector plane) since this represents lost photons. If we use PbSe or InSb deposited directly on the silicon, then this is not an issue. If however we use the silicon microthermopile array, then the angle for total internal reflection is about 17°. This creates a relation between the length of the grating l_g, the length of the detector array l_d and the distance between the two d that is given by:

$$l_g \approx l_d < 2d \tan(17°)$$

For example, if the grating and detector array are both 1 cm long, then the distance between them must be at least 1.6 cm or about $\frac{5}{8}$ -inch to avoid total internal reflection at the detector facet. If the grating is larger or smaller (in length) than the detector, then the distance increases.

Flat Grating

We have used a cylindrical grating in our design to focus as well as diffract the light into its component wavelengths. The shorter the focal length, the more curved (the shorter the radius of curvature of) the cylindrical surface. This presents a challenge of processing if the grating is to be defined by lithography since it is nearly impossible to obtain a uniform photoresist thickness on a curved surface. For this reason it is desirable to develop a focusing grating on a flat surface. Ideally, we would use a holographic grating but such gratings are exceedingly difficult to design and fabricate. However we may be able to both focus and diffract the light with a flat grating similar to a Fresnel zone plate.[1] The question is, would we be able to fabricate the grating lines if

APPENDIX -- PCT APPLICATION NO. PCT/US99/07781

Data Compression - *Principal component analysis* (PCA) addresses the compression of data and removal of noise. Using eigenfunction decomposition, a set of mutually orthonormal vectors (also know as factors or loading vectors) that span the spectral data are determined. These vectors can then be ordered according to the amount of variance captured A subset of these vectors which capture a desired amount of variance is retained. By projecting the original data set upon this subset, the dimensionality of the data can be reduced while capturing a significant amount of the variance.

The feature extraction methods vary from simple linear regression [Wold, et al., 1987, Lorber, et al., 1987] (e.g. PCR, ridge regression) to nonlinear function approximation [Qin and McAvoy, 1992; White, 1995; Sanger, 1989] (e.g. neural networks). Our plan is to investigate three basic approaches; PCR, PLS and neural network based learning algorithms. A mathematical description of PCA and related methods can be found in [Jackson, 1981; Jolliffe, 1986; Wold, et al., 1987; MacGregor, 1989].

As shown in Figure 5.1, coordinates x_1 and x_2 indicate two zero-centered measurement variables with sampled data represented by the black points. The projections of the standard deviation of the data, σ_1 and σ_2 onto vectors v_1 and v_2 provide information regarding the natural coordinates of the data. By rotating the original axes x_1 and x_2 onto the more natural coordinates v_1 and v_2, an orthogonal space is found where the primary axes align along the directions of maximum variance. In the shaded example, the experimental data indicates a linear relationship between the two measured variables x_1 and x_2. By rotating the coordinate system along the direction of maximum variance in the data, the two measured variables could be well-represented by one variable v_1. PCA provides the direction of the maximum variance in the data and compresses the dimensionality of the data from 2 to 1.

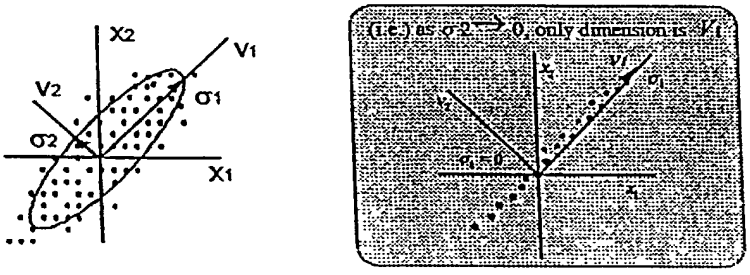

Figure 5.1 *Principal Components Analysis*

Once the principal components are determined, subsequent measurements can be projected onto the natural coordinates or principal components to reduce dimensionality. Once these projections are complete, the components can be plotted to determine linear correlations in the data or indicate variables which may be truncated.

An example of such a correlation using a polysilicon etch in a plasma reactor is provided in Figure 5.2. Each point represents a particular operating condition from a design of

we reduce the size of the spectrograph? In the initial 3" prototype, the grating line widths were about 5 μm

The radii for the zone plate are given by

$$\frac{m\lambda}{2} = \frac{r_m^2}{2}\left(\frac{1}{a} + \frac{1}{b}\right)$$

where r_m are the radii, λ is the wavelength of the light in the medium, a is the distance from grating to source, b is the distance from grating to detector, and m is an integer If we assume a waveguide dimension of one-inch and maintain the 2:1 entrance path length to exit path length ratio, then the equation reduces to

$$r_m^2 = 1.69 \cdot m\frac{\lambda}{n}$$

in centimeters, where n is the index of refraction of the waveguide (n_{Si} = 3.4). For a one inch waveguide, the grating length (maximum r_m) could be no more than 1 cm. Then for a wavelength of 4 μm, m = 5029. This means the line spacing at its finest would be $r_{5028} - r_{5029} \approx 1.0$ μm. Though challenging, this is well within the capability of state-of-the-art lithography. Therefore, it is clear that we can reduce the size of the spectrograph to at least one-inch, possibly ¾-inch diameter when using a detector with 50 μm pixels. Shrinking the spectrograph further will mean making the detector pixels proportionately smaller (very possible) but should relax the lithography requirement since m is proportional to grating length squared.

5.3.2 Deconvolution

For a single species, it is straightforward to determine the concentration of gas in a plume by measuring either emission (or equivalently absorption over some known path). We demonstrated that our phase 1 optical breadboard can do this, without any additional signal processing. In phase 2 we will address the real-life situation with multiple species and the consequent need to both recognize which species are present and then determine the absolute concentration of each species. This is also a general problem faced by IR spectroscopists and instrument designers working with multiple sensor or transducer inputs. Following earlier work in the literature, References [Hashem, 1994; Lewis, 1995], we will team with the neural network experts at Neurodyne to apply neural network processing to solve the deconvolution problem.

The ability to extract concentrations from emission spectra is severely constrained by both chemical and instrumental factors when either a narrow spectral region, or only a few wavelengths are used for the measurement. The intent is to avoid or mitigate the influence of these problems by acquiring high resolution, detailed spectra with good signal-to-noise.

Spectral information can be very useful for characterizing multi-species environments. However this information is usually buried in thousands of variables captured over a wide range of wavelength. Chemometric methods attempt to separate the useful information from noise and redundancy by determining relevant correlations in the data. There are two fundamental steps in these approaches. The first is the compression of data and the second is the extraction of interesting characteristics.

APPENDIX - - PCT APPLICATION NO. PCT/US99/07781

experiments PCA was performed on the data and the first few components were found to account for 96% of the variation in the data. Projections of the optical emission spectral measurements onto the first two principal components indicates clustering along %HBr feedgas ratios labeled next to each point. In Figure 5.3, a secondary ordering is shown along magnetic field orientation. This is an example to indicate the ability of PCA in spectral data analysis. There are a number of more advanced methods which combine linear regression and neural networks to extract useful data from complex spectral measurements

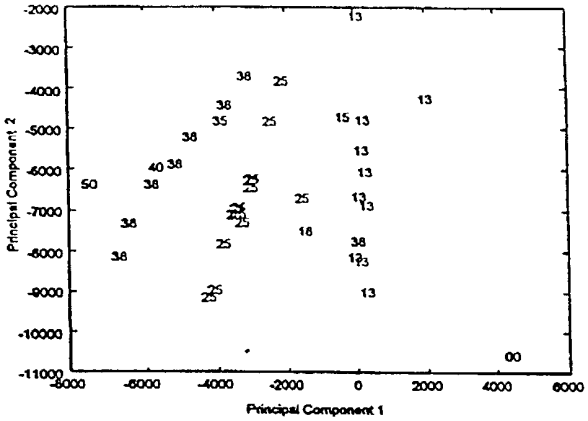

Figure 5.2 *Optical Emssion Spectral Projections by Gas Flow*

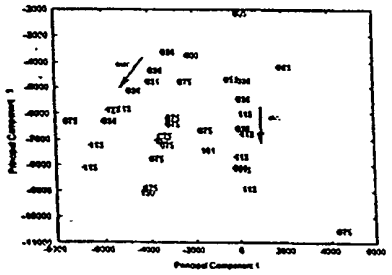

Figure 5.3 *Optical Emission Spectral Projections by Magnetic Field Orientation*

In most applications of PCA [7, 15, 9], it is desired to reduce the dimensionality and complexity of n-dimensional space to that which enables easier classification of the data. This is done by effectively rotating the $r \times n$ data matrix M onto the new orthogonal basis spanned by n eigenvectors of the $n \times n$ covariance matrix C=cov(M). Finally the eigenvector matrix of C, also referred to as principal components, is shown to transform the matrix M to an orthogonal matrix T of scores which have no cross-correlation and reduce the dimensionality of M.

APPENDIX - - PCT APPLICATION NO. PCT/US99/07781

In general, the r x n matrix of raw data L is formatted such that each element L_{ij} is the jth measurement over n total variables measured during the ith run over r total runs. The r x n raw data matrix L is mean-centered to produce the r x n data matrix M where the elements

$$M_{ij} = (L_{ij} - \bar{L}_j) \text{ for } 1 \le i \le r \text{ and } 1 \le j \le n \tag{1}$$

are mean-centered using the sample mean $\bar{L}_j$ of each column (or channel) j over the total number of experimental runs (r). The n x n sample covariance matrix C measures the dependence between variables of mean-centered matrix M can be written as

$$C = \left(\frac{1}{r-1}\right) \cdot M^T M \tag{2}$$

The eigenvectors of the covariance matrix are linear combinations of the original variables that represent orthogonal components of the variance in the data and are referred to as principal components. The right eigenvectors of the covariance matrix C can be calculated by solving the equation:

$$CV = V\Lambda \tag{3}$$

where $V = [v_1 \quad \cdots \quad v_n]$ is the n x n matrix containing n eigenvectors and Λ is an n x n diagonal matrix of eigenvalues. In equation (3), each n dimensional eigenvector v_j corresponds to the jth eigenvalue λ_j. Once calculated, the associated eigenvalues and eigenvectors are ordered in a descending manner such that $\lambda_1 \ge \lambda_2 \ge \ldots \ge \lambda_n$. Therefore the eigenvector v_1 associated with the largest eigenvalue λ_1 of C indicates the direction of maximum variance and the eigenvector associated with the smallest eigenvalue indicates the direction of minimum variance. The variance in any direction v_j may be measured by dividing the associated eigenvalue λ_j by the sum of the n eigenvalues or the trace of covariance matrix C.

$$\% \text{ variation in eigenvector } (v_j) = \frac{\lambda_i}{\sum_j \lambda_j} \cdot (100) = \frac{\lambda_i}{trace(C)} \cdot (100) \tag{4}$$

$$Mv_j = t_j \text{ for } 1 \le j \le n \tag{5}$$

If we project M onto the eigenvector v_j of the covariance matrix C we obtain an r -dimensional vector called a score t_j. If we project M onto the eigenvector matrix V, we obtain an r x n matrix T composed of n such column vectors. This transformation produces a new representation of the data. By projecting M onto the basis vectors in V, the new matrix T has orthogonal columns and retains all of the variance Λ in M:

$$MV = T \tag{6}$$

APPENDIX - - PCT APPLICATION NO. PCT/US99/07781

$$(MV)^T MV = T^T T \tag{7}$$

$$V^T M^T MV = T^T T \tag{8}$$

$$(r-1)V^T CV = T^T T \tag{9}$$

$$V^T V\Lambda = \left(\frac{1}{r-1}\right)T^T T \tag{10}$$

$$\Lambda = \left(\frac{1}{r-1}\right)T^T T \tag{11}$$

Since the principal components or eigenvectors of C are ordered along directions of maximum to minimum variance, the column dimension n of matrix V can be reduced to a more manageable number while capturing as much variance as possible. For example if the y most significant principal components or eigenvectors (e.g. y=4) capture 99% of the variation in the data we could reduce the n x n eigenvector matrix V to an n x y matrix $\hat{V}$. Data matrix M can then be projected onto these principal components reducing the measured data from an r x n matrix T to the r x y matrix, $\hat{T} = [t_1, t_2, .., t_y]$.

$$M\hat{V} = \hat{T} \tag{12}$$

As with matrix M, the rows of $\hat{T}$ correspond to experimental runs 1 through r. The vectors of scores 1 through y represent the majority of variance in the data while reducing the column dimension by (n-y).

Feature Extraction - The feature extraction methods vary from simple linear regression [Wold, Kowalski] (e.g. PCR, ridge regression) to nonlinear function approximation [White, McAvoy] (e.g. neural networks). Our plan is to investigate three basic approaches; PCR, PLS and neural network based learning algorithms.

Principal Component Regression (PCR) and Partial Least Squares, (PLS) Methods Both PCR and PLS begin by using PCA to determine the orthonormal vectors that span the spectral data. The subset of these vectors are mapped to spectral characteristics (e.g. species concentrations) using regression. Using PCR, an ill-conditioned matrix of spectral data can be reduced to a subset of principal components and then fit to concentration or process variables. Partial Least Squares (PLS) generates a subset of orthogonal vectors for not only the spectral data but for the concentrations as well. PLS rotates the spectral and concentration factors in order to optimize the regression fit from the measured spectra to concentrations.

Both PCR and PLS utilize the decomposition of a matrix of input data X and the linear regression of output data matrix Y upon X.

$$Y = XB + e \tag{13}$$

APPENDIX - - PCT APPLICATION NO. PCT/US99/07781

In PCR, X is transformed by the orthogonal matrix of eigenvectors of $X^T X$ to a matrix of scores T (as shown in equation 6 above).

$$XV = T \tag{14}$$

The matrix output matrix Y is then regression upon the reduced subset of scores, $\hat{T}$. To accomodate the variance in Y, PLS weights the covariance matrix by the addition of positive definite matrix YY^T to $X^T X$, providing a new covariance matrix $X^T YY^T X$. In this new form, those elements of Y that are close to zero reduce the effect of associated rows of X and thus we do not try to predict noise [6]. The addition of Y containing elements that are close to zero (e.g. noise) results in the associated rows of X to not be used [6]. In this case, the weighted covariance matrix is decomposed into a matrix of eigenvectors, R and eigenvalues, D.

$$X^T YY^T X = RDR^T . \tag{15}$$

The matrix X is then transformed using the eigenvector matrix R to an orthogonal matrix of scores, T as described in (2) above. The output matrix Y is then regressed upon T, as performed in PCR.

In terms of the physical interpretation of PCA, PLS involves the rotation of the components of X and Y such that the resulting distance is minimized. This is accomplished by iteratively regressing on the selected components of X and Y and stopping when the components of X are no longer near those of Y.

Nonlinear Relationships Between Measurements and Concentrations There are often nonlinear relationships between spectral data and characteristics reflected in species concentrations, the influence of plume temperature noted above is a good example. In order to fit these relationships, a nonlinear function approximation method (e.g. locally weighted regression, polynomial networks, multi-layer perceptron networks) may be used. Often these methods are lumped into the general class of neural network or learning algorithms. Perhaps the most applicable learning algorithm to the application described herein are spatially localized learning algorithms. The most generic form of training a multilayer perceptron (MLP) network uses gradient descent where the weights are adjusted proportional to the derivative of error between the actual output and target values. This approach can best be visualized as a ball traveling along a bowl shaped surface along the steepest direction until the minimum is achieved.

Locally weighted regression is a function approximation method used with memory based learning [Cleveland and Delvin, 1988; Atkeson et al, 1995]. The training data for the learning algorithm is simply stored in memory. When a query is requested, locally weighted regression is done about the query point to make a prediction. For nonlinear modeling we assume that there is a locally linear model (holds in a spatial locality about the given query point). Global regression implicitly weights each data point equally in the regression. In local regression each data point is weighted according to its distance from the point being queried. Since only the points in the spatial neighborhood of the query point contribute strongly to its prediction, this method can accurately model globally nonlinear functions. Note that global regression is cheap because the

APPENDIX -- PCT APPLICATION NO. PCT/US99/07781

model parameters are solved once for all future queries where local regression is more expensive because new weights and a new solution for beta is required for each query There are methods of making this computation efficient, however [Deng and Moore, 1995].

Multi-Layer Perceptron Neural Network - Although there exists several nonlinear function approximation approaches to select from, several neural network approaches have demonstrated benefits over traditional regression techniques in several semiconductor applications [3,5,9,14].

Often referred to as a neural network, this method uses a multilayer perceptron connectionist network with a backpropagation learning algorithm to fit multivariable data. Although basic knowledge regarding gradient descent based learning algorithms is necessary, the neural network offers an advantage over many nonlinear function approximation approaches in that one need not know much about the structure or order of the mapping. The most generic form of training a multilayer perceptron (MLP) network uses gradient descent where the weights are adjusted proportional to the derivative of error between the actual output and target values. This approach can best be visualized as a ball traveling along a rough bowl shaped surface along the steepest direction until a minimum is achieved.

There are many forms of backpropagation learning, most developed to speed convergence. In our approach, weight updates are achieved through Levenberg-Marquardt optimization [4] adapted for use with the MLP architecture. (A more thorough analysis of model based estimation and optimization using neural networks is provided in [14].) As with any learning algorithm, MLP networks can be overtrained thus reducing the generalization capabilities. To prevent this, leave-one-out cross validation can be used to achieve sufficient generalization.

APPENDIX -- PCT APPLICATION NO. PCT/US99/07781

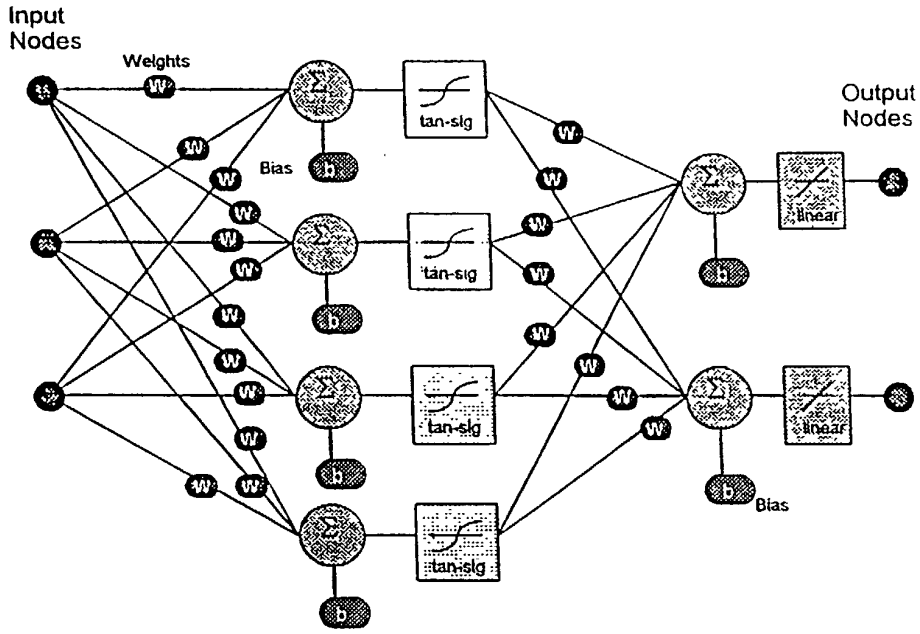

Figure 5.4 *Multilayer Perceptron Architecture*

5.3.3 Packaging and Instrumentation

The thrust of this Task will be to solidify system and sub-system designs and fabrication procedures with respect to producibility or adaptability to cost-effective production. While a large part of the design analysis will have been performed in previous tasks to optimize system performance, this task will re-evaluate the system with emphasis on how readily the design lends itself to high volume fabrication, manufacturing, and assembly. It is entirely possible that the best design from a performance standpoint will be compatible with volume manufacturing, while it is also possible that compromises will be required to make an effective and producible system. This evaluation will be carried out in conjunction with industrial partners, potential customers, and finally with the relevant outside vendors.

As an adjunct part of this activity, to be funded by the company, we will conduct market research, which we will expand and revise as the system becomes more fully developed and refined. At the time of the writing of this proposal the largest short-term commercial potential appears to be with the simple spectrograph which can be incorporated into many existing IR sensing systems. This has the appeal that there is an existing market of equipment manufacturing companies with established customer bases who have shown an interest based only on our

preliminary results Ultimately we may choose to bring the complete instrument system to market, but in the short-term we will be more effective in providing them with this breakthrough spectrograph. Options for production-scale fabrication, marketing, and distribution will be investigated. Revenues from sales of the spectrograph, hopefully initiated before the end of Phase II, will solidify the Ion Optics business base, and support the aggressive development and commercialization of infrared sensors and instruments.

5.3.4 Calibration and Accuracy

Establishing NIST traceablity for the instrument will be a critical stage in the development and acceptance of our plume spectrometer. NIST's Radiometric Physics Division, in keeping with its charter to promote accurate and useful radiation measurement technology in the UV, visible, and infrared spectral regions, takes an active role in pyrometry and spectral radiance calibrations and the preparation of calibration protocols. We plan to utilize the Division's personnel and facilities to relate total and spectrally resolved *puls*IR output to those of a NIST reference blackbody, thus establishing traceablility to the source used to certify the secondary standards employed by instrument manufacturers and calibration laboratories.

To accomplish this, Ion Optics will coordinate with NIST to produce a calibration plan whose objective is to develop the pulsIR flat-pack as transfer standard. This will require working with personnel in the NIST laboratories, revising the plan to incorporate their recommendations, and finally resubmitting it to NIST for final review and approval. The approved certification plan will then be carried out in the appropriate facilities in the Physics Division's laboratories.

These facilities include a high accuracy cryogenic radiometer (HACR) whose intrinsic uncertainty is 0.01% or better (one sigma) over the range 0.2 to 11 μm; it serves as the basis for most of the calibrations offered by the Division. While the HACR is extremely accurate and widely employed to characterize the absolute spectral response, spatial uniformity, and linearity of photodetectors, the low background infrared (LBIR) facility (Figure 5.5) is likely to be the facility of choice. Using an absolute cryogenic radiometer capable of measuring irradiance at its aperture from a few nW/cm^2 to 10 $\mu W/cm^2$ with better than 1% uncertainty (two sigma), the LBIR provides accurate calibrations of IR sources, spectrophotometers, and low background detectors over the range from 0.2 to 25 μm.

APPENDIX -- PCT APPLICATION NO. PCT/US99/07781

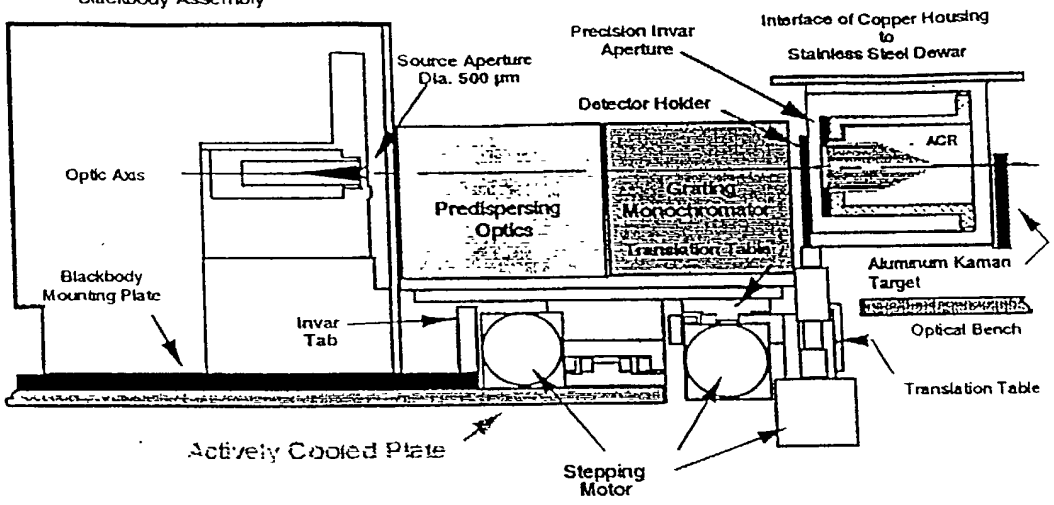

Figure 5.5 *A cross-sectional view of the low background infrared facility, its blackbody, and its absolute cryogenic radiometer.*

5.3.5 Brassboard Device Integration and Test

The assembled system will be subjected to a series of tests to validate its accuracy and reliability. To the extent possible, we will work with other organizations to achieve an absolute wavelength and intensity calibration of the system against secondary sources and NIST-traceable references. Stability tests will consist of measuring the system's response to known samples under controlled laboratory conditions and then subjecting the system to vibration, thermal cycling, and pressure changes. Throughout these environmental variations the systems response to the constant sample will be recorded and compared to the initial indication.

As an evaluation of the system's stability, these measurements will be performed continuously over a period of several weeks. Measurements performed under identical conditions will be compared to evaluate system stability. Based on the results of these evaluations, the design of the individual components, their assembly, and the packaging will be re-evaluated and modified as necessary.

After the iterative component and system analysis has been completed, the refined prototype system will be demonstrated in an actual field test. This test will consist of installing the instrument at SSC. By mounting the prototype system next to established monitoring equipment, we will be able to verify its reliability and accuracy for use as a sole source of information in plume testing on actual engines at SSC.

The most important part of the Phase II effort will be demonstration of the capabilities of the instrument, particularly in field trials. We will work with SSC and other potential customers to arrange for actual tests in the laboratory and in on-site tests. As illustrated by the attached

APPENDIX -- PCT APPLICATION NO. PCT/US99/07781

1. Introduction

NASA has a need for low-cost, low-power, low-mass, highly integrated spectral data acquisition instruments that enable data acquisition and feed back control from both ground based testing facilities and on spacecraft. We are building a novel, monolithically integrated, infrared micro-spectrograph. It is fabricated from silicon to address this need. This device will incorporate the silicon micro spectrograph, simple focusing optics, and an electrical interface for power input and remote readout. The silicon micro spectrograph is a slab of high purity, optical grade silicon, with a holographic diffraction grating and linear detector array monolithically integrated right on the surface. . This system will be lightweight, compact, rugged, alignment-free, calibration-free, and low-cost. During the first quarter of this project, we have modeled and redesigned the 3" prototype device into a 1" device with improvements providing 4 times the resolution and sensitivity of the Phase I instrument. We have completed the design modifications and are preparing for the fabrication of the first test beds.

Already at this stage of integration, we have shown that a micro machined silicon device can achieve resolution and throughput comparable to off-the-shelf 1/8 meter monochromators which are ten times larger and heavier. Work for the next quarter will concentrate on fabrication of the next generation prototype, about 1/4 the size of the device currently operating in our laboratory.

2. Technical Overview

This past quarter has seen the re-evaluation of the Phase I design, determination of its week points and the development of an improved design. The process we followed to achieve this included: modeling the spectrometer system to determine minimum detectable signal strengths, determining the spectral bandwidth over which the system must operate, and determining minimum spectral resolution requirements. We have conceived and developed a new design for an easier to manufacture optical bench. After ray tracing and optimizing the optics, we have achieved a factor of 4 improvement in optical throughput. We have also finalized the selection of the detector array, developed a miniature integrated chopper design, and developed a fabrication plan with our vendors.

3. Technical Accomplishments

Significant progress has been made since the start of the program. System modeling, optical redesign, detector selection, fabrication procedures and preliminary mechanical housings have been developed. A detailed discussion of our accomplishments follow.

APPENDIX -- PCT APPLICATION NO. PCT/US99/07781

3.1 Reevaluation of Phase I Spectrometer

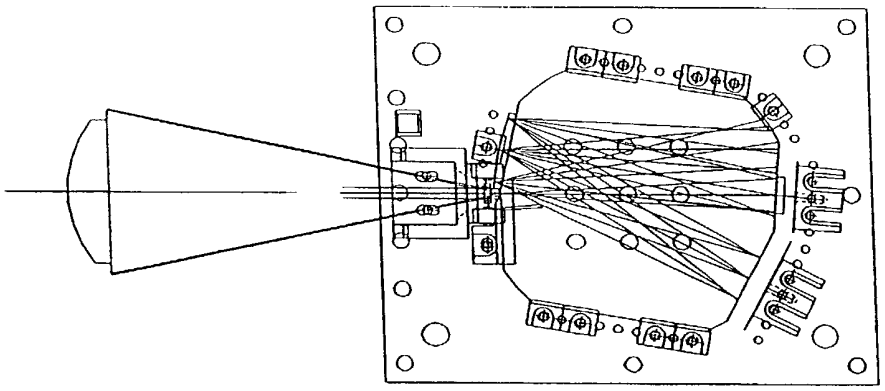

Figure 3.1 Phase I optical bench and lay out showing input lens, silicon slab, grating, detector plane, chopper, and filter.

The Phase I block spectrograph was reevaluated to uncover the lessons learned and to find areas of improvement for the Phase 2 miniaturization redesign. The following lists some of the key points:

•*Size* - The Phase I design is too large, does not provide an advantage over more conventional designs, and is relatively complex and expensive to manufacture.

•*Facets* - The Phase I block had 4 active facets, which were at precise odd angles to one another, two of which require AR coating.

•*Fabrication* - The Phase I design called for the grating to be fabricated onto a cylindrical surface whose radius was smaller than the block. This proved impossible to fabricate, since it would require acute inside corners in the silicon block. In the Phase I design we solved this problem by applying the curvature to an external piece and contact coupling it to the block. This functioned correctly but proved to be lossy and provided reflection ghosts in the system.

•*Grating Design* - The design utilized a chirped grating to flatten the image field of the Rowland circle optical design. This required an expensive holographic setup. The curvature of the grating substrate made it difficult to etch the grating into the silicon uniformly, resulting in uneven optical efficiency across the grating.

APPENDIX -- PCT APPLICATION NO. PCT/US99/07781

•*Readout Electronics* - The 16 channel lock-in amplifier of the Phase I device was superior in performance to the digital lock-in initially used. However it required two 4" x 6" PC boards, much too bulky for the Phase II miniature device.

•*Chopper Design* - The tuning fork chopper used in the Phase I device has magnetic coil drivers, which radiate EM interference. This interference is at the chopping frequency and can not be filtered from the signal. This is an intrinsic short coming of the tuning fork design.

•*Light baffle* - The internal baffle cut in the block proved to be a tremendous scattering sight, greatly increasing the background radiation reaching the detector and reducing the optical signal discrimination.

•*Entrance Slit* - The entrance slit, built from a separate piece of machined aluminum, caused scattering from its edges, contributing to the background noise.

•*AR Coatings* - The system requires anti reflection coatings on its entrance and exit facets, this will reduce the losses by 50%. However since the facets are at odd angles this could be difficult and expensive to accomplish. Since the detectors are contact coupled to the silicon, special matching AR coatings must be devised to match the detector to the silicon index. This is a development task of its own.

These factors along with the discoveries we made from the system model were used to design a new spectrometer lay out and detection system, whose advantages are discussed in section 3.5.

3.2 System Modeling

A system model was created to determine the detectivity of the system. The basic question to be answered was how much radiance must the target provide in order to be detected by the spectrographic system. The intuitive answer is to make the system with the highest detectivity. However within the limitation of the detectors and spectrometer throughput what can we reasonably expect to see, and is that sufficient to make measurements to detect the chemicals of interest. Two aspects of this question have been explored, the first is to determine what temperature of the target (a measure of radiance) is required to get a signal to noise of 1 out of the detectors at each wavelength. This assumes that the sample radiates like a black body. The second aspect is what spectral features are we looking for in the sample gasses, what resolution is required to resolve them, and are they within our spectral sensitivity.

We directed our consultant Dr. A. Tuchman of AVI to develop a system model that took into account temperature of the target, spectral throughput of the lens and optical

APPENDIX -- PCT APPLICATION NO. PCT/US99/07781

bench, efficiency of the grating, spectral separation, and detectivity of the detector array. The model produced the following results:

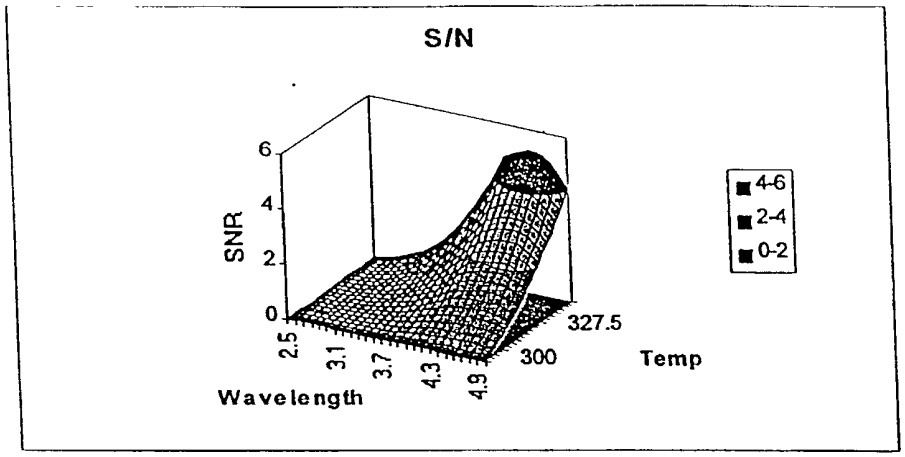

FIGURE 3.2 This figure shows the detectivity of the spectrometer system. The horizontal axis indicate the spectral band and the thermal temperature (radiant intensity), the vertical axis indicates the signal to noise ratio. It shows that at longer wavelengths and higher temperatures the signal to noise is higher (system will detect better).

The effort in the next quarter of Phase II will include estimates of S/N over the regions of interest and relative to the detectors being purchased under Phase II. This effort will be coupled with a determination as to what the spectral features are within the sample gasses, and what species are within our spectral sensitivity.

3.3 Spectral Analysis

We have subcontracted Neurodyne, Inc. (NDI) to develop gas identification software. The objective is to pick out the individual gas constituents from the compound spectral data. This is particularly difficult because the signals are overlapped, distorted, and vary rapidly with time. The neural net approach they will use will identify gas species not by their single prominent peaks alone, but will use all the spectral components in parallel. It is hoped that they will not only identify each species but also the concentration of each gas in the plume. An added benefit of this approach is that any non linearity in the system is accounted for in the calibration of the software, easing the design requirements.

The approach utilized data from a high resolution FTIR spectrograph. By averaging adjacent measurements, the resolution of the spectra was reduced to match that

obtained by our lower resolution device. The next step is to added these spectra together in various weights, and to test the software to see if they can identify the component spectra and the weights.

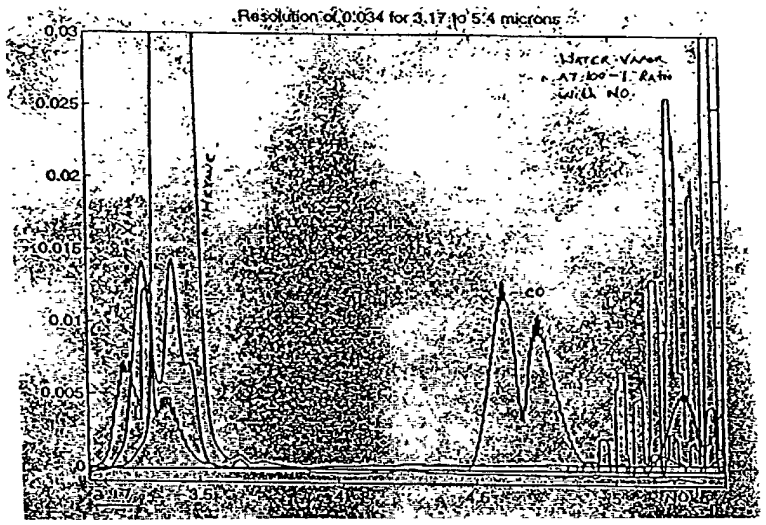

Figure 3.3 Chemical spectra selected are water vapor, carbon dioxide, carbon monoxide, sulfur dioxide, hydrogen sulfide, ammonia, methane, and ethane. In this figure the high resolution spectra obtained from FTIR spectrograph have been blurred to simulate the lower resolution of the 64 channel micro spectrograph.

The results of their analysis indicates that the spectral resolution is sufficient, but the spectral range needs to be translated slightly. A wavelength range of 3.17 to 5.42 um at a resolution of 0.034 um is acceptable for measuring hydrocarbons, CO, CO_2, and NO. This range will allow us to see the hydrocarbon major peaks from 3.2 to 3.6 microns, the CO_2 peaks from 4.2 to 4..4 microns, the CO peaks from 4.5 to 4.8 microns and the NO peaks from 5.1 to 5.4 microns.

Our initial design called for 2.5 to 5 um spectral range, this allowed us to use un-cooled PbSe detectors. However after the NDI analysis, it is apparent that important spectral feature exist out to 5.5 um, and that there are no significant features below 3.17 um. Therefore we have varied our optical design to operate from 3.17 to 5.5 um. This has also required the change of the detection scheme, requiring us to utilize TE cooled PbSe detectors. By cooling the detectors the spectral sensitive cut-off moves from 5 um to 5.5 um, with the added benefit that the D* improves by a factor of 2. However

the cooling will require a more complex housing to seal out moisture, a driver for the TE cooler with thermal feed back control, and a heat sink.

To develop a plume gas data base, NDI has utilized auto exhaust emissions. These emission contain similar gasses to that of the plume, are readily available, and can be provided in measured mixture by NDI's engine lab facility in West Virginia. Emission samples were taken from a diesel engine operated over a number of engine load conditions. The samples were evaluated using a MIDAC FTIR system. Macros were written to pull out key peaks in various ranges which would help deconvolve NO_x from water vapor. From their preliminary analysis, the water vapor is the most difficult problem, overlapping and masking the other gas constituents. They have been examining combustion equations to look for correlations that can be exploited in analyzing the spectra. One solution would be to correlate the CO_2 line with water vapor since their production is strongly associated within the combustion process.

NDI has requested information on rocket plume spectral data. We are in the process of trying to collect that data from sources such as NASA and the Air Force. We plan to submit a formal request for that data shortly.

3.4 Optical Front End

From the analysis of the Phase I device and the results of our system models we have developed an improved design that will greatly increase the utility of the spectrometer. We have completed the baseline silicon block spectrometer optic design. It uses a modified 'Ebert' layout fabricated from a single piece of machined silicon.

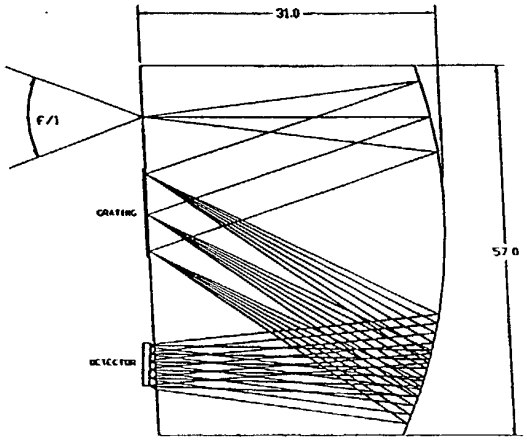

APPENDIX -- PCT APPLICATION NO. PCT/US99/07781

Figure 3.4 Phase II optical bench raytrace. This layout has only two optical surfaces, greatly simplifying fabrication and increasing reliability by eliminating tolerance stack up inaccuracies. The flat grating design increases the grating's efficiency and makes the device easier to manufacture. Its F/1 design allows for twice the throughput of the Phase I design, and its air gap at the detectors provide for focusing and permits the use of conventional AR coats. Dimensions are in mm.

In the 'D' shaped optic IR light enters the entrance slit, an AR coated area defined by thin film deposited layer. The radiation illuminates a cylinder mirror which collimates the light. The high refractive index of silicon greatly reduces the angle of the cone of light, this permits the use of an F/1 lens at the entrance aperture. It also reduces the size of the cylinder mirror, and permits the spectrograph to operate near the diffraction limit. The collimated beam is reflected off a gold coated diffraction grating. The grating disperses the IR spectrum, which is re-imaged after a second reflection off the cylinder mirror. The light exits the block through an AR coated surface and is imaged onto the detector plane. The detector plane is at a slight angle in order to flatten the field across the image. The air gap permits the detector plane location to be adjusted, allowing for manual focusing. As the rays exit the block the large cone angle of the rays is restored, more fully filling the acceptance angle of the detector.

The grating produces a number of lower energy unwanted diffraction orders. In our earlier design these orders were trapped in the block and were scattered and added to unwanted background signal on the detector. The new design permits the exit of these unwanted orders out of the flat surface where they will be captured by a light trap.

The following table addresses all the pros and cons of this new "D" shaped design.

APPENDIX -- PCT APPLICATION NO. PCT/US99/07781

Requirement	Phase 1Design	Phase 2 Design	Pro / Con
Size/weight/volume	3" dia. x .25" thk 1.75 cu. in.	1" x 1.5" x .040" thk 0.06 cu .in.	Provides a 30x decrease in optical bench weight
Number of Facets	6 - 4 on block and 2 on contact coupled grating	2 - each facet used multiple times	4 reflection design significantly decreases size
Grating	Chirped grating on separate curved surface	Conventional flat grating	Easier to manufacture, and maintain uniform efficiency, etched into block prohibits the exchange of gratings
Chopper	Tuning fork	PZT bimorph	No radiated fields, chopper not required with micro thermopile detector
Scattering	No exit for higher diffracted order, no beam dump, scattering internal baffle	AR coated exit for higher orders, external beam dumps, no internal baffles,	Decreases signal noise by eliminating scattered light to detector
AR coating	AR coating on two odd angle surfaces	AR coating on 1 surface	Cheaper to manufacture
Spectral band	2.5 - 5 um	3.13 - 5.5	Better spectral features, but requires TE cooling of the PbSe detecotr
Spectral Resolution	0.15 um	0.039 um	Higher resolution required for gas identification
Detector	PbSe 16 element	TE cooled PbSe 64 element or micro thermopile	Required to find spectral features, PbSe cooling improves SNR
Read out electronics	16 channel lock-in amplifier	64 Channel multiplexed w/ digital lock-in; or w/ 64 hybrid lock-in amplifiers	Greatly reduces space, Hybrid has fewer noise sources in system but is more bulky
Filter	External	Used as window on vacuum package	Dual use saves components
Package	Open air, large	Sealed, for dry gas or vacuum	Needed to keep condensate off TE cooled detector, more expensive
Detector/block interface	Contact coupled	Air gap	Provides for focusing, eases exchange of detectors.
Slit	Free standing to provide focus	Deposited on block	Deposited slit is finer, less scattering and ghosts

It was concluded that the new design was superior to the Phase I design, and the technical risk was small enough to make it worth pursuing.

APPENDIX -- PCT APPLICATION NO. PCT/US99/07781

3.5 Fabrication

Due to the uniqueness of the design we have worked closely with our vendors to develop a fabrication plan that is consistent with the inexpensive mass production of the front end. This consist of the following:

Optical blanks. "D" shaped optical blanks are purchase from VA Optical, a silicon supplier. Their main business is to produce substrates for the micro-chip industry. For this reason they can produce superior flat polish on both sides of the optic. The near net shape will include all the polished flats but not the cylinder surface.

Cylinder. The blanks will be sent to Digital Optics Corporation who will stack 20 parts into a monolithic block, then shape the block into a cylinder lens. They possess the interferometric equipment necessary to measure and produce the necessary surface on the cylinder mirror. They will gold coat the mirror and AR coat the flat.

Grating. The gratings will be built by Diffraction Limited. They will produce a grating in photoresist on the surface and etch it into the silicon. They will also work with the elements assembled in a stack. Once the grating is made they will add gold reflector overcoat and deposit the entrance slit.

Assembly. The part will be returned to Ion Optics where its performance will be measured. This is done by feeding the block with a lab spectrometer and measuring the quality of the output image with an IR camera. Once its performance is verified the device will be integrated into the housing with the detector and focused.

3.6 Mechanical

The design requires the precise alignment of the optical bench, the chopper, the detector array and the filter. This is all accomplished with a precision sealed package. The package holds the chopper, filter and detector in position and provides for a vacuum seal.

The miniature chopper we developed consists of a piezo-electric (PZT) bimorph strip with a flag on the end. The bimorph strip is a sandwich of PZT and stainless steel bonded to together. The bimorph curls like a bimetallic, as a voltage is applied across the PZT causing it to change length. This provides very fast chopping of the optical beam with minimum volume and no EMI.

The electronic read out will be fit into the vacuum package so the signals are amplified and multiplexed before leaving the package. This provides for a minimum number of

electrical feed through. It also provides a modularity of the design, so the spectrometer optics package can be traded out with little effort.

The detector mount will hold the back side of the TE cooler to which the detector array is bonded. The mount will allow the detector to be precisely positioned with micrometer screw adjusts and then locked into place. Heat from the TE cooler will be conducted through the mount and into the base of the package.

The package will have a removable cover that will permit the components to be aligned prior to the cover being applied. The cover will contain the entrance window that will be coated to act as a cut off filter in the system. The package will also incorporate a mount to hold the input lens or an input fiber optic.

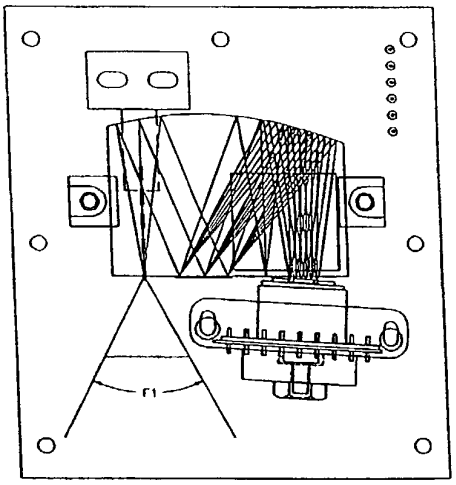

FIGURE 3.5 The preliminary design of housing, heat sinks, chopper, detector mount, and alignment fixtures have been completed. These will be further refined and detailed once the detector configuration has been finalized.

3.7 Detectors

When it comes to determining system performance, no other component will have as much effect perhaps than the detector. For this reason, we have extensively researched detectors applicable for our requirements. However criteria other than performance must be considered when evaluating detector systems for our portable, handheld spectrometer. These include cost, size, complexity and flexibility. For example, photoconductive devices typically suffer from low frequency or 1/f noise which can be reduced by chopping the input signal and AC coupling the output from the

detector. However this low noise detection scheme increase the level of complexity of the optical system and the read out electronics.

After considering the wide range of detector arrays available, we have narrowed our options to two choices: a PbSe photoconductive array and a micro-thermopile linear array. A thermoelectrically cooled PbSe array provides the best performance with moderate cooling requirements in our spectral region of interest. When cooled to between 145 and 250 K, low noise performance is obtained. We intend to use solid state thermoelectric coolers, which are rugged, low cost devices that can provide sufficient cooling for the PbSe device.

We have completed an extensive survey and contacted many of the PbSe array detector vendors in the U.S. Out of this survey we located only one, Optoelectronics Texton, with an operating multiplexed PbSe array. We spent several months in good faith effort, developing an array design, operating parameters, and package. However when it came time to formalize our purchase order, Opto provided a price three times that of the budgetary figures we had discussed (their quote approached $100K). This cost is well outside our budget, and the episode has been a major schedule set back to the program. We have now developed an alternative detector plan, and have begun to carry it out.

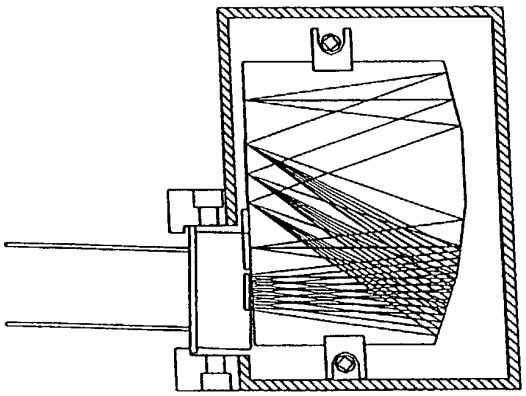

Figure 3.6 This is the package design that utilizes the Optoelectronics/Textron integrated multiplexor and PbSe detector array.

After investigating a number of other PbSe detector array sources, we have selected New England Photoconductor (NEP) as the detector array vendor. NEP is a local manufacturer of photoconductive arrays that supplied the array used in the Phase 1 system. Their performance under that contract was very favorable. NEP quoted the lowest price for a custom 64 element linear array and will integrate their array with a

newly developed custom integrated multiplexor circuit. We are in the process of evaluating the technical risk and system performance of this developmental multiplexor, and its possible impact on system performance. Its major advantage is that an integrated multiplexor will significantly reduce the size, cost, and complexity of the readout electronics.

We have also investigated the use of a 64 element micro-thermopile detector. There are many advantages to using the micro-thermopile: it is sensitive over a wide range of wavelengths, it does not suffer from 1/f noise and so does not require a chopper, and it does not have to be cooled. Conventional thermopiles are not as sensitive as a PbSe detector, however a source at JPL believes that they can produce a micro machined thermopile in the configuration we desire with a D* of 10^9, equivalent to PbSe. Although this device is experimental, we hope to incorporate this device into a prototype spectrometer and evaluate its performance. Although we believe we need the sensitivity of a PbSe detector at this time, the micro-thermopile is a very attractive alternative, that could be used in spectrographs that range from 1 - 20 um (the full IR spectrum).

3.8 Readout Electronics

Typically, a modulated or chopped detector signal is recovered using a lock-in amplifier or synchronous detection scheme. The large number of pixels and the use of a multiplexor complicates the extraction of the modulated signal from our PbSe detector. We are currently investigating extracting the modulated output digitally. The serial output of the multiplexor will be digitized with a high speed, high resolution A/D converter. The sampled outputs from each pixel will be collected from multiple scans and processed digitally. For example, by performing a Fast Fourier Transform (FFT) on the data collected for each one pixel, the energy content at the modulation frequency can be determined. The FFT acts as a narrowband filter at the modulation frequency. This energy can be averaged over time to further increase signal to noise. We plan to evaluate this approach using an off-the-shelf A/D board and a standard analysis package running on a personal computer. This allows us to rapidly prototype and test different processing techniques.

In order to reduce our technical risk, we have also specified and received a proposal for a hybrid multi-channel lock-in amplifier. This device will replace the multiplexor. It is assembled from un-packaged die and mounted on a thick film circuit; an eight channel device occupies 2.56 square inches. Although this approach is fairly large and costly, it has a low technical risk and guaranties maximum performance.

APPENDIX -- PCT APPLICATION NO. PCT/US99/07781

3.9 Processing

The continued growth of the digital signal processing market has resulted in a number of low cost DSP processors for embedded applications. We are currently investigating several processors for our application. In particular, we are evaluating the DSP56L811 from Motorola. This processor is a cost-effective solution that combines the prodigious number crunching of a digital signal processor with the versatile functionality of a microcontroller. This processor could perform the signal processing necessary for signal extraction and chemical detection and also control a display and keypad; a serial interface will be used for communication with an external computer. An off-the-shelf development board will facilitate the rapid prototyping of the final spectrometer unit.

4. Plans For Next Quarter

4.1 Fabrication of the Silicon Spectrometer Optic.

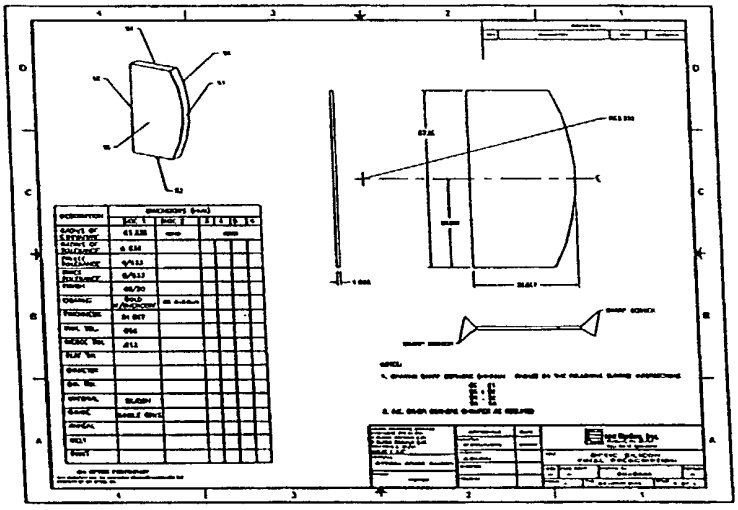

Figure 4.1 Detailed drawing of optical bench ready for fabrication.

The drawing package has been sent out for quotation. We intend to contract three vendors to build the assembly in stages.

1. The silicon wafer and optical substrate fabricator will produce the silicon optic without the cylindrical optical surface and optical coatings.
2. The lens fabricator will finish the cylindrical surface and AR coat the opposite flat.

3. The grating fabricator will etch and gold coat the grating

At this point the Silicon Spectrometer Slab is complete and will be characterized for spectral resolution, through-put, and scattered light.

The goal of these three steps is to define a manufacturing process to maximize yield and operating characteristics.

4.2 Optical Chopper

A vendor has been selected and a quote obtained for five chopper assemblies based on the proof of concept prototype. The purchase order will be executed as soon as the final drawing package for the optical bench is released. This is anticipated to occur early June, 1997.

4.3 Detector Assembly

We are currently evaluating the multiplexed detector from NEP. The characterization will be completed shortly. We can then place the order for the multiplexed detector array. Delivery will be in about 8-10 weeks. At this point, the design of the data acquisition and signal processing circuitry will be initiated.

4.4 Packaging

The next major mechanical design task will be the case for the instrument. Particular emphasis will be placed on designing a low cost package that is easy to assemble.

5. Marketing

To investigate commercial markets for this spectrographs we have contacted several spectrograph vendors, and started a market survey of users. To assist in this we have produced a preliminary spec sheet showing two embodiments of the device. The first is the handheld spectrometer and the second is the OEM bench. In the coming months we hope to refine these specs by contacting various potential end users and OEM customers.

APPENDIX -- PCT APPLICATION NO. PCT/US99/07781

MICRO-SPEC®

The world's smallest IR spectrograph

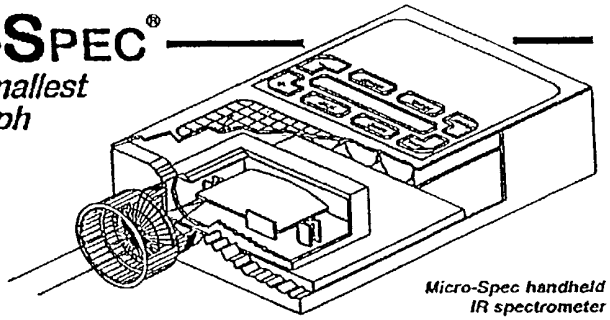

Micro-Spec handheld IR spectrometer

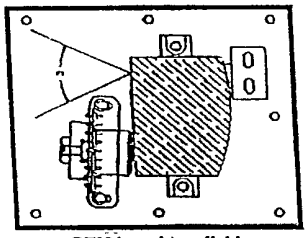

OEM bench available
1/4 meter monochrometer in a 3 inch package

The miniature Micro-Spec infrared spectrometer is the smallest, near/mid IR grating spectrometer available. The patent-pending design, developed for the space program, is now available for commercial users. It's unique waveguide construction provides four times the throughput of conventional designs. Monolithic construction provides vibration immunity and thermal stability. Designed for infrared gas detection (CH_4, CO, CO_2, NO, NO_2, H_2O), the system can be used for chemical identification in the field or on the loading dock.

PRELIMINARY SPECIFICATIONS
January 1, 1997

Input:	F/1 lens or fiber optic
Sensitivity:	3 - 5.5μm (1.5 - 3μm alt.)
Resolution:	0.04μm
Throughput:	F/1
Computer Output:	RS232
Grating:	Blazed Holographic
Slit:	0.07 x 1mm
Detector:	PbSe 64 element
Dimensions:	3" x 6.5" x 1.2"
Weight:	50oz
Display:	LCD Graphic
Power:	Battery (10W @ 12V)

Ion Optics, Inc.
Innovative Technology Building IR Products

411 Waverly Oaks Road, Suite 144, Waltham, MA 02154
Telephone (617) 788-8777 • Fax (617) 788-8811

Figure 5.1 Preliminary spec. sheet showing product concept.

APPENDIX -- PCT APPLICATION NO. PCT/US99/07781

6. Cumulative Costs

The cumulative costs for this PHASE II project are $197,346. Current expenditure is in line with the projected cost to complete.

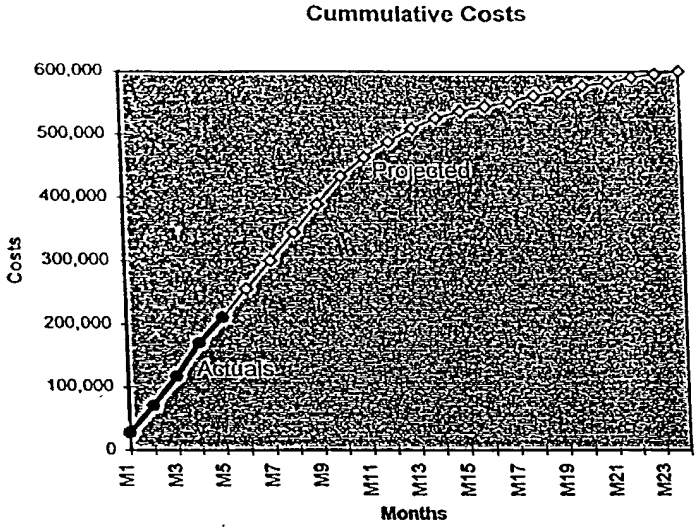

7. ESTIMATED PERCENT OF TECHNICAL EFFORT COMPLETE

The technical effort is estimated to be 35% complete.

APPENDIX -- PCT APPLICATION NO. PCT/US99/07781

CLAIMS

1. A monolithic spectrometer system, comprising:

a slab waveguide having an input surface for accepting optical radiation and an exit surface;

a diffraction grating disposed with a third surface of the waveguide;

a detector array aligned adjacent to the second surface;

a first reflective mirror coated on the waveguide such that the radiation transmitted within the waveguide is reflected and collimated to the grating, wherein light energy diffracted from the grating is dispersed to the mirror for subsequent refocus through the second surface and onto the array.

2. A system according to claim 1, wherein the waveguide comprises silicon.

3. A system according to claim 1, wherein the detector array is selected from the group consisting essentially of microbolometers, PbSe, PbS, and CCD.

4. A system according to claim 1, further comprising input optics to focus optical radiation onto the first surface.

5. A system according to claim 1, further comprising an electronics subsystem for collecting signals from the array, for processing the signals, and for correlating the signals to reference data so that a chemical species of the radiation spectrum is determined.

APPENDIX -- PCT APPLICATION NO. PCT/US99/07781

Abstract

The invention includes a solid optical grade waveguide coupled to a line array of detectors. Light from a source (e.g., earth emissions transmitted through gases) is focussed at a first surface of the waveguide, reflected from an internal mirror to a diffractive surface, which diffracts the light to a second reflector. The reflector refocusses the diffracted light onto the array at a second surface of the waveguide. The detectors are preferably microbolometers or made from PbS or PbSe material. The waveguide is typically silicon to transmit IR radiation with relatively high index of refraction. Other materials can be used. Electronics, responsive to user input, processes detector signals and determines spectral characteristics of the light such as to indicate the presence of a chemical species.

APPENDIX -- PCT APPLICATION NO. PCT/US99/07781

1/2

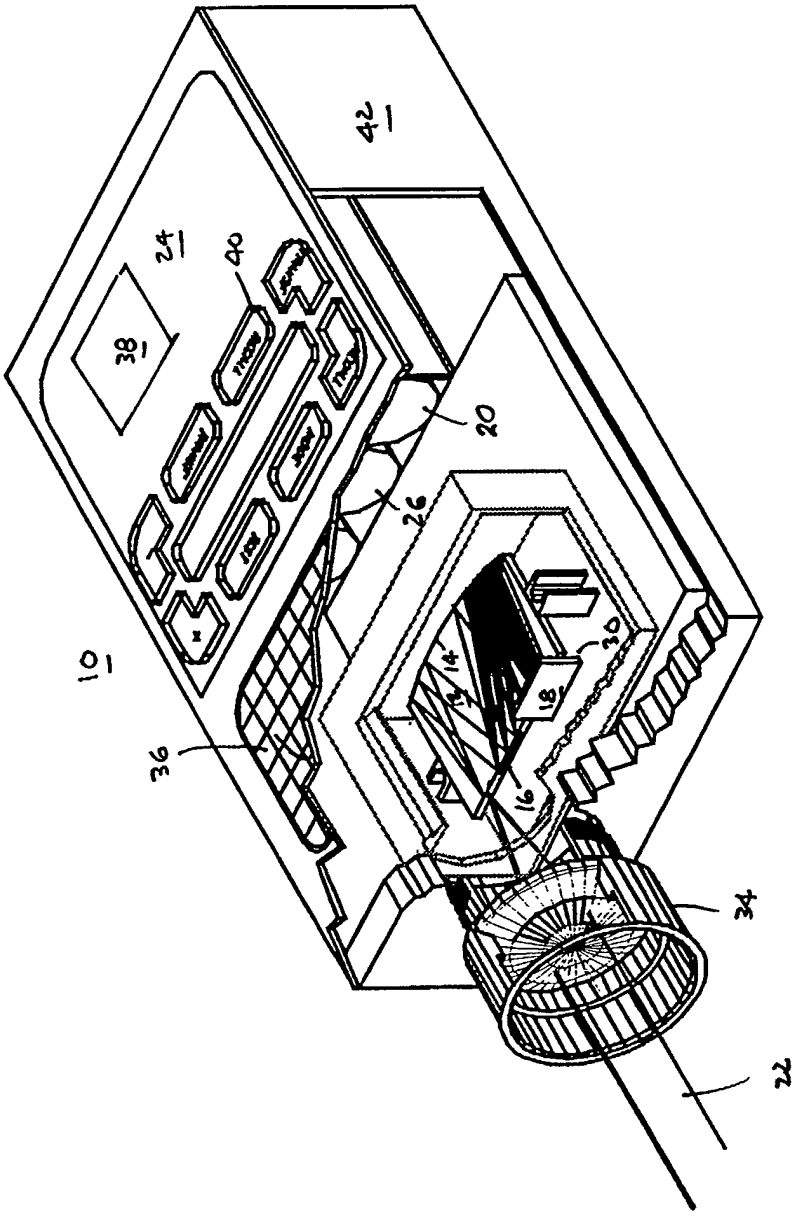

FIG. 1

APPENDIX -- PCT APPLICATION NO. PCT/US99/07781

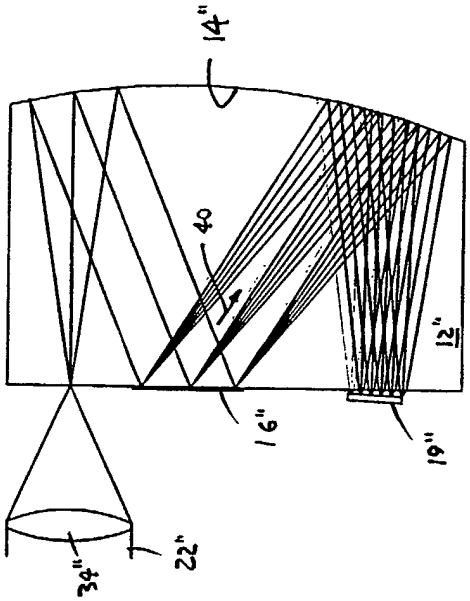

FIG. 3

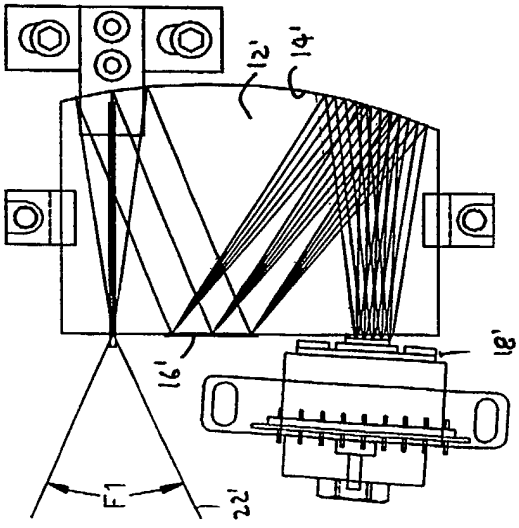

FIG. 2

CLAIMS:

1. A narrow band incoherent radiation emitter detector comprising:

a planar filamental emission/detection element characterized by a predetermined spectral range of emitted/detected radiation and a emission/detection width dl/l less than about 0.1, where l is the wavelength of said radiation.

2. An emitter detector according to claim 1 wherein said spectral range includes relatively long wavelengths and excludes relatively short wavelengths.

3. An emitter/detector according to claim 2 wherein said emission/detection width is substantially determined by surface features of said emission/detection element.

4. An emitter/detector according to claim 1 wherein said emission/detection width is substantially determined by surface features of said emission/detection element.

5. An emitter/detector according to claim 1 wherein said spectral range is near an infrared absorption line of a predetermined material.

6. An emitter/detector according to claim 5 wherein said emission/detection width is substantially determined by surface features of said emission/detection element.

7. An emitter/detector according to claim 1 wherein said spectral range excludes relatively long wavelengths and relatively short wavelengths and includes a range of intermediate wavelengths therebetween.

8. An emitter/detector according to claim 7 wherein said emission/detection width is substantially determined by surface features of said emission/detection element.

9. An emitter/detector according to claim 8 wherein said range of intermediate wavelengths includes an infrared absorption line of a predetermined material.

10. An emitter/detector according to claim 8, further comprising a detector for photons characterized by a wavelength within said intermediate range.

11. An emitter/detector according to claim 8 further comprising a thermal detector for detecting Infrared energy characterized by a wavelength in said intermediate range.

12. An emitter/detector according to claim 8 wherein said emission/detection element is a suspended filament made of a metal foil.

13. An emitter/detector according to claim 8 wherein said emission/detection element is a suspended filament made of a back-etched semiconductor.

14. An emitter/detector according to claim 8 wherein said emission/detection element is a resistive element having an emission surface to control said spectral range.

15. A gas detector comprising:

A. a planar filamental emission/detection element characterized by a predetermined spectral range of emitted/detected radiation and a emission/detection width dl/l less than about 0.1, where l is the wavelength of said radiation, said emission/detection element having an input/output axis, and

B. a first reflector disposed along said input/output axis and opposite to said emission/detection element, whereby an optical path is defined from said emission/detection element to said first reflector to and back to said emission/detection element, wherein said optical path between said emission/detection element and said first reflector passes through a gas test region.

16. A gas detector according to claim 15, further comprising:

C. a driver for driving said emission/detection element to emit radiation propagating along said optical path toward said first reflector.

17. A gas detector according to claim 14 further comprising:

D. a processor responsive to said emission/detection element for generating an output signal representative of radiation incident thereon.

18. A gas detector according to claim 15 wherein said spectral range includes a wavelength corresponding to an absorption line of a predetermined gas.

19. A gas detector according to claim 15 further comprising:

a second reflector extending from points near said emission/detection element along said input/output axis,

wherein said second reflector is disposed along said optical path, whereby said optical path extends from said emission/detection element to said second reflector to said first reflector to said second reflector to said emission/detection element, and wherein said optical path between said second reflector and said first reflector passes through said gas test region.

20. A gas detector according to claim 19, further comprising:

C. a driver for driving said emission/detection element to emit radiation propagating along said optical path toward said first reflector.

21. A gas detector according to claim 20 further comprising:

D. a processor responsive to said emission/detection element for generating an output signal representative of radiation incident thereon.

22. A gas detector according to claim xx4 wherein said second reflector is a beam-forming reflector and said second reflector is substantially planar.

23. A gas detector comprising:

A. a planar filamental emission element characterized by a predetermined spectral range of emitted radiation and an emission width dl/l less than about 0.1, where l is the wavelength of said emission element having an output axis,

B. a first reflector disposed along said output axis, and

C. a planar filamental detection element characterized by a predetermined spectral range of detected radiation and a emission/detection width dl/l less than about 0.1, where l is the wavelength of said detection element having an input axis, whereby an optical path is defined from said emission element to said first reflector and to said detection element, wherein said optical path between said emission element and said first reflector, or between said first reflector and said detection element or both, passes through a gas test region.

24. A gas detector according to claim 23 further comprising:

a second reflector disposed along said optical path between said first reflector and said detection element whereby said optical path extends from said emission element to said first reflector to said reflector to said detection element, and wherein said optical path between said first reflector and said second reflector passes through said gas test region.

25. A gas detector according to claim 23, further comprising:

C. a driver for driving said emission element to emit radiation propagating along said optical path toward said first reflector.

26. A gas detector according to claim 23 further comprising:

D. a processor responsive to said detection element for generating an output signal representative of radiation incident thereon.

27. A gas detector according to claim 23 wherein said spectral range includes a wavelength corresponding to an absorption line of a predetermined gas.

28. A multi-wavelength radiation emitter/detector array comprising:

an array of planar emission/detection elements, each element being characterized by a predetermined spectral range of emitted/detected radiation and an emission/detection width dl/l less than about 0.1, when l is the wavelength of said radiation.

29. An array according to claim 28 wherein said array is adopted to emit/detect information representative of a planar image.

PCT

WORLD INTELLECTUAL PROPERTY ORGANIZATION
International Bureau

INTERNATIONAL APPLICATION PUBLISHED UNDER THE PATENT COOPERATION TREATY (PCT)

(51) International Patent Classification 6 :
H05B 3/26

A1

(11) International Publication Number: WO 00/07411

(43) International Publication Date: 10 February 2000 (10.02.00)

(21) International Application Number: PCT/US99/17338

(22) International Filing Date: 30 July 1999 (30.07.99)

(30) Priority Data:

60/094,602	30 July 1998 (30.07.98)	US
60/096,133	10 August 1998 (10.08.98)	US

(71) Applicant *(for all designated States except US)*: ION OPTICS, INC. [US/US]; Suite 144, 411 Waverly Oaks Road, Waltham, MA 02454 (US).

(72) Inventors; and

(75) Inventors/Applicants *(for US only)*: JOHNSON, Edward, A. [US/US]; 38 Old Stagecoach Road, Bedford, MA 01730 (US). BODKIN, W., Andrew [US/US]; 37 Forest Street, Needham, MA 02492 (US). WOLLAM, John, S. [US/US]; 53 Alcott Street, Acton, MA 01720 (US). DALEY, James, T. [US/US]; 35 Pattys Lane, Mansfield, MA 02048 (US).

(74) Agents: LAPPIN, Mark, G. et al.; Lappin & Kusmer LLP, 200 State Street, Boston, MA 02109 (US).

(81) Designated States: AU, CA, JP, US, European patent (AT, BE, CH, CY, DE, DK, ES, FI, FR, GB, GR, IE, IT, LU, MC, NL, PT, SE).

Published
With international search report.

(54) Title: INFRARED RADIATION SOURCES, SENSORS AND SOURCE COMBINATIONS, AND METHODS OF MANUFACTURE

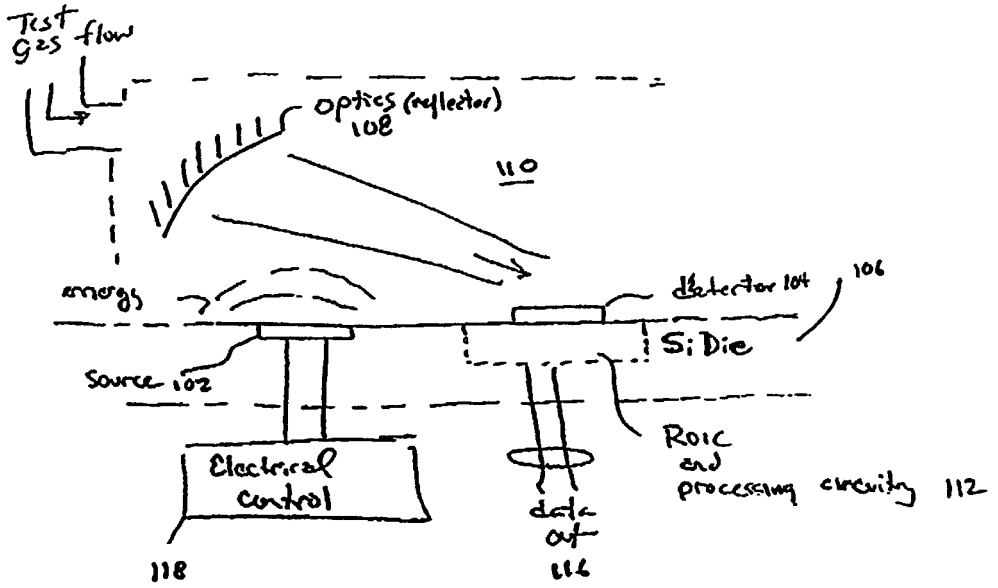

(57) Abstract

A blackbody radiation device (110) includes a planar filament emission element (102) and a planar detector (104) for respectively producing and detecting radiation having width d1/1 less than about 0.1 to test a sample gas, where 1 is the wavelength of the radiation; a reflector (108); a window (W); an electrical control (118); and a data output element (116).

FOR THE PURPOSES OF INFORMATION ONLY

Codes used to identify States party to the PCT on the front pages of pamphlets publishing international applications under the PCT.

AL	Albania	**ES**	Spain	**LS**	Lesotho	**SI**	Slovenia
AM	Armenia	**FI**	Finland	**LT**	Lithuania	**SK**	Slovakia
AT	Austria	**FR**	France	**LU**	Luxembourg	**SN**	Senegal
AU	Australia	**GA**	Gabon	**LV**	Latvia	**SZ**	Swaziland
AZ	Azerbaijan	**GB**	United Kingdom	**MC**	Monaco	**TD**	Chad
BA	Bosnia and Herzegovina	**GE**	Georgia	**MD**	Republic of Moldova	**TG**	Togo
BB	Barbados	**GH**	Ghana	**MG**	Madagascar	**TJ**	Tajikistan
BE	Belgium	**GN**	Guinea	**MK**	The former Yugoslav Republic of Macedonia	**TM**	Turkmenistan
BF	Burkina Faso	**GR**	Greece			**TR**	Turkey
BG	Bulgaria	**HU**	Hungary	**ML**	Mali	**TT**	Trinidad and Tobago
BJ	Benin	**IE**	Ireland	**MN**	Mongolia	**UA**	Ukraine
BR	Brazil	**IL**	Israel	**MR**	Mauritania	**UG**	Uganda
BY	Belarus	**IS**	Iceland	**MW**	Malawi	**US**	United States of America
CA	Canada	**IT**	Italy	**MX**	Mexico	**UZ**	Uzbekistan
CF	Central African Republic	**JP**	Japan	**NE**	Niger	**VN**	Viet Nam
CG	Congo	**KE**	Kenya	**NL**	Netherlands	**YU**	Yugoslavia
CH	Switzerland	**KG**	Kyrgyzstan	**NO**	Norway	**ZW**	Zimbabwe
CI	Côte d'Ivoire	**KP**	Democratic People's Republic of Korea	**NZ**	New Zealand		
CM	Cameroon			**PL**	Poland		
CN	China	**KR**	Republic of Korea	**PT**	Portugal		
CU	Cuba	**KZ**	Kazakstan	**RO**	Romania		
CZ	Czech Republic	**LC**	Saint Lucia	**RU**	Russian Federation		
DE	Germany	**LI**	Liechtenstein	**SD**	Sudan		
DK	Denmark	**LK**	Sri Lanka	**SE**	Sweden		
EE	Estonia	**LR**	Liberia	**SG**	Singapore		

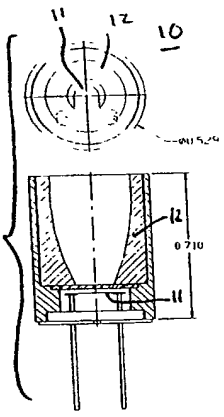

FIG 1A

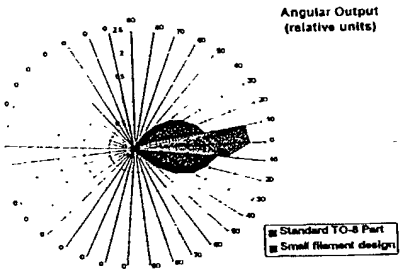

FIG 1B

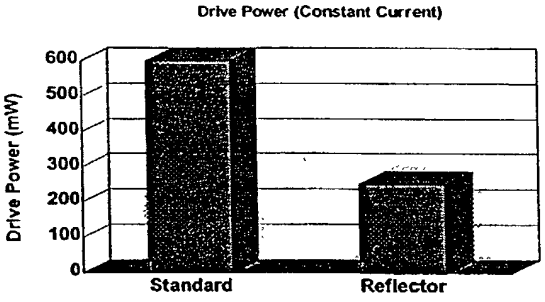

FIG 1C

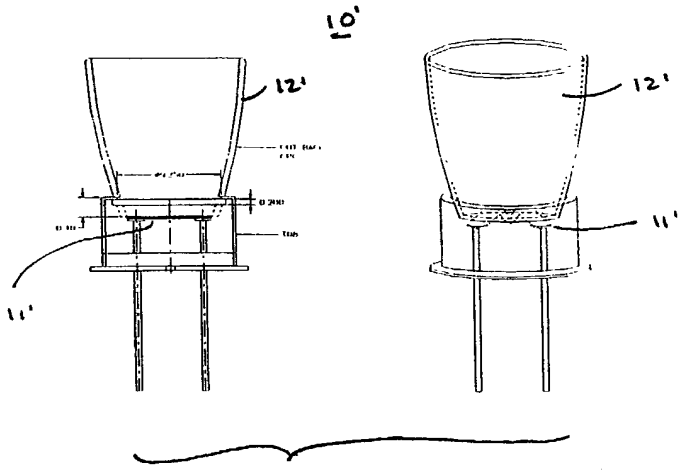

FIG 1D

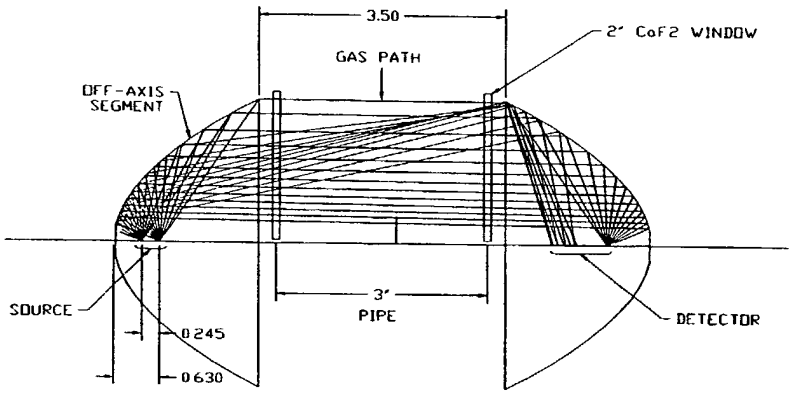

FIG 2

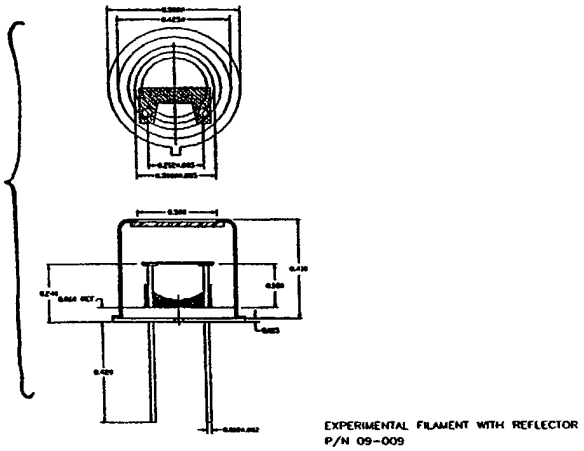

FIG 3A

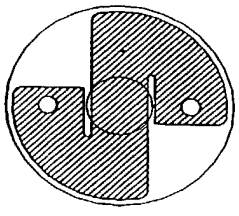

FIG 3B

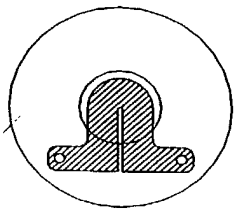

FIG 3C

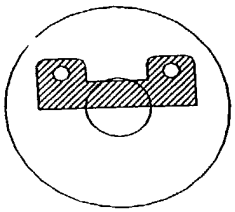

FIG 3D

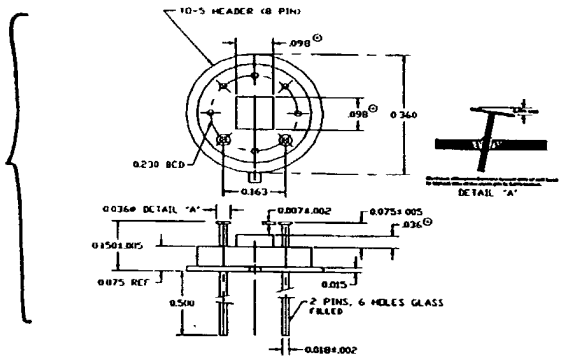

FIG 4

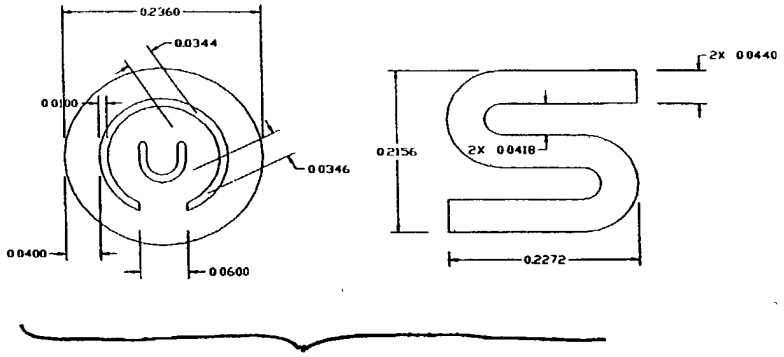

FIG 5

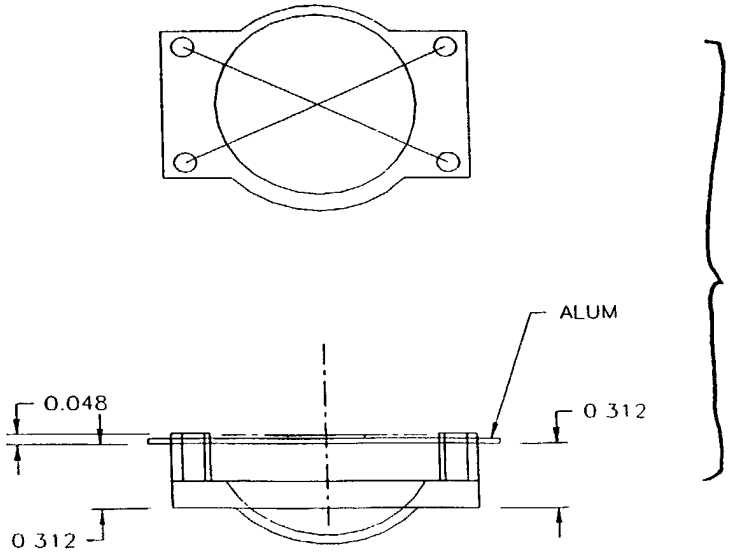

FIG 6

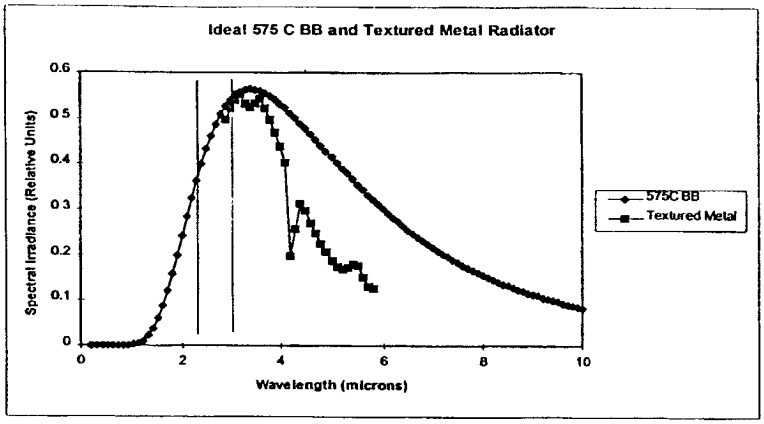

FIG 7

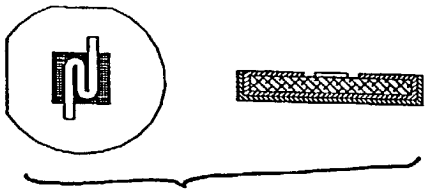

FIG 8A

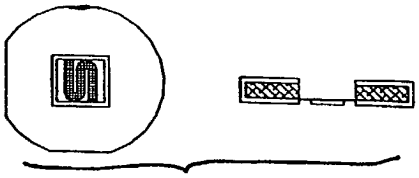

FIG 8B

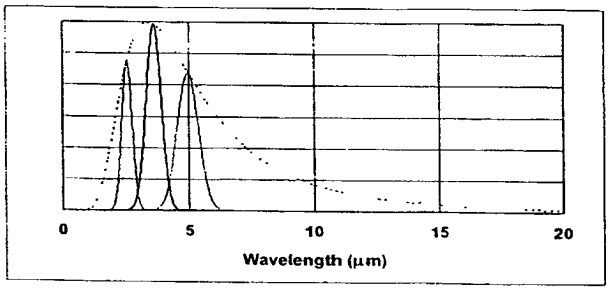

FIG 9A

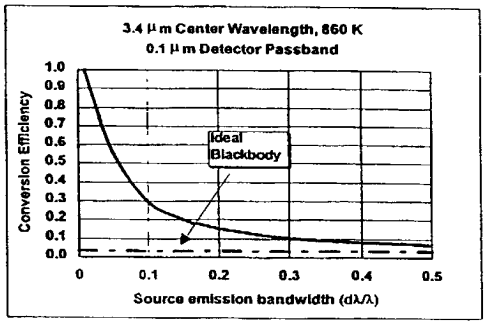

FIG 9B

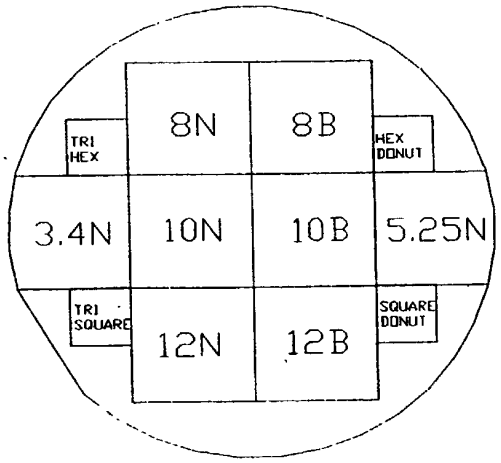

FIG 7A(a)

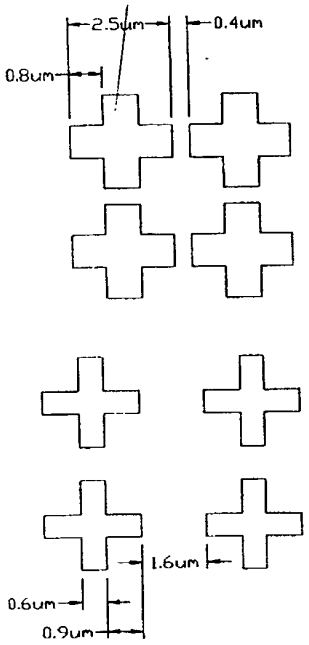

FIG 7A(b)

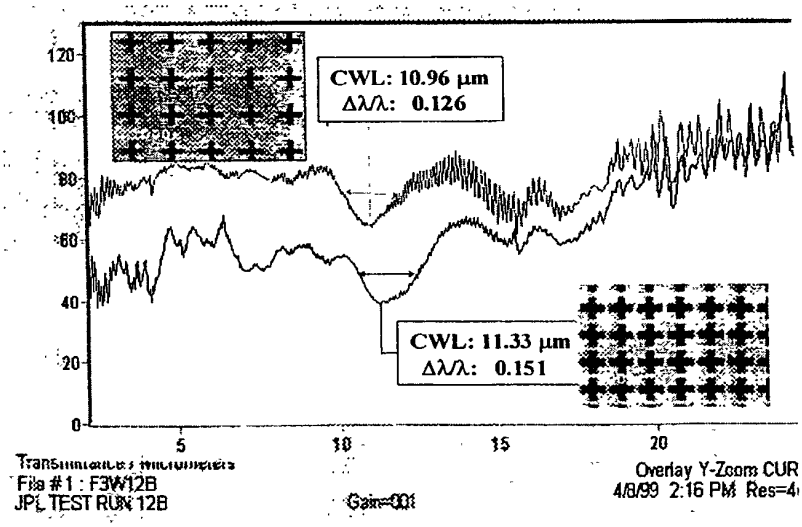

FIG 7A(c)

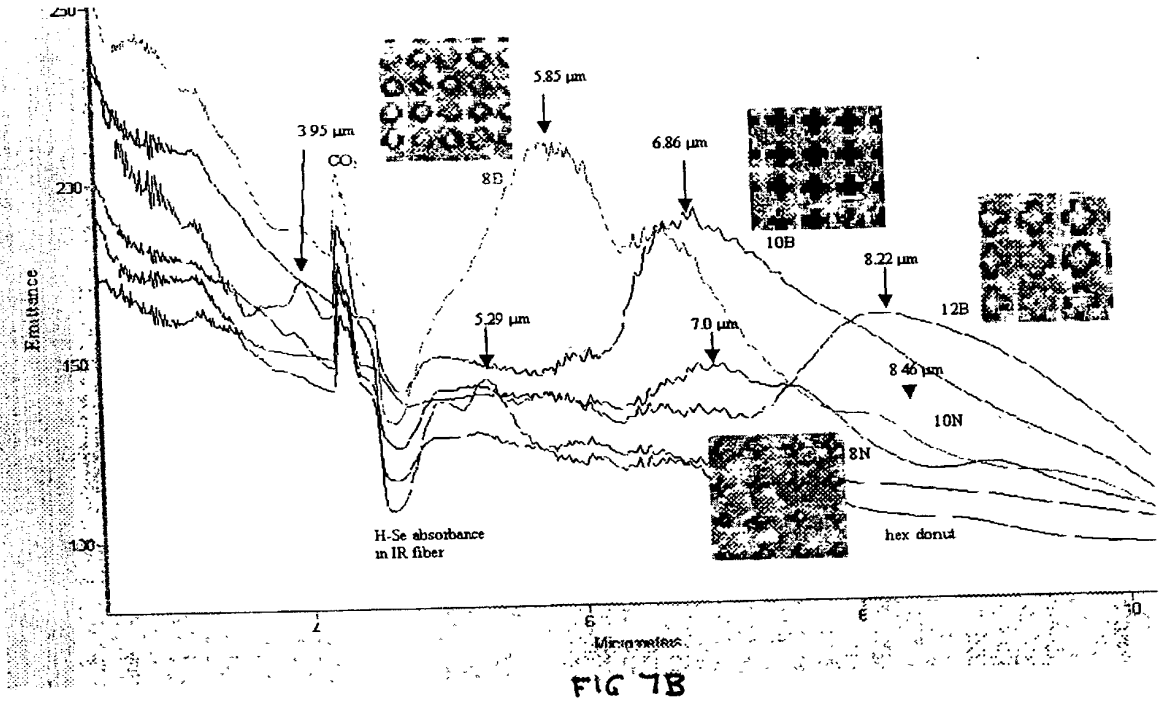
Emittance
250
200
150
100
3.95 µm
CO2
5.85 µm
8B
6.86 µm
10B
8.22 µm
12B
5.29 µm
7.0 µm
8.46 µm
10N
8N
H-Se absorbance
in IR fiber
hex donut
Micrometers

FIG 7B

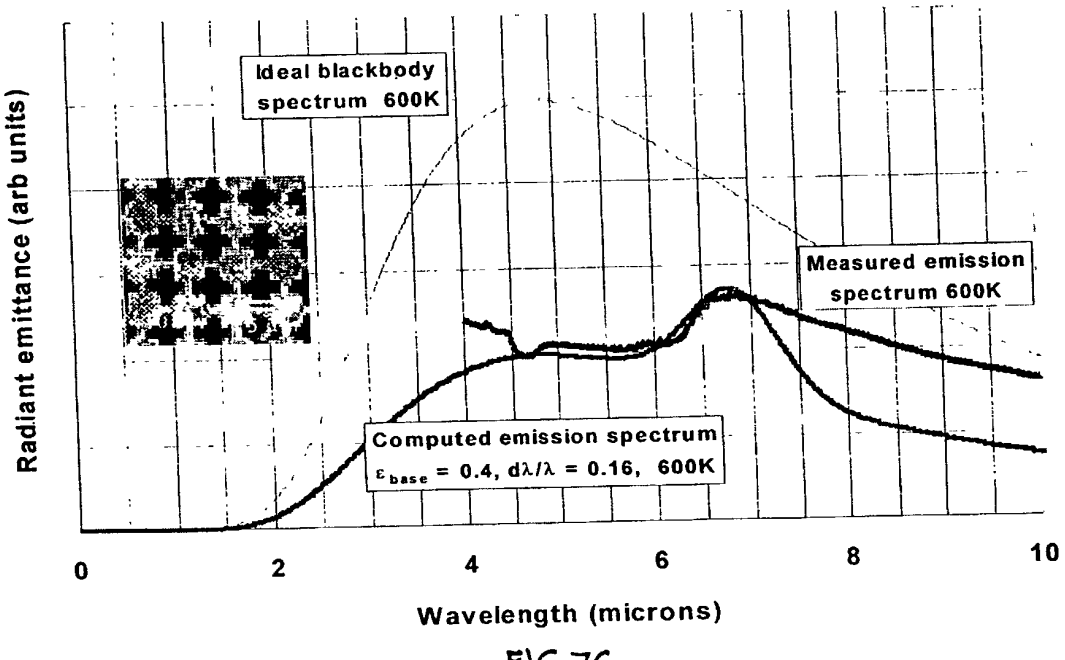
Ideal blackbody
spectrum 600K
Measured emission
spectrum 600K
Computed emission spectrum
ε base = 0.4, dλ/λ = 0.16, 600K
Radiant emittance (arb units)
0
2
4
6
8
10
Wavelength (microns)

FIG 7C

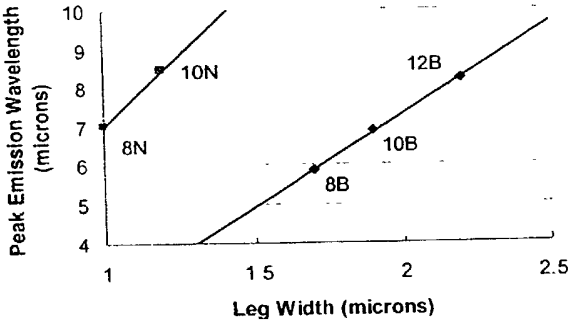

FIG 7D(a)

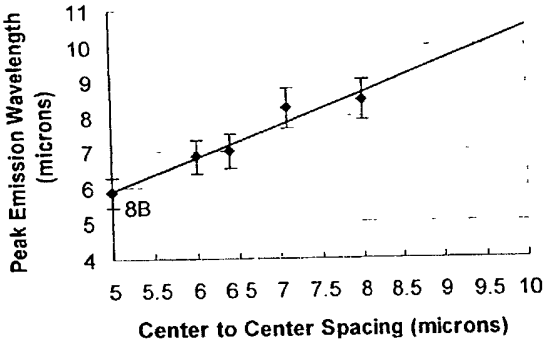

FIG 7D(b)

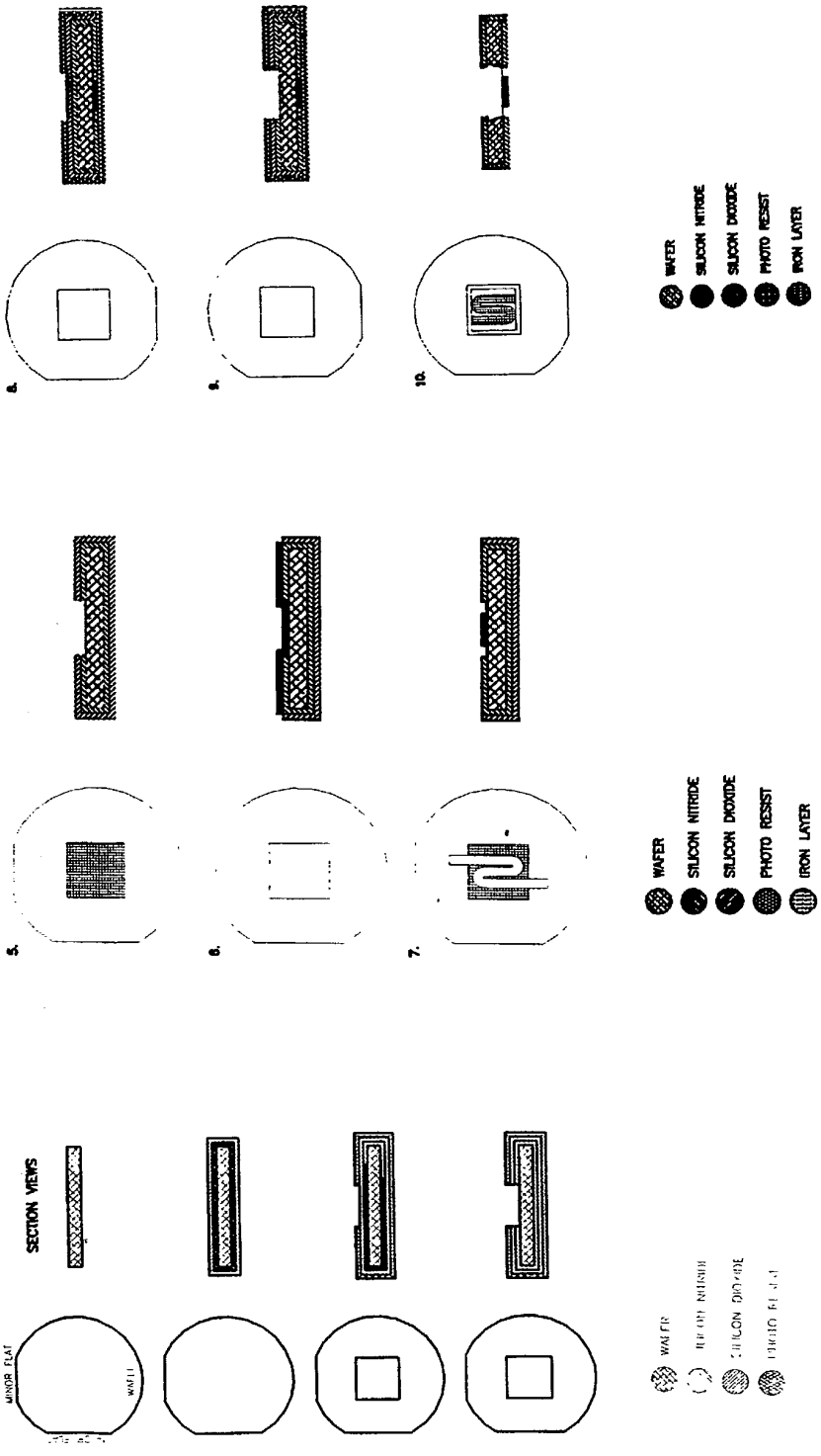
WAFER
SILICON NITRIDE
SILICON DIOXIDE
PHOTO RESIST
IRON LAYER
SECTION VIEWS
MINOR FLAT

FIG 8A

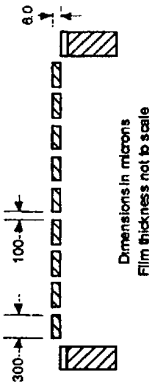

FIG 8B(c)

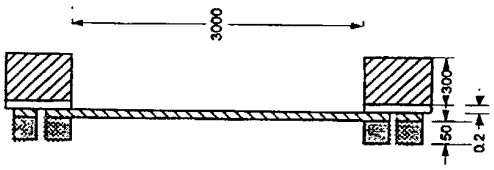

FIG 8B(b)

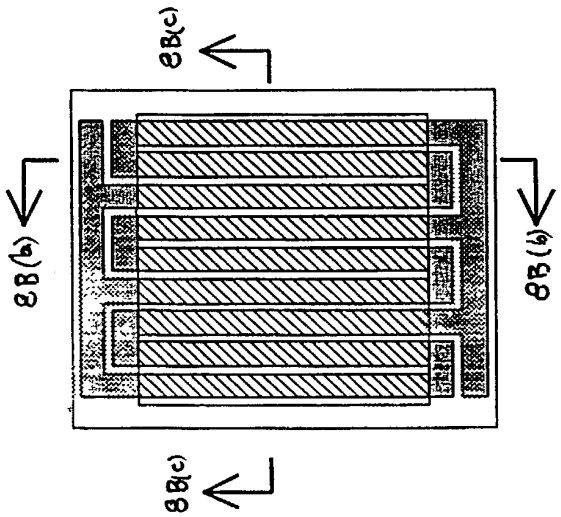

FIG 8B(a)

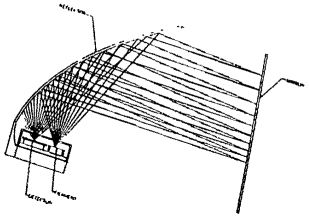

FIG 10

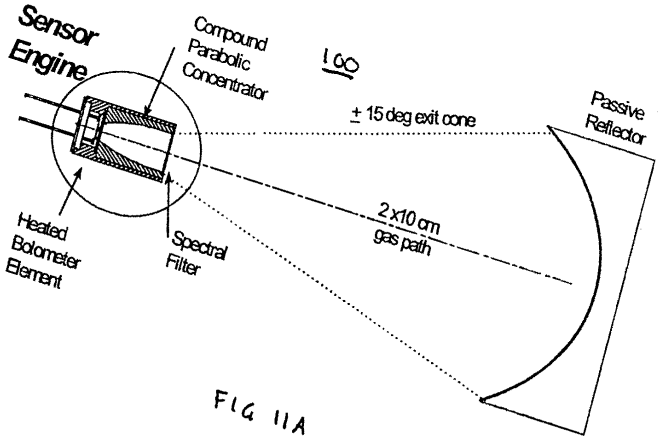

FIG 11A

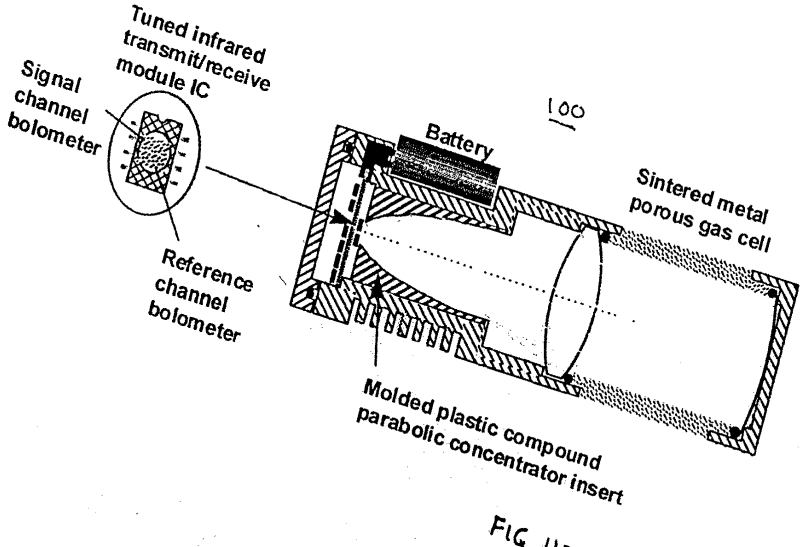

FIG 11B

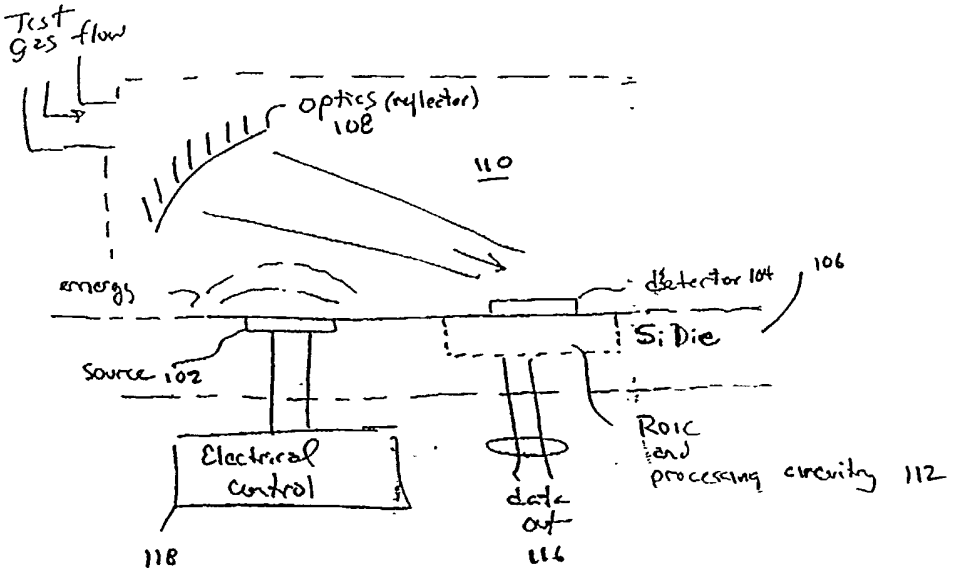

FIG 11C

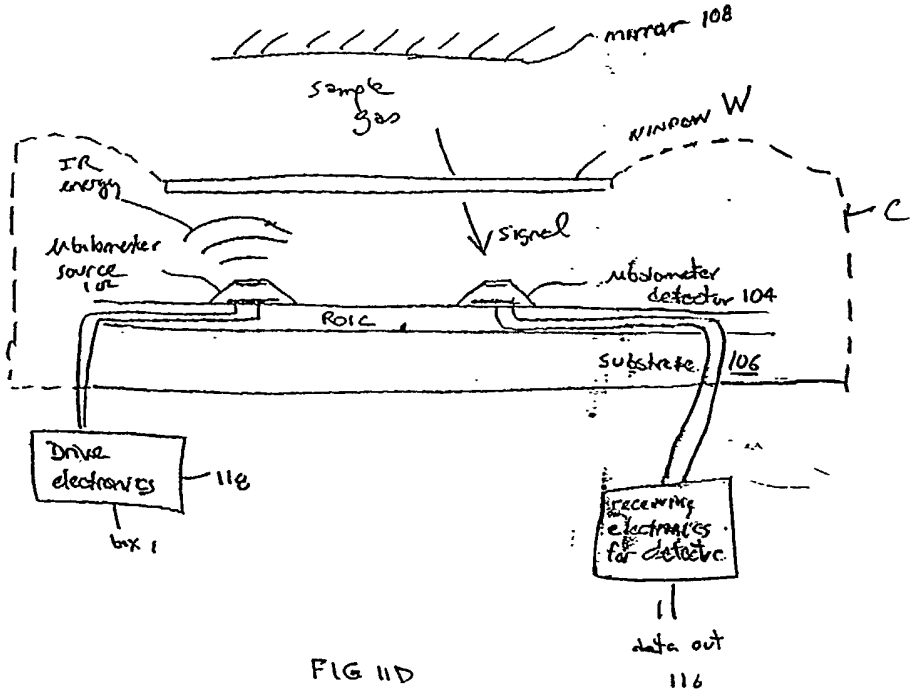

FIG 11D

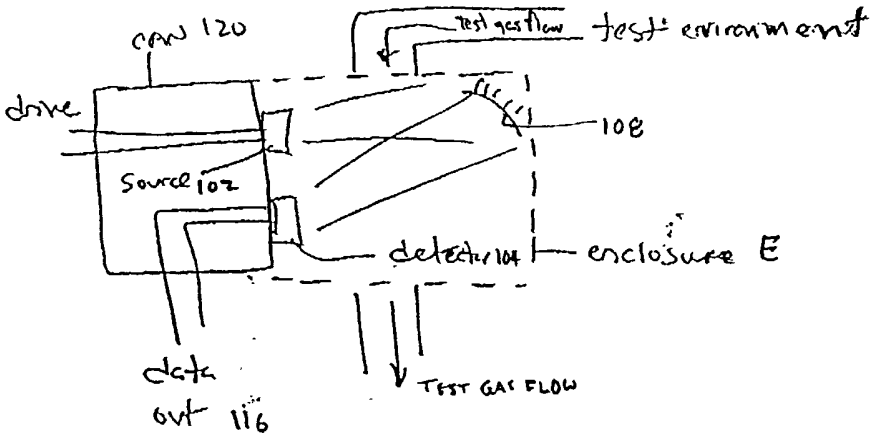

FIG 11E

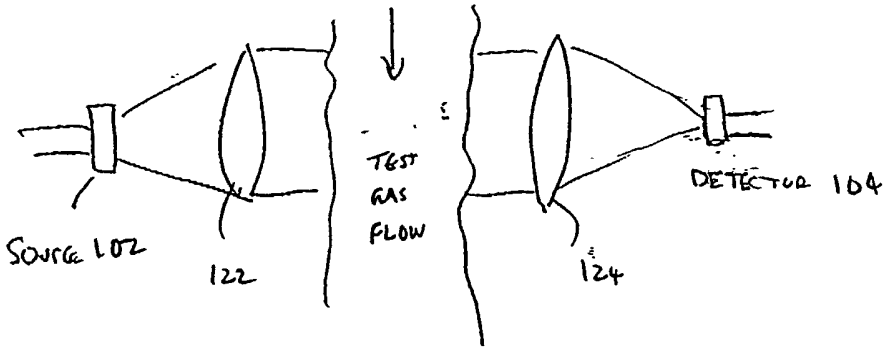

FIG 11F

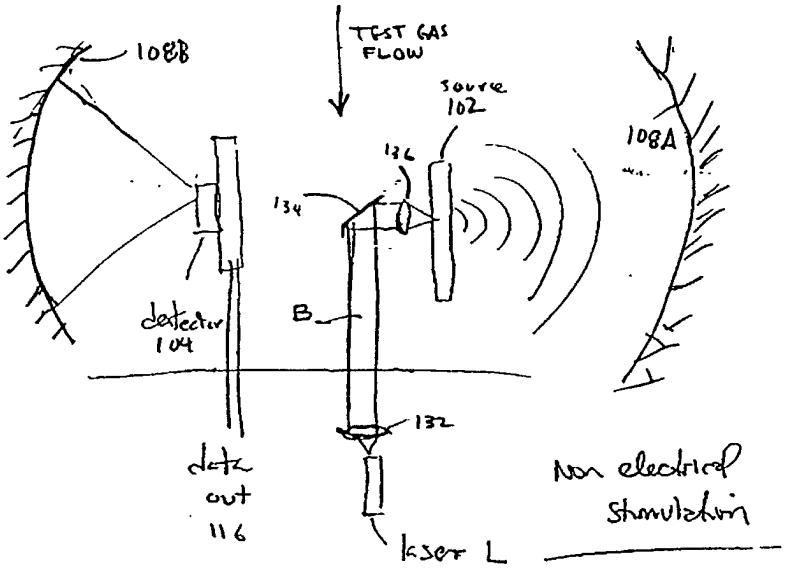

FIG 11G

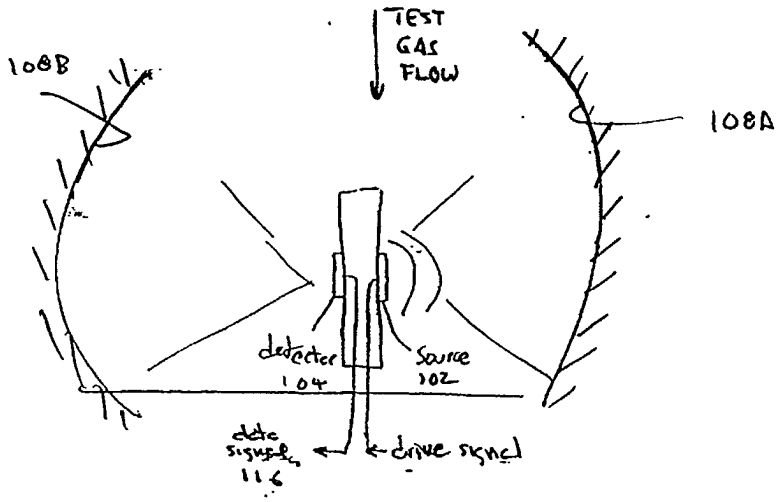

FIG 11H

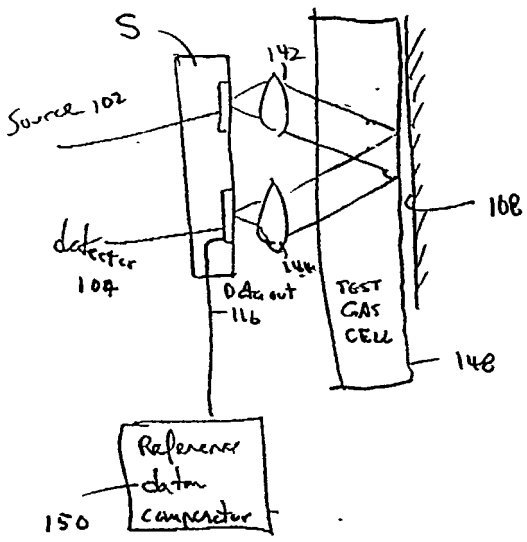
S
142
Source 102
detector
104
144
Data out
116
TEST
GAS
CELL
108
148
Reference
data
computer
150

FIG 11 I

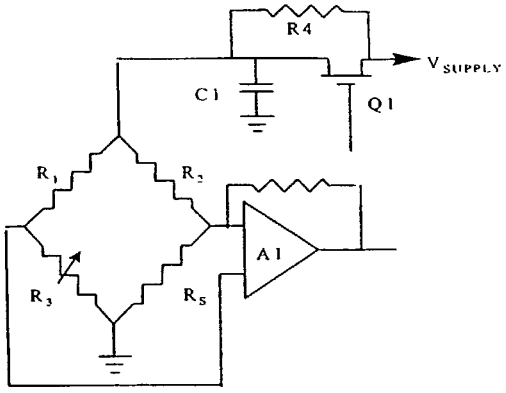

FIG 12

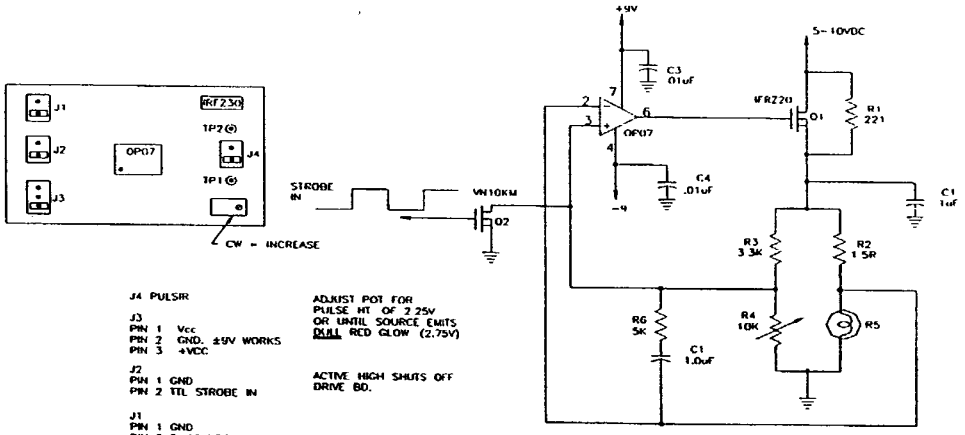

FIG 13

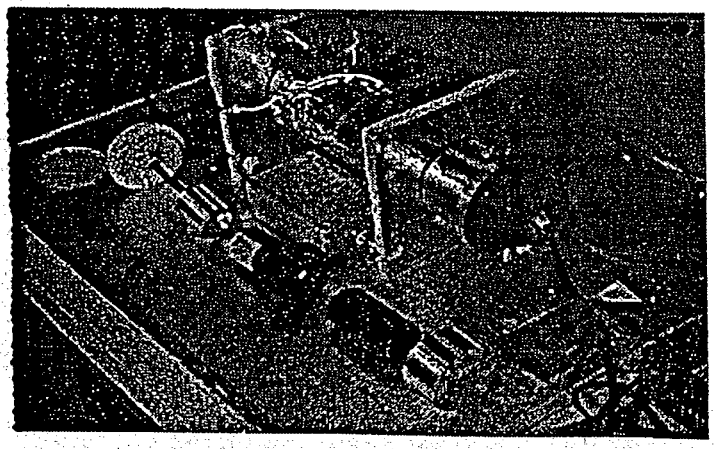

FIG 14A

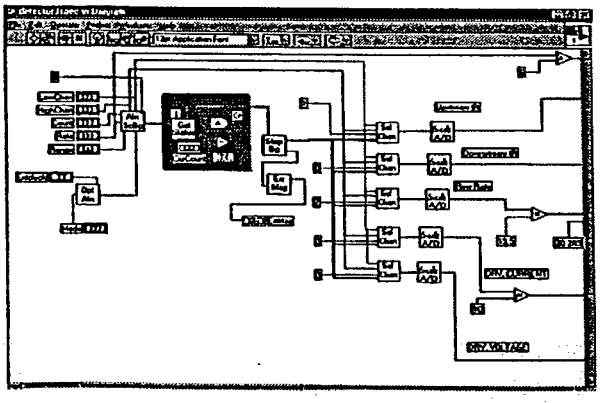

FIG 14B

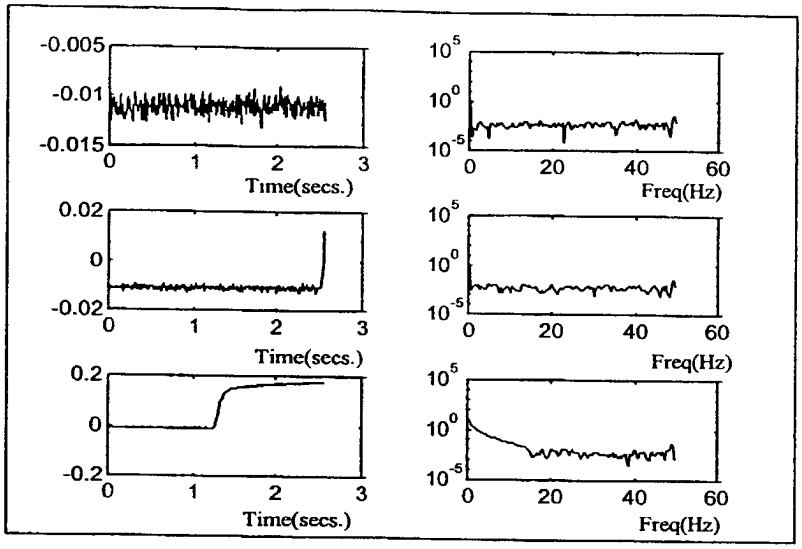

FIG 15

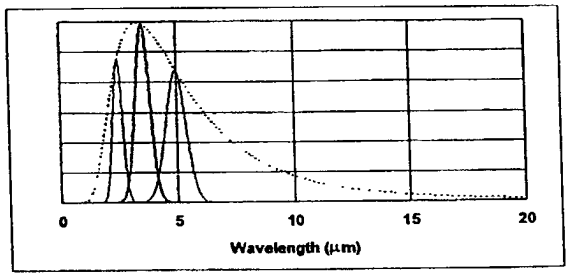

FIG 16

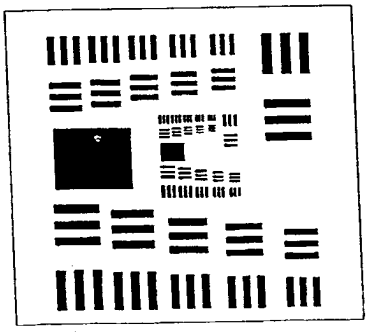

FIG 17A

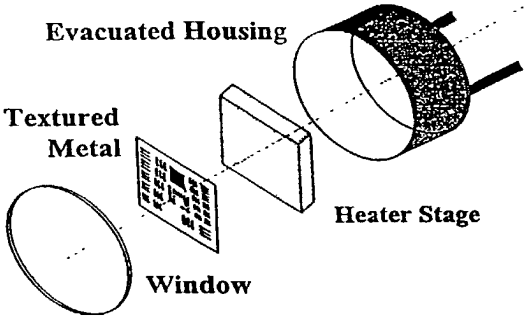

FIG 17B

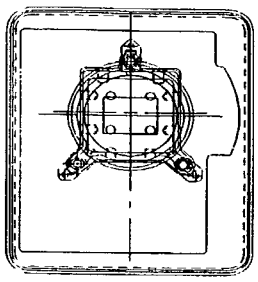

FIG 16A

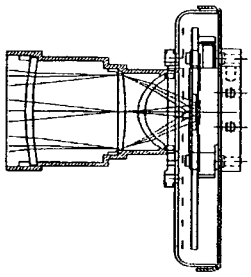

FIG 18B

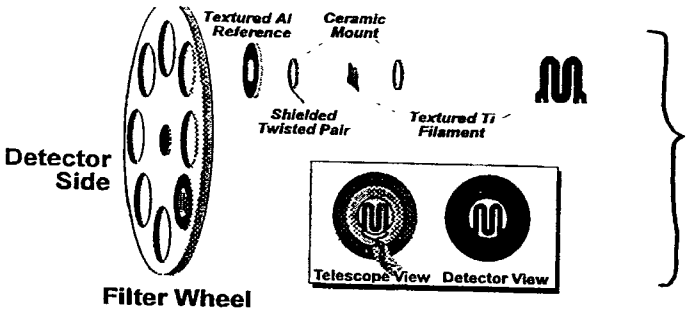

FIG 19A

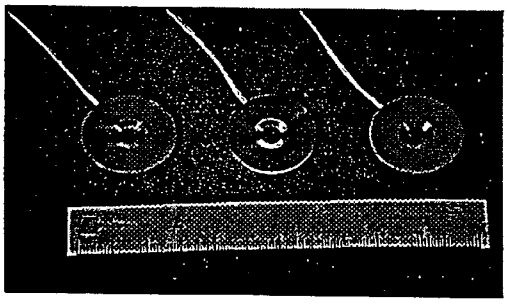

FIG 19B

Docket No.
56362-032 (IOPL-007)

Declaration and Power of Attorney For Patent Application

English Language Declaration

As a below named inventor, I hereby declare that:

My residence, post office address and citizenship are as stated below next to my name,

I believe I am the original, first and sole inventor (if only one name is listed below) or an original, first and joint inventor (if plural names are listed below) of the subject matter which is claimed and for which a patent is sought on the invention entitled

the specification of which

(check one)

☐ is attached hereto.

☒ was filed on January 30, 2001 as United States Application No. or PCT International Application Number 09/762,077

and was amended on _____
(if applicable)

I hereby state that I have reviewed and understand the contents of the above identified specification, including the claims, as amended by any amendment referred to above.

I acknowledge the duty to disclose to the United States Patent and Trademark Office all information known to me to be material to patentability as defined in Title 37, Code of Federal Regulations, Section 1.56.

I hereby claim foreign priority benefits under Title 35, United States Code, Section 119(a)-(d) or Section 365(b) of any foreign application(s) for patent or inventor's certificate, or Section 365(a) of any PCT International application which designated at least one country other than the United States, listed below and have also identified below, by checking the box, any foreign application for patent or inventor's certificate or PCT International application having a filing date before that of the application on which priority is claimed.

Prior Foreign Application(s)			Priority Not Claimed
(Number)	(Country)	(Day/Month/Year Filed)	☐
(Number)	(Country)	(Day/Month/Year Filed)	☐
(Number)	(Country)	(Day/Month/Year Filed)	☐

I hereby claim the benefit under 35 U.S.C. Section 119(e) of any United States provisional application(s) listed below:

60/094,602	**July 30, 1998**
(Application Serial No.)	(Filing Date)
60/096,133	**August 10, 1998**
(Application Serial No.)	(Filing Date)
(Application Serial No.)	(Filing Date)

I hereby claim the benefit under 35 U. S. C. Section 120 of any United States application(s), or Section 365(c) of any PCT International application designating the United States, listed below and, insofar as the subject matter of each of the claims of this application is not disclosed in the prior United States or PCT International application in the manner provided by the first paragraph of 35 U.S.C. Section 112, I acknowledge the duty to disclose to the United States Patent and Trademark Office all information known to me to be material to patentability as defined in Title 37, C. F. R., Section 1.56 which became available between the filing date of the prior application and the national or PCT International filing date of this application:

PCT/US99/17338	**30 July 1999**	**Pending**
(Application Serial No.)	(Filing Date)	(Status) (patented, pending, abandoned)
(Application Serial No.)	(Filing Date)	(Status) (patented, pending, abandoned)
(Application Serial No.)	(Filing Date)	(Status) (patented, pending, abandoned)

I hereby declare that all statements made herein of my own knowledge are true and that all statements made on information and belief are believed to be true; and further that these statements were made with the knowledge that willful false statements and the like so made are punishable by fine or imprisonment, or both, under Section 1001 of Title 18 of the United States Code and that such willful false statements may jeopardize the validity of the application or any patent issued thereon.

POWER OF ATTORNEY: As a named inventor, I hereby appoint the following attorney(s) and/or agent(s) to prosecute this application and transact all business in the Patent and Trademark Office connected therewith. *(list name and registration number)*

Mark G. Lappin, Reg. No. 26,618
Toby H. Kusmer, Reg. No. 26,418
Elizabeth A. Levy, Reg. No. 24,275
David M. Mello, Reg. No. 43,799
Ronald R. Demsher, Reg. No. 42,478
Elizabeth E. Kim, Reg. No. 43,334
Jeffrey J. Miller, Reg. No. 39,773
Scott A. Ouellette, Reg. No. 38,573
John T. Prince, Reg. No. 43,019
All registered attorneys of McDermott, Will & Emery

Send Correspondence to: **Mark G. Lappin, P.C.**
McDermott, Will & Emery
28 State Street
Boston, MA 02109

Direct Telephone Calls to: *(name and telephone number)*
Mark G. Lappin; (617) 535-4000 (tel); (617) 535-3800 (fax)

Full name of sole or first inventor **Edward A. Johnson**
Sole or first inventor's signature — Date 17 JUN 09
Residence **38 Old Stagecoach Road, Bedford, Massachusetts 01730** MA.
Citizenship **USA**
Post Office Address **38 Old Stagecoach Road, Bedford, Massachusetts 01730**

Full name of second inventor, if any **W. Andrew Bodkin**
Second inventor's signature — Date
Residence **37 Forest Street, Needham, Massachusetts 02192**
Citizenship **USA**
Post Office Address **37 Forest Street, Needham, Massachusetts 02192**

2-00

Full name of third inventor, if any
John S. Wollam

Third inventor's signature — Date: 7/17/01

Residence
~~53 Alcott Street, Acton, Massachusetts 01720~~ 37 Carlson Lane, Falmouth, Massachusetts 02540

Citizenship
USA MA.

Post Office Address
~~53 Alcott Street, Acton, Massachusetts 01720~~ 37 Carlson Lane, #9, Falmouth, Massachusetts 02540

Full name of fourth inventor, if any
James T. Daly

Fourth inventor's signature — Date

Residence
35 Pattys Lane, Mansfield, Massachusetts 02048

Citizenship
USA

Post Office Address
35 Pattys Lane, Mansfield, Massachusetts 02048

Full name of fifth inventor, if any

Fifth inventor's signature — Date

Residence

Citizenship

Post Office Address

Full name of sixth inventor, if any

Sixth inventor's signature — Date

Residence

Citizenship

Post Office Address

Full name of third inventor, if any **John S. Wollam**
Third inventor's signature Date
Residence **53 Alcott Street, Acton, Massachusetts 01720**
Citizenship **USA**
Post Office Address **53 Alcott Street, Acton, Massachusetts 01720**

3-01

Full name of fourth inventor, if any **James T. Daly**
Fourth inventor's signature James T Daly Date 6/22/01
Residence **35 Pattys Lane, Mansfield, Massachusetts 02048** MA.
Citizenship **USA**
Post Office Address **35 Pattys Lane, Mansfield, Massachusetts 02048**

Full name of fifth inventor, if any
Fifth inventor's signature Date
Residence
Citizenship
Post Office Address

Full name of sixth inventor, if any
Sixth inventor's signature Date
Residence
Citizenship
Post Office Address